



Provided by the author(s) and University of Galway in accordance with publisher policies. Please cite the published version when available.

Title	Towards improved performance of mediated glucose oxidising enzyme electrodes for biosensing and biopower applications
Author(s)	Bennett, Richard W.
Publication Date	2019-11
Publisher	NUI Galway
Item record	http://hdl.handle.net/10379/15775

Downloaded 2024-04-26T23:26:52Z

Some rights reserved. For more information, please see the item record link above.



Towards improved performance of mediated glucose oxidising enzyme electrodes for biosensing and biopower applications

Submitted by:

Richard W. Bennett M.Sc.

Thesis is submitted for the Ph.D degree by research of the National University
of Ireland Galway



School of Chemistry

Month and year of submission: November 2019

Head of School: Dr. Patrick O'Leary

Supervisor: Professor Dónal Leech

Declaration

The contents of this thesis, except where otherwise stated, are based entirely on my own research which was carried out in the Biomolecular Electronics Research Laboratory based in the School of Chemistry and Ryan Institute, National University of Ireland Galway. I have not obtained a degree at NUI Galway or any other university on the basis of this research.

Richard W. Bennett

November 2019

Acknowledgements

I would like to thank everyone who helped me get to this point and assisted me through my many years of study.

Firstly to my supervisor, Professor Dónal Leech, for giving me the opportunity to join his research group. I am grateful for his guidance and support as well as encouraging me to strive for more. I consider myself privileged to have been part of the BERL.

To all my friends associated with the BERL group for being so supportive on both the good days and bad! In particular I would like to thank Dr. Conan Mercer and Dr. Peter Ó Conghaile for their guidance and taking me under their wing in the beginning.

To all my friends in the Chemistry department, especially the members of Tagnesium, for providing some great memories outside of lab hours!

To all my friends, thank you for providing a much needed outlet and constantly reminding me that there is more to life than obtaining a PhD!

To my brother Jack for putting up with me and always being there.

To anyone pursuing a Ph.D.; *“Ever tried. Ever failed. No matter. Try Again. Fail again. Fail better.”* – Samuel Beckett.

Finally to my parents and uncle John, thank you for your never ending support and constant encouragement. I have been given a life filled with opportunity thanks to you. Without your support this would not have been possible.

Table of Contents

ACKNOWLEDGEMENTS	3
ABSTRACT	6
CHAPTER 1: INTRODUCTION	8
1 INTRODUCTION.....	8
1.1 FUEL CELLS.....	9
1.1.1 <i>Biofuel cells</i>	11
1.3 ENZYME CATALYSTS	14
1.3.1 <i>Glucose oxidase</i>	15
1.3.2 <i>Dehydrogenases</i>	17
1.4 ELECTRON TRANSFER FROM ENZYME TO ELECTRODE	19
1.4.1 <i>Osmium based redox mediators</i>	21
1.5 IMMOBILISATION STRATEGIES	23
1.6 NANOSTRUCTURED SUPPORTS IN ENZYME ELECTRODES	24
1.7 OPTIMISATION STRATEGIES	25
1.8 PERMSELECTIVE MEMBRANES	26
1.9 ENZYMATIC FUEL CELLS.....	28
1.10 ELECTROANALYTICAL TECHNIQUES	29
1.10.1 <i>Voltammetric and amperometric techniques</i>	30
1.11 THESIS PROPOSITION	34
1.12 REFERENCES.....	36
CHAPTER 2: BIO-INSPIRED STRATEGY FOR SURFACE IMMOBILISATION OF ENZYME AND OSMIUM REDOX CENTRES USING POLY(L-DOPA).	51
INTRODUCTION.....	51
EXPERIMENTAL	52
RESULTS.....	53
CONCLUSIONS	60
REFERENCES	61
CHAPTER 3: DESIGN OF EXPERIMENTS APPROACH TO PROVIDE ENHANCED GLUCOSE-OXIDISING ENZYME ELECTRODE FOR MEMBRANE-LESS ENZYMATIC FUEL CELLS OPERATING IN HUMAN PHYSIOLOGICAL FLUIDS	67
ABSTRACT	68
INTRODUCTION.....	68
EXPERIMENTAL	70
MATERIALS	70
RESULTS AND DISCUSSION.....	72
CONCLUSIONS	84
ACKNOWLEDGEMENTS.....	84
REFERENCES	85
CHAPTER 4: EFFECT OF INDIVIDUAL PLASMA COMPONENTS ON THE PERFORMANCE OF A GLUCOSE ENZYME ELECTRODE BASED ON REDOX POLYMER MEDIATION OF A FLAVIN ADENINE DINUCLEOTIDE-DEPENDENT GLUCOSE DEHYDROGENASE	87
ABSTRACT	88
INTRODUCTION.....	89
EXPERIMENTAL	90
RESULTS AND DISCUSSION.....	91
CONCLUSION	99
ACKNOWLEDGMENTS.....	100
REFERENCES	100
CHAPTER 5: IMPROVED OPERATIONAL STABILITY OF MEDIATED GLUCOSE ENZYME ELECTRODES FOR OPERATION IN HUMAN PHYSIOLOGICAL SOLUTIONS	108
ABSTRACT.....	109
INTRODUCTION.....	110

EXPERIMENTAL SECTION	111
RESULTS AND DISCUSSION.....	112
CONCLUSIONS	119
ACKNOWLEDGEMENTS.....	120
REFERENCES	120
SUPPORTING INFORMATION	126
CHAPTER 6: CONCLUSIONS AND FUTURE DIRECTIONS	128
CONCLUSIONS	128
FUTURE DIRECTIONS	129
REFERENCES	131
APPENDIX	134
PUBLICATIONS.....	134
ORAL PRESENTATIONS	134
POSTER PRESENTATIONS	134
AWARDS.....	135

Abstract

Energy produced through enzymatic catalysis at electrodes, namely oxidation of glucose and reduction of oxygen may be used to power devices. The goal of powering implantable or semi-implantable medical devices through enzymes has driven forward the field of enzymatic bioelectrochemistry. Significant challenges must be overcome prior to their inclusion as a power source for medical devices such as low power output, poor operational stabilities and biocompatibility issues. Similar challenges hinder the development of continuous use enzymatic biosensors with poor operational stabilities and biocompatibility preventing long term deployment. This thesis aims to build on work carried out previously in the area of enzyme electrode assembly for fuel cell and biosensor development to improve the understanding and performance of glucose oxidising enzyme electrodes for enhanced operation. Novel enzyme electrode immobilisation strategies are investigated and compared with previously published enzyme electrode assemblies. Enzyme electrodes were prepared using the electropolymerisation of L-Dopa to poly(L-Dopa) as an immobilisation strategy. Improved optimisation methodologies are reported and used to assemble glucose oxidising electrodes with higher current output than those previously described. Enzyme electrodes consisting of co-immobilised redox polymer with FADGDH, MWCNTs and PEGDGE achieved current densities of $1.22 \pm 0.10 \text{ mA cm}^{-2}$ in PBS containing 5 mM glucose were achieved, 52 % higher than those using one factor at a time optimisation approaches. Enzyme electrodes consisting of co-immobilised redox polymer with FADGDH, MWCNTs and PEGDGE were tested in test solutions containing individual plasma components to investigate the reduced performance of enzyme electrodes in human physiological solutions. Electrodes tested in the presence of uric acid generated the lowest current responses and the lowest operational stabilities of all individual plasma components. Current densities of $0.9 \pm 0.10 \text{ mA cm}^{-2}$ were observed at 5 mM glucose concentrations in the presence of uric acid compared to $1.5 \pm 0.10 \text{ mA cm}^{-2}$ in PBS with no uric acid present. 46 % of the initial current remained after 12 hours continuous operation in the presence of uric acid compared to 72 % for PBS with no uric acid present. In comparison, glucose oxidase based electrodes maintained identical operational stabilities of 70 % with and without uric acid present while cellobiose dehydrogenase electrodes maintained 86 % stability in PBS, with 33 % stability in the presence of uric acid. Enzyme electrodes were prepared with Nafion coatings to minimise the effect of plasma on the enzymatic film. Current densities of $8.0 \pm 2.0 \text{ mA cm}^{-2}$ were recorded in 100 mM for glucose oxidase enzyme electrodes prepared with a 0.5 % w/v Nafion coating with an operational stability of 84 % for 12-hour

continuous operation when tested in artificial plasma. FADGDH based electrodes in the same test conditions produced current densities of $4.5 \pm 0.70 \text{ mA cm}^{-2}$ and an operational stability of 58 %. Further work is required to fully understand changes to enzyme electrode performance in physiological solutions and strategies to minimise the impact of these solutions for operation *in-vivo* to allow for higher power outputs and longer operational lifetimes for prototype devices.

Chapter 1: Introduction

1 Introduction

Since the development of the first external electrical heart stimulation by Zoll, there have been huge strides made in the field of medical intervention and medical devices. [1] The current definition for an implantable medical device includes any device which is intended to be totally or partially introduced, surgically or medically, into the human body or by medical intervention into a natural orifice, and which is intended to remain after the procedure. [2,3] In the decades since 1952, scientists and engineers have developed a range of devices for implantation such as bladder stimulators, cochlear implants, cardiac defibrillator and cardiac pacemakers. [4–7] Advancements in biomedicine have led to further miniaturization of devices for implantation in the body. All implantable and semi-implantable devices require a power source for operation. Power generated electrochemically is the most efficient method for powering of such devices when compared to alternative methods such as mobile solar cells or mechanical to electrical power generation. This is due to lower cost and higher power density. [8] Electrochemical power generation can be split into two major sub-groups, batteries and fuel cells. The first report of electrochemical power generation for an implantable device was from Charles Simmons in 1913 with the Zn/NH₄Cl/MnO₂ cell. [9] By the 1980s the first fully implanted pacemaker in humans was launched, containing two nickel-cadmium battery cells capable of producing 60 mAh. [10,11] The current state of the art is a fully implantable, battery powered, leadless pacemaker. Over 700,000 pacemakers are implanted worldwide annually with the two available leadless pacemakers produced by St. Jude Medical and Medtronic. [12–14]

Despite these advances in battery powered implantable devices, several key issues are associated with their implementation. Further miniaturisation of such devices is limited by the size of the battery. These batteries require casings, membranes and seals to isolate the toxic components from the human body and from each electrode to avoid short circuiting. [15–17] The pacemaker requires eventual replacement due to the limited lifetime of the battery. This requires further surgery and its accompanying risks. Power generation through fuel cells offer an alternative to battery-based power. In theory, a fuel cell which operates using substrates present in the body would allow for continuous power generation throughout the lifetime of an implanted device. Fuel cells which operate through the oxidation of glucose and the reduction of molecular oxygen would accomplish this as both glucose and oxygen are present *in-vivo*. Traditional metal-based fuel cells based on catalytic surfaces such as platinum are unattractive

due to their lack of specificity, propensity for surface fouling and inability to operate under physiological conditions. [18,19] Enzymatic fuel cells (EFCs) offer a promising route towards powering implantable or semi-implantable devices. The EFC works through immobilisation of a glucose-oxidising enzyme at the anode and an oxygen-reducing enzyme at the cathode. The advantages over traditional metal-based fuel cells include specificity of the electrode reaction due to the inherent nature of the enzymatic active site and capacity to operate under physiological conditions. This allows for further miniaturisation, as the membrane associated with batteries and metal-based fuel cells is redundant if sufficient specificity of the enzymes at each electrode is obtained. [8,20] Despite the advantages of implementing EFCs as power sources in implantable and semi-implantable devices certain obstacles need to be addressed. Research is required to improve current density at each electrode to improve overall power density, to improve the operational lifetime through stability in current output and to mitigate the foreign body response to which all implanted or semi implanted devices are subject.

This thesis presents steps towards improved understanding and performance of glucose oxidising electrodes for the development of enzymatic fuel cells and biosensing devices. These steps are presented as chapters, with three of the chapters (3,4 and 5) published as research articles, with me as first author. Chapter 2 focuses on the electropolymerisation of L-Dopa as an immobilisation strategy for preparation of glucose oxidising enzyme electrodes. This is followed by chapter 3 which details a design-of-experiments approach towards optimisation of surface component amounts to provide a glucose oxidising enzyme electrode of high current density for fuel cell application operating under pseudo-physiological conditions. Chapter 4 investigates the effect of individual components present in human plasma on glucose oxidising enzyme electrode performance in an attempt to understand why current density output decreases when EFC operate in complex solutions such as human plasma or blood. This is followed by chapter 5 which focuses on improving the operational stability of glucose oxidising enzyme electrodes through the application of Nafion over-coating to mitigate the effect of some plasma components on the enzyme electrode performance.

This introductory chapter is aimed at providing a general overview of the literature relating to experimental and theoretical aspects not covered in detail in chapters 2-5 of the thesis.

1.1 Fuel Cells

Fuel cell technology is based around two central processes, the oxidation of fuel at the anode and the reduction of an oxidant at a cathode. These electrochemical processes when coupled

together result in the flow of electrons to produce electricity. Pioneering experiments performed by Sir Humphry Davy which were reported on in 1807 led to Sir William Grove reporting the first fuel cell in 1842. [21,22] The power generated in a fuel cell (P_c) is the product of the potential difference in the cell (V_c) and the current produced (I_c) (equation 1.1). The power is measured in Watts, with the potential and current measured in Volts and Amperes, respectively.

$$P_c = V_c \times I_c \quad \text{Equation 1.1}$$

The standard cell voltage as determined by the difference in standard reduction potentials of the cathode and anode undergoes irreversible losses under the current load and results in the operational voltage of the cell differing from the theoretical standard cell voltage (equation 1.2). These irreversible losses are called the overpotential (η) and occur due to mass transport limitation, kinetic losses due to the electrochemical reaction and losses due to resistance against electronic and ionic conduction. [23,24]

$$V_c = (E^o_c - E^o_a) - \eta \quad \text{Equation 1.2}$$

Fuel cells and batteries operate by harnessing the energy in chemical bonds and converting it to electricity. Batteries differ in that they contain a finite internal supply of chemical energy and are defined as closed thermodynamic systems. Fuel cells convert chemical energy from an external source and are open thermodynamic systems. [23] This suggests that a fuel cell can operate continuously as long as it is supplied with fuel and oxidant whereas this is not the case with batteries.

A well-known example of a fuel cell is the proton exchange membrane fuel cell (PEMFC) which oxidises hydrogen at the anode and reduces oxygen at the cathode. Fig. 1 depicts an operational PEMFC with the flow of electrons and transfer of ions across the membrane. Molecular hydrogen is oxidised at the anode by a catalyst, producing protons and electrons. This is usually achieved through use of a metal catalyst such as platinum. The protons cross the proton exchange membrane while the electrons flow through the external circuit to the cathode. Molecular oxygen is reduced to form water at the cathode, again by use of a catalyst such as platinum. [25] The standard cell voltage for a hydrogen/oxygen fuel cell is 1.23 V. [26]

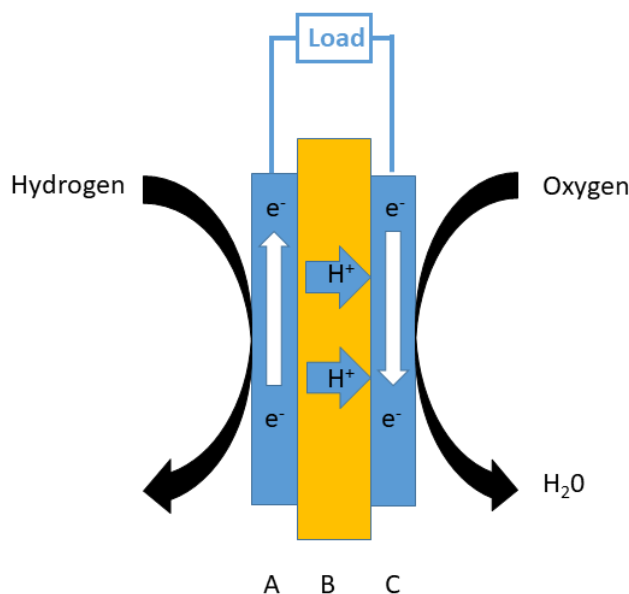


Figure 1: Schematic showing a working PEMFC with anode (A), proton exchange membrane (PEM) (B) and cathode (C). Hydrogen is oxidised at the anode with oxygen reduced at the cathode, creating a flow of electrons with hydrogen ions passing through the PEM.

While platinum is an excellent catalyst, there are disadvantages associated with its use. Platinum is a non-specific catalyst meaning that in the setup described it is capable of catalysis of both oxidation and reduction processes. The surface of the platinum electrode can easily be fouled or passivated, making the fuel cell less effective over time. The lack of specificity means that a membrane is required to isolate anolyte from catholyte to avoid short circuiting the fuel cell. Furthermore, platinum is expensive and is not a very effective catalyst under mild conditions such as those present in the human body (pH 7.4, 37 °C). All of the disadvantages associated with platinum-based fuel cells suggest that advancements in fuel cell research require more specific catalysts that are active under physiological conditions.

1.1.1 Biofuel cells

Biofuel cells (BFCs) are based on use of a biological catalyst (microorganisms or enzymes) at an electrode or in the electrolyte to convert chemical energy to electricity. [27] BFCs operate in an identical manner to metal-based fuel cells with oxidation of a fuel at the anode and reduction of an oxidant at the cathode. Microbial fuel cells use microbial colonies present at an anode to oxidise the fuel present and can be coupled to either an enzymatic, metal based or bacterial cathode. The MFC is usually compartmentalised to separate the anode from the

cathode. [28] Enzymatic fuel cells operate by isolating redox enzymes capable of either oxidation or reduction from organisms and immobilising them at the appropriate electrode surface. [29] As the research carried out in this thesis is on enzymatic biosensors/fuel cells, the area of MFCs will only be briefly discussed.

1.1.1.1 Microbial fuel cells

Microbial fuel cells operate by usually using microorganisms at an anode to oxidise organic substrates. This allows for the generation of electricity from previously unused fuel sources such as wastewater. The prospect of power generation from wastewater has resulted in MFC technology receiving considerable interest. MFCs are well established in scientific literature with their first appearance over 100 years ago. They were first reported by Potter and his research group in 1912,[30] using a fuel cell that generated electricity from the fermentation of microbes in glucose solution. A typical MFC is made up of an anode connected through an external circuit to a cathode. The anode and cathode are separated by a membrane to allow for transfer of ions. Oxidation of the substrate (wastewater for example) at the anode produces protons and electrons. The protons cross through the membrane to reach the catholyte while electrons are forced through the external circuit to the cathode. Oxygen interacts with the hydrogen ions and electrons to form water at the cathode, similar to the PEMFC. Most MFCs operate using a metal catalyst to reduce oxygen to water. [31] Fig. 2 below shows a simple schematic illustrating a typical MFC setup.

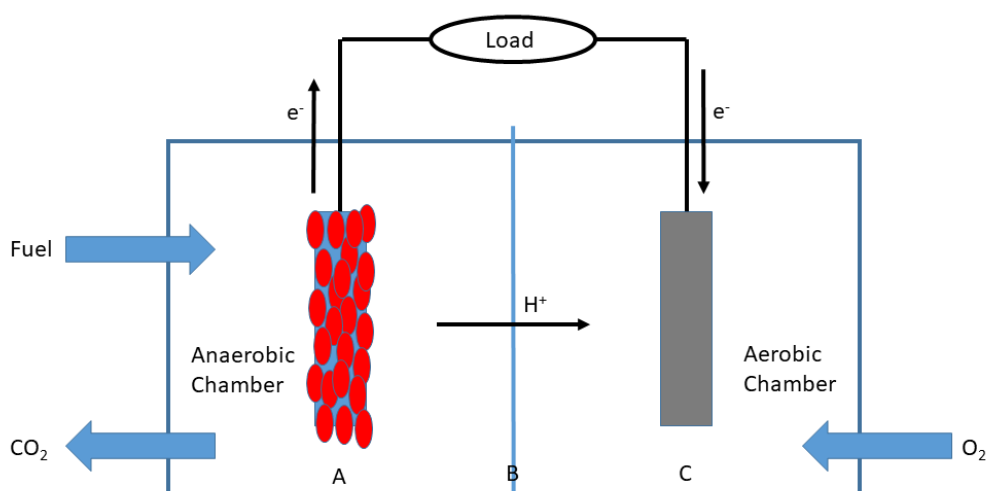


Figure 2: Schematic showing a simple microbial fuel cell setup with anode (A), proton exchange membrane (PEM) (B) and cathode (C) where red-filled ovals depict presence of bacterial cells on the anode.

1.1.1.2 Enzymatic fuel cells

EFCs work in a similar manner to traditional metal-based fuel cells and MFCs but the catalytic processes at one, or each, electrode are performed by enzymes immobilised at the electrode surface. The pioneering work by Yahiro *et al.* in 1960 [32] was the first example of a fuel cell operating using glucose and oxygen where one of the half reactions was catalysed by an enzyme. Typically, the enzymes utilised in a fuel cell are isolated from native organisms such as fungi and immobilised at an electrode. Enzymes which oxidise a fuel such as glucose are used as anodic enzymes while enzymes capable of reducing an oxidant such as oxygen are used as cathodic enzymes. This particular EFC setup is the most commonly reported in the literature as both glucose and oxygen are present in the body making it an attractive route towards powering medical devices. [33–35] Fig. 3 below shows a schematic highlighting a typical enzymatic glucose/oxygen fuel cell setup. As this thesis focuses solely on glucose oxidation using enzymes for application in fuel cells and biosensors, other classes of redox enzymes will not be discussed.

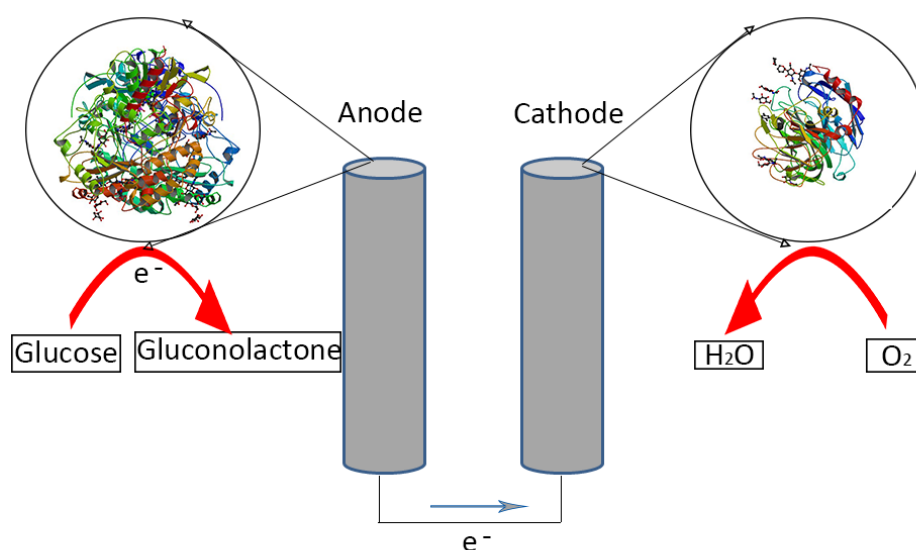


Figure 3: Schematic showing a typical setup for a glucose/oxygen fuel cell. A glucose oxidising enzyme is immobilised at the anode with an oxygen reducing enzyme at the cathode. Electrons flow from the anode to the cathode with hydrogen ions migrating through the electrolyte to the cathode.

While it is an interesting challenge to create power from substrates present *in-vivo* there are numerous limitations associated with deployment of EFCs. The two main drawbacks associated with enzyme electrodes are low power densities and poor operational stability. These are significant hurdles to overcome prior to EFCs becoming a legitimate alternative to battery powered implantable or semi-implantable devices. Enzyme electrodes must produce

sufficient current density and maintain operational stability under physiological conditions (5 mM glucose, 150 mM NaCl, pH 7.4, 37 °C for electrodes operating in human blood). Current battery technology allows for implantation and continuous operation of a lithium-based cell for 5-10 years. [36] The latest trends in implantable battery technology is in the area of energy harvesting through mechanical, physical or electrical routes. [37,38] When considering timescales for continuous operation by EFCs, hours are used instead of years. More recently, work carried out by El Ichi-Ribault *et al.* demonstrated operation of an enzymatic fuel cell implanted in a rabbit for 2 months, although this was not used continuously. [39] It is difficult to forecast if EFCs will ever be capable of overtaking batteries as power sources for implantable devices due to their limitations. However, EFCs used to power short term devices that can be replaced are more viable applications of the technology. Printing of EFCs on readily disposable patches, paper or cartridges to power devices is a way of minimising the two biggest drawbacks of EFCs; low power density and poor operational stability.

1.3 Enzyme catalysts

Traditional metal-based catalysts for the oxidation of glucose and reduction of oxygen, such as platinum, have numerous drawbacks. While a platinum electrode is excellent at catalysing these reactions, the surface is non-specific, can be easily poisoned and operates most efficiently under harsh conditions. Enzyme catalysts can be specific, requiring therefore no membrane to separate fuel from oxidant, and can operate under physiological conditions. [33,40,41] In addition to these advantages, enzymes electrodes can be based on enzymes immobilised at catalytically less active, carbon-based, electrodes: these are cheaper than platinum-based electrodes and avoid crossover reactions occurring that can short-circuit a membraneless fuel cell. For these reasons, there has been extensive research on improving the performance of enzyme electrodes for application to fuel cells. [20,42,43] A promising route towards providing sufficient power output and operational lifetime of EFCs involves the genetic engineering of enzymes prior to immobilisation at an electrode surface. This can be done to widen the substrate specificity to incorporate more fuels or to enhance the catalytic efficiency of an enzyme. [44–46] As the primary aim of this research is to optimise the performance of glucose oxidising enzyme electrodes, the following sections will introduce each of the glucose oxidising enzymes used throughout the thesis.

1.3.1 Glucose oxidase

Glucose oxidase (GOx) is a glucose oxidising enzyme with a molecular weight of 160 kDa. It is a dimeric glycoprotein consisting of two subunits each weighing 80 kDa, see Fig. 4. Flavin adenine dinucleotide (FAD) in the active site is buried approximately 1.5 nm inside the protein shell and acts as the initial electron acceptor. Upon oxidation of glucose to produce gluconolactone, the FAD is reduced to FADH₂ which is in turn oxidised by the final electron acceptor, molecular oxygen, back to FAD. [33,35,41] The reduction and oxidation of FAD is presented in the equations 1.3 and 1.4 below.

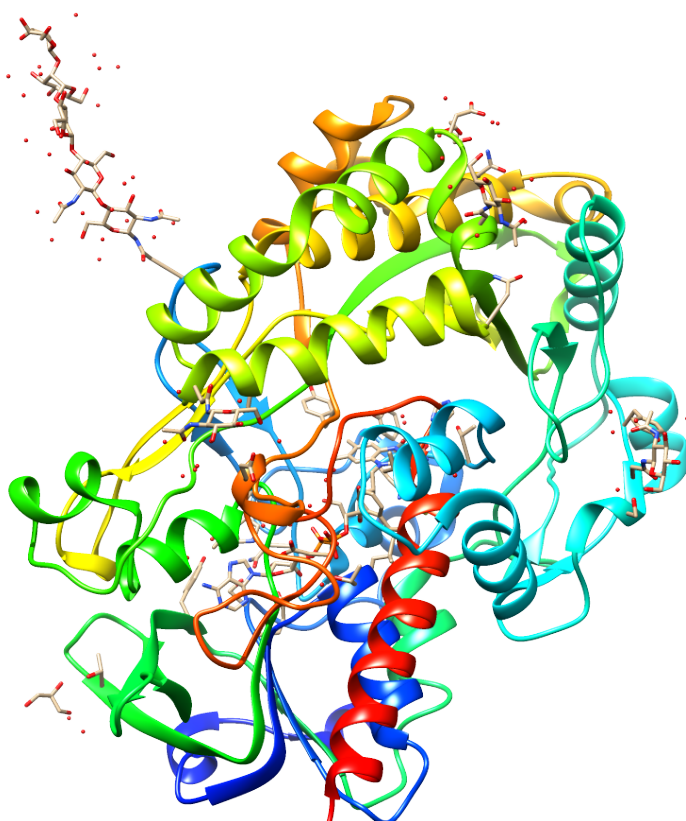
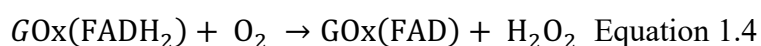
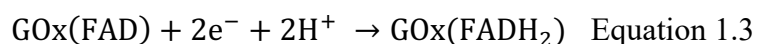


Figure 4: Crystal structure of the *Aspergillus niger* glucose oxidase. (PDB ID: 3QVP, Kommoju *et al.*) [47] This image was generated using the UCSF Chimera package.



Molecular oxygen acts as the natural co-substrate and final electron acceptor for the enzyme. Glucose oxidase cannot undergo direct electron transfer to donate electrons to a solid electrode,

despite multiple publications stating this to be the case. [48] In order to facilitate electron transfer between active site and electrode, a redox mediator is thus required. Redox mediators can compete with oxygen to accept electrons from the enzyme active site for wiring of the enzyme active site to the electrode surface. This mediated electron transfer occurs at lower overpotentials when compared to oxidation of the enzyme co-product peroxide or reduction of enzyme co-substrate oxygen (eqn 1.4). However, coupling of a GOx-based anode with an oxygen reducing cathode in a membraneless fuel cell then creates significant issues. The oxygen required in solution for the cathode to function competes with the redox mediator as an electron acceptor. This parasitic effect results in lower current produced at the anode. The second issue is the production of hydrogen peroxide as co-product when oxygen acts as the final electron acceptor. Peroxide affects the performance of enzyme electrodes as it is damaging to these biological macromolecules. [49] For these reasons, replacement of GOx as glucose oxidising enzyme with an oxygen insensitive enzyme, such as a dehydrogenase is desirable. However, due to GOx being commercially available, relatively stable and substrate specific it is a useful benchmark to evaluate the performance of alternate enzyme electrodes. [35,50]

Historically GOx-based enzyme electrodes for sensing of glucose focused on the oxidation of hydrogen peroxide at an electrode surface to monitor blood glucose levels. These sensors operated at high potentials (0.6 V vs. Ag/AgCl) and suffered from interference through direct oxidation of compounds such as uric acid and ascorbic acid present in blood. [51,52] The introduction of redox mediators to shuttle electrons from active site to the electrode surface allowed for glucose sensors to operate at lower potentials, which limited the effect of interfering compounds. The first demonstration of mediated electron transfer using GOx was by Cass *et al.* who used ferrocene-based compounds as mediators. GOx was co-immobilised on a pyrolytic graphite electrode alongside ferrocene to produce a glucose sensor which operated at 0.35 V vs. Ag/AgCl. [53] More recently Meredith *et al.* reported GOx crosslinked with ferrocene modified linear poly(ethyleneimine) polymer on electrodes produces 2 mA cm⁻² in the presence of 100 mM glucose at 0.13 V vs. Ag/AgCl in PBS. [54] Despite improvements to ferrocene mediated GOx enzyme electrodes, issues remain with the use of ferrocene derivatives such as the fact that ferrocene in its oxidised form ferricenium is unstable in aqueous solution and that ferrocene derivatives are not readily soluble leading to complications with electrode assembly. [55] This resulted in the introduction of a range of alternative metal-based mediator replacements to overcome the limitations of ferrocene and its derivatives. For example Zakeeruddin *et al.* synthesised a range of tris-(4,4'-substituted-2,2'-bipyridine)

complexes of iron(II), ruthenium(II) and osmium(II) mediator compounds for application as mediators in GOx-based enzyme electrodes. [56] These mediator systems will be discussed further in section 1.4.1.

1.3.2 Dehydrogenases

Dehydrogenases such as glucose dehydrogenase (GDH) and cellobiose dehydrogenase (CDH) are oxidoreductase enzymes capable of oxidising glucose and transferring the electrons to co-factors such as flavin adenine dinucleotide (FAD), nicotinamide adenine dinucleotide (NAD) or pyrrolo-quinoline quinone (PQQ). [57–59] Biosensing and fuel cell devices utilising dehydrogenases have become more widespread in recent years as the enzymes do not donate electrons to oxygen as co-substrate and therefore do not produce hydrogen peroxide as co-product. An FAD-dependent glucose dehydrogenase (FADGDH) was first isolated in 1951 from *Aspergillus oryzae*. [60] Dehydrogenases remained mostly unexplored until their application as biocatalysts for glucose oxidation and since then have received increased attention. [61–63] Yoshida *et al.* reported on the structure of fungus-derived FADGDH, see Fig. 5. The 3-D structure consists of two major domains; a C-terminal domain and an FAD-binding domain and it was found to be structurally similar to fungal GOx (Fig. 5). [64] Amino acid residues believed to associate with molecular oxygen in GOx are not conserved while differences in the binding cavity may account for the substrate recognition differences observed between the two enzymes. The FAD domain is bound within the enzyme and undergoes a two proton, two electron redox reaction. The flavin has a reported redox potential of -0.23 V versus a standard hydrogen electrode (SHE) at pH 7. [65]

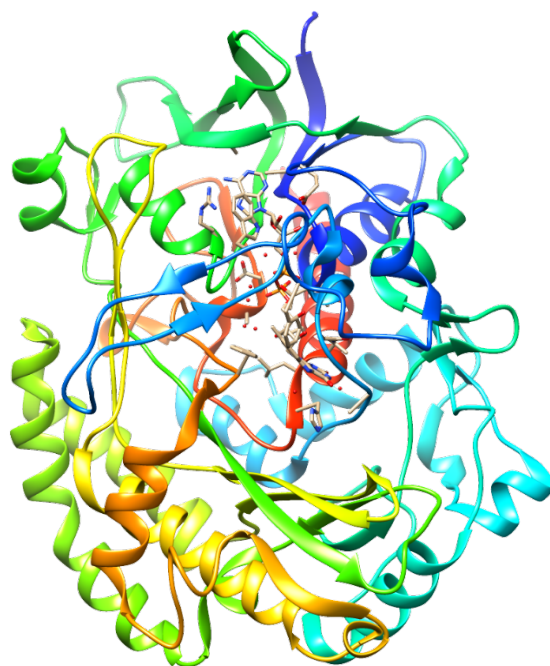


Figure 5: Crystal structure of the Crystal structure of the *Aspergillus* sp. flavin adenine dinucleotide dependent glucose dehydrogenase. (PDB ID: 4YNT, Yoshida *et al.*) [64] This image was generated using the UCSF Chimera package.

Cellobiose dehydrogenase is a monomeric protein with a heme b-containing cytochrome domain connected to a flavin-containing dehydrogenase domain. [66] The study of CDH enzymes for application as enzyme electrodes has focused on electrodes that operate through direct electron transfer from the cytochrome domain. A variant of the CDH enzyme has been applied in direct electron transfer electrode assemblies for lactose detection. [67] The cellobiose dehydrogenase used in Chapter 4 was from the *Corynascus thermophilus* species (*CtCDH*) for comparison with other glucose oxidising enzymes, as it has better selectivity for glucose compared to CDHs used for lactose detection. To facilitate comparison with other mediated glucose oxidising electrodes the flavodehydrogenase domain of the *CtCDH* was heterologously expressed using *Pichia pastoris*, a methylotrophic yeast, and purified prior to use. This resulted in a protein of only 60 kDa, compared to 85 kDa for the original, untruncated enzyme, and it is this recombinant enzyme, *rCtCDH* that is reported on in Chapter 4 of this thesis. [68,69]

In summary three glucose oxidising enzymes were used for comparison in this research; GOX, FADGDH and *rCtCDH*.

1.4 Electron transfer from enzyme to electrode

One of the major concerns for selection of enzyme catalyst in biosensing and biopower applications is efficient electron transfer between active site and electrode surface. There are two routes through which electrons can transfer from active site to the electrode. These are direct electron transfer (DET) and mediated electron transfer (MET) (Fig. 6). [55,70] In DET systems, electrons transfer directly from the enzymatic active site to the electrode surface. In order for this to occur the enzyme active site must be within suitable distance of the electrode surface with fast electron transfer restricted to distances less than 0.8 nm. [48] As an example, using cytochrome c and a zinc substituted cytochrome c as a model system, the rate of electron transfer decreased by approx. 10^4 when the distance was increased to 1.7 nm from 0.8 nm. [71,72] This puts a limit on the amount of enzyme that can be wired directly to the electrode surface and the type of enzyme to be wired, as not all enzymes can undergo DET. An important consideration for DET systems is the orientation of the enzyme on the electrode surface. Stochastic positioning of enzymes at an electrode surface leads to inefficient direct wiring. Therefore, orientation strategies based on chemical bonding and surface treatments are required. [73] This complicates enzyme electrode assembly and can often be difficult to achieve while currents produced are low when compared to MET based enzyme electrodes. [74]

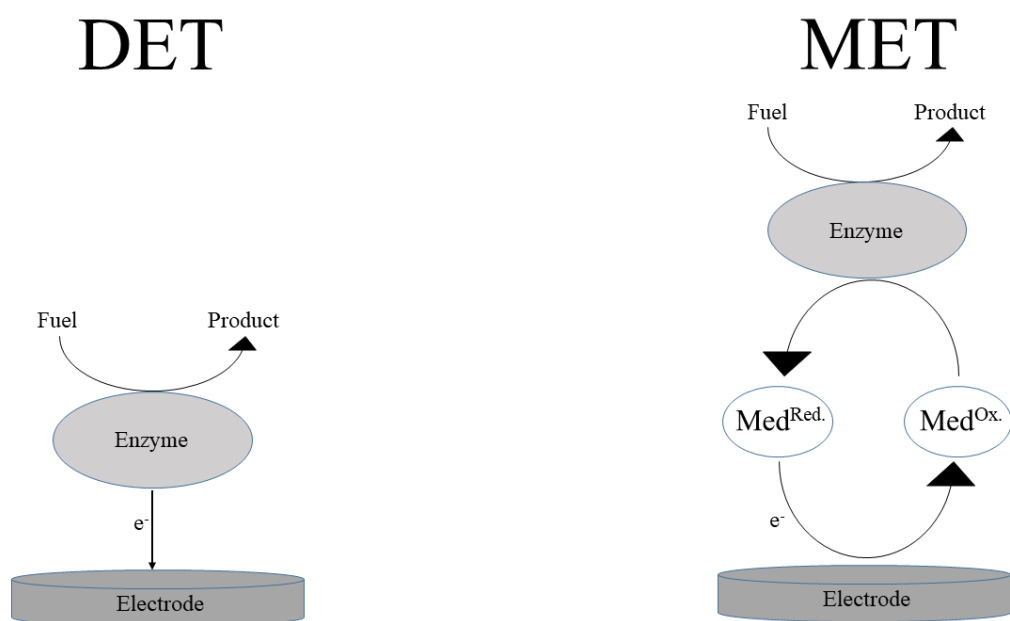


Figure 6: Simplified schematic highlighting the major differences between direct electron transfer (DET) and mediated electron transfer (MET).

For example, GOx has a bulky shell surrounding its FAD active site, which acts as the catalyst in a ping-pong mechanism, making DET with GOx impossible. [75] Artificial mediators are capable of communicating with the redox-active centre of the enzyme and efficiently shuttling electrons from the enzyme to the electrode, instead of the oxygen electron acceptor. The re-oxidation of the mediator occurs at potentials lower than the peroxide product of oxygen reduction. [76] Electrode assembly can be more straightforward when including the mediator due to wiring of the active site to the electrode surface such that that proximity and orientation of the enzyme is not as important as it is to achieve DET. Redox mediators are capable of shuttling electrons across a multi-layer film of enzymes allowing for greater amounts of enzyme to be connected to the electrode surface compared to monolayers of enzyme for DET. In order for effective electron transfer to occur between the active site and the artificial mediator, an appropriate redox potential for the mediator is required to make the transfer thermodynamically favourable. [41,55,77] For fuel cell application, an appropriate redox potential is required to compromise between sufficient current generation and the cell voltage. The rate at which electron transfer occurs between enzyme and mediator can be described by Marcus theory where the rate varies exponentially with reaction free energy until it becomes limited by mass transport. [78] Furthermore, in order for the mediator to operate over long timeframes, it needs to be stable in both oxidised and reduced states. This is to allow for continuous regeneration of the oxidised form of the mediator for shuttling of electrons from enzyme to active site. Osmium-based polypyridyl redox complexes and polymers are attractive candidates as mediators due to their stability in oxidised and reduced forms, tunable redox potential, ease of co-immobilisation and ability to operate at low potentials. [79–82] The tunable nature of the osmium redox potential allows for inclusion of osmium mediators in both anodic and cathodic processes. [77,83] Osmium based polypyridyl redox centres have been connected to polymer backbones for a range of sensing and fuel cell applications. [84] The structure of one of the most widely used redox polymers, $[\text{Os}(2,2'\text{-bipyridine})_2(\text{polyvinylimidazole})_{10}\text{Cl}]^+$ ($\text{Os}(\text{bpy})\text{PVI}$), is presented in Fig. 7.

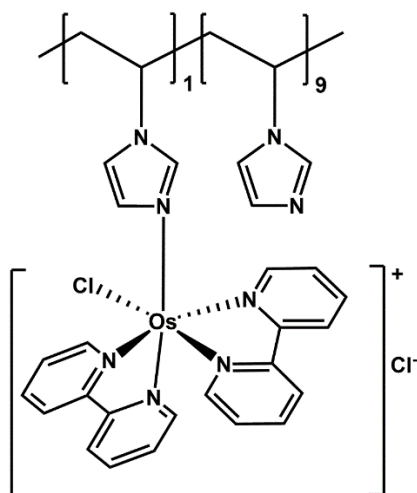


Figure 7: Structure of the redox polymer [Os(2,2'-bipyridine)₂(poly-vinylimidazole)₁₀Cl]⁺ (Os(bpy)PVI).

1.4.1 Osmium based redox mediators

From the initial development of mediated glucose oxidising electrodes by Cass *et al.* to the development of tris substituted polypyridyl osmium, ruthenium and iron complexes by Zakeeruddin *et al.*, there has been much interest in the area of mediator development for glucose oxidising electrodes. [53,56] Osmium based mediators are advantageous as they have operate at lower potentials and have faster electron self-exchange rates. [56] The basis of this research is on improving glucose oxidising electrodes using osmium redox complexes (Chapter 2) and redox polymers (Chapters 3, 4 and 5) so alternative mediators will not be discussed. The overall synthetic strategy for Os complexes and polymers can be seen in Fig. 8. The introduction of tetherable Os complexes allows for various crosslinking and preparation strategies for enzyme electrode assembly. [77,85] Enzyme electrodes based on Os-containing redox polymer allow for crosslinking, using a di-epoxide crosslinker, to add structural stability to the film. Crosslinked polymer films allow for entrapment and/or crosslinking of redox active enzymes, adding to the operational stability of the enzyme electrode by avoiding leaching from the surface. [79,86]

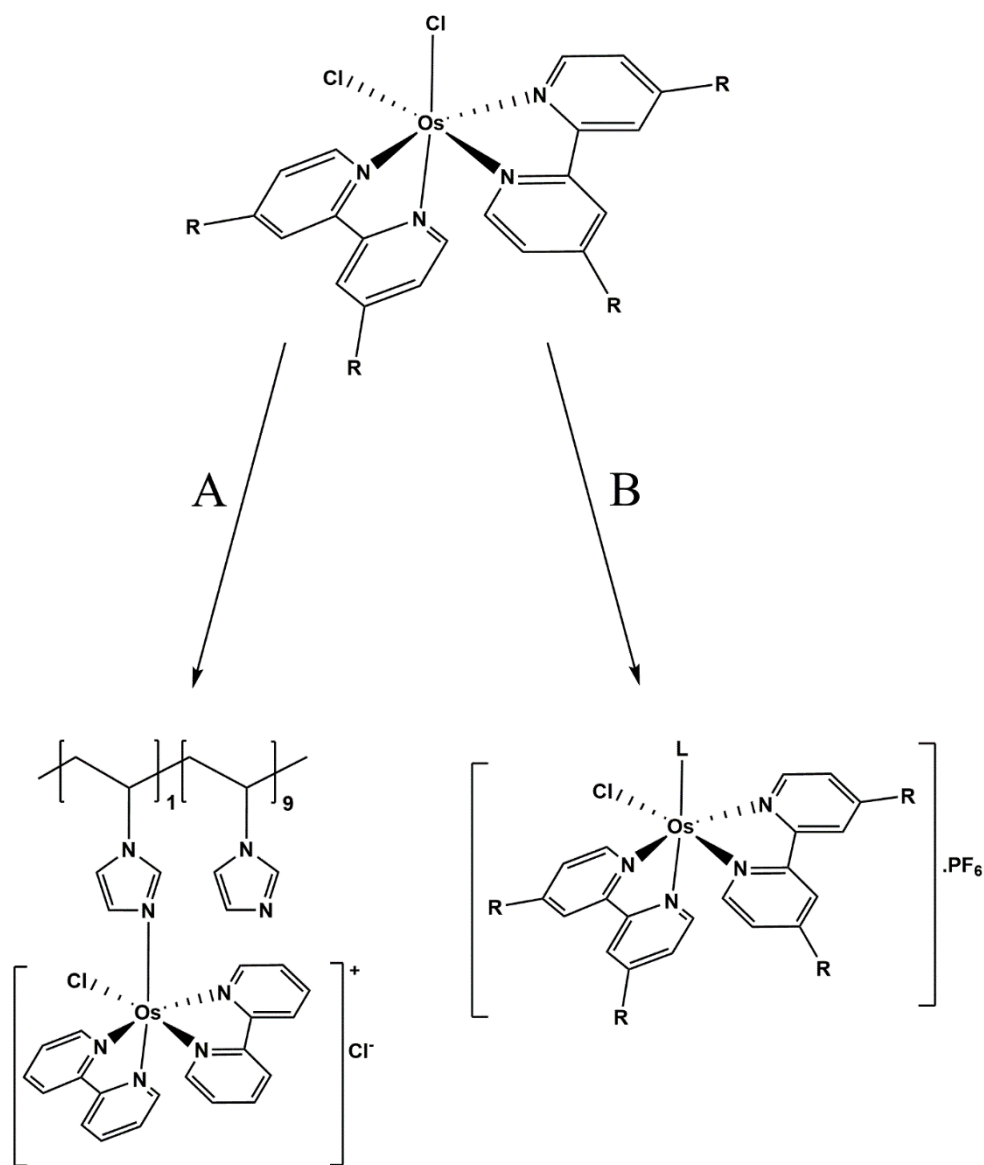


Figure 8: Schematic showing the general structure of the starting complex $[\text{Os}(2,2'\text{-bipyridine})_2\text{Cl}]^+$ with route A showing the synthesis of $[\text{Os}(2,2'\text{-bipyridine})_2(\text{poly-vinylimidazole})_{10}\text{Cl}]^+$ through reaction with a PVI polymer. Route B shows the synthetic strategy for an osmium complex with introduction of a tetherable ligand to the osmium complex of general formula $[\text{Os}(2,2'\text{-bipyridine})_2(\text{L})\text{Cl}]^+$ where $\text{R} = \text{NH}_2, \text{OCH}_3, \text{CH}_3, \text{H}, \text{Cl}$.

Crosslinking of redox polymers with enzymes at the electrode surface is achieved using bifunctional crosslinkers to give a redox hydrogel with reduced leaching of components from the film. Electron transfer through these hydrogels is proposed to happen through self-exchange between oxidised and reduced osmium moieties along the polymer backbone and/or between moieties on adjacent polymer strands. Collisions between oxidised and reduced neighbouring osmium centres tethered to the polymer backbone result in electron exchange (see Fig. 9). [87]

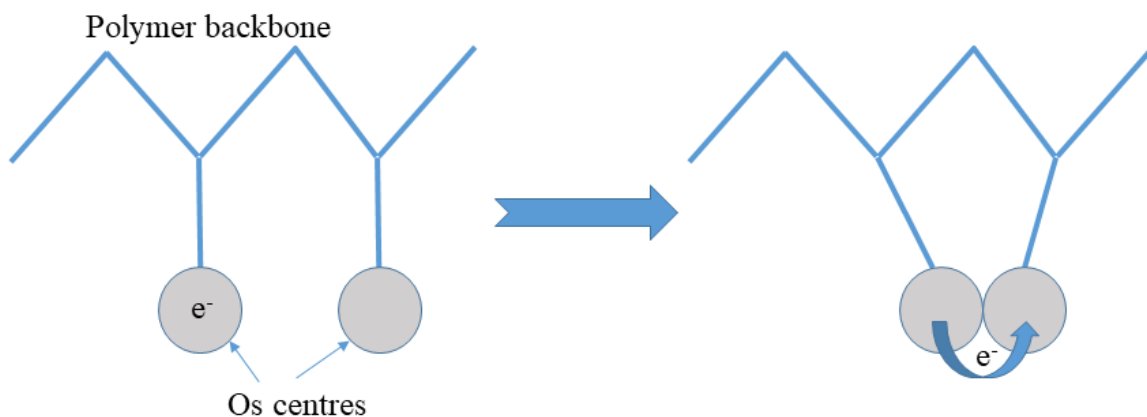


Figure 9: Simplified schematic showing collisions between neighbouring osmium centres resulting in electron transfer through redox hydrogels. The exchange occurs when oxidised and reduced centres are within a certain distance of each other. [88,89]

1.5 Immobilisation strategies

Poor operational stability is one of the major challenges associated with the application of enzyme electrodes to continuous use biosensing and biofuel cells. One of the main reasons for poor operational performance is leaching of components from the electrode surface into the bulk solution. There are numerous approaches for the immobilisation of components at the electrode surface such as covalent attachment, physisorption, entrapment and crosslinking all with the aim of enhancing operational stability through minimising leaching. [90]

Considerable progress has been made in the area of electrochemical immobilisation, with electropolymerisation of polymers at electrode surfaces the most well-known approach. Electrode assemblies using conducting polymers such as polypyrrole and non-conducting polymers such as polyphenol have been studied. [91] In Chapter 2 enzyme electrodes were prepared using electropolymerisation of L-Dopa to produce poly(L-Dopa) to entrap components at the surface. The electropolymerisation scheme to convert L-Dopa to poly(L-Dopa) is shown in Fig. 10. The process is similar to work published previously using poly(dopamine) and chemical polymerisation of L-Dopa. [92–94] This was tested as an alternative to existing crosslinking strategies for enzyme electrode preparation such as use of a di-epoxide crosslinker, described in the next section.

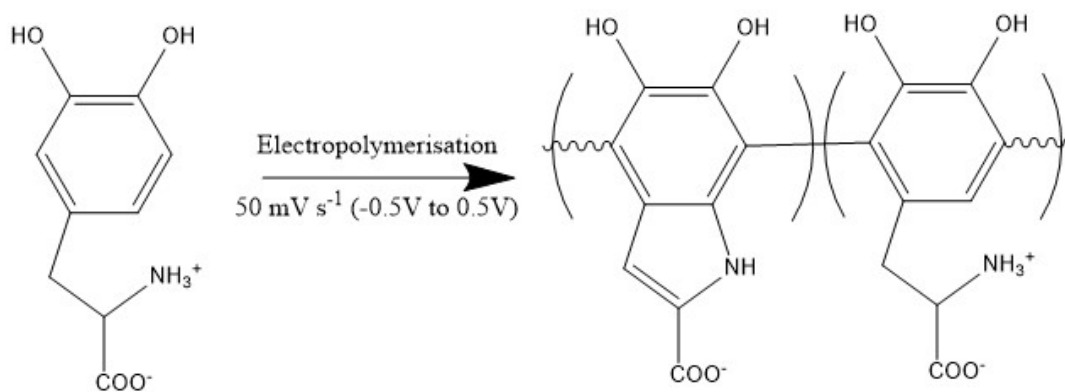


Figure 10: Schematic showing the conversion of L-Dopa to poly(L-Dopa) through electropolymerisation.

Gregg and Heller developed a strategy for entrapment of enzyme and mediator using epoxide-based crosslinkers to assemble three dimensional redox hydrogels. [95] These three dimensional redox hydrogels are hydrophilic in nature and swell when immersed in solution thus improving self-exchange redox conduction and aiding mass transport. [96] Various crosslinking strategies have been developed in order to improve the stability and connectivity of redox films on electrode surfaces. O'Hara *et al.* prepared crosslinked enzyme electrodes consisting of Os(bpy)PVI, GOX and the crosslinker poly(ethylene glycol) diglycidyl ether (PEGDGE) (Fig. 11). [97] De Lumley-Woodyear *et al.* compared PEGDGE as a crosslinker with enzyme electrodes co-immobilised using either glutaraldehyde solution, suberic acid bis(N-hydroxysuccinimide ester) or dimethyl suberimidate. [81] More recently MacAodha *et al.* compared enzyme electrodes prepared using PEGDGE with those prepared using glutaraldehyde vapours for the immobilisation of GOx, redox polymer and MWCNTs. [50,98] PEGDGE was used as a crosslinker in electrode preparation in Chapter 3, 4 and 5.

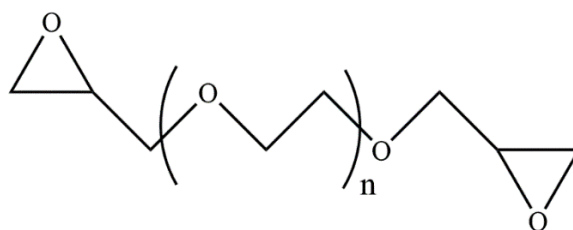


Figure 11: General structure of poly(ethylene glycol) diglycidyl ether (PEGDGE).

1.6 Nanostructured supports in enzyme electrodes

The development of nanostructured supports is an active area of research in materials chemistry. Nanostructures such as gold nanoparticles, graphene sheets, buckypaper and carbon nanotubes (CNTs) have been included in enzyme electrode preparation. [99–103] CNTs were

first developed in 1991 and have been the focus of extensive research for many applications since due to their intrinsic electrical conductivity. The CNT structure is formed through rolled layers of graphene sheets to give tubular structures. Variations of CNTs can be produced depending on how they are synthesised. Multiwalled CNTs (MWCNTs) can be produced when multiple layers of graphene sheets are rolled into tubular structures. [104] The inclusion of MWCNTs in enzyme electrode preparation is of interest as they contribute to higher current densities and operational stabilities due to the increase in surface area of the electrode. [90,103,105] MWCNTs can be treated prior to electrode preparation to functionalise their surface, such as introduction of carboxylate groups to enhance dispersion in aqueous solvent and to aid in crosslinking. [83,90,106,107] Due to the increased current density and operational stability of electrodes prepared with MWCNTs, each chapter presented includes MWCNTs as nanostructured supports in the co-immobilisation process along with enzyme, redox mediator and crosslinker.

1.7 Optimisation strategies

The traditional approach towards improving an experimental process typically involves changing one variable while holding the other variables steady. This means that the variables' effect on the experimental outcome is measured in isolation of the other factors. This methodology is referred to as a one factor at a time (OFAT) approach. Determining the relationship between the output of a process (experimental result) and the factors affecting that process through the selection of factorial experimental designs is a more efficient and thorough route for optimisation of an experimental process (Fig. 12). [108,109] A design of experiments (DoE) approach is one particular route towards optimisation of an experimental process providing structure to experimental procedures. Once the experimental design phase has been completed, relationships between experimental outcomes and experimental factors can be established. [109,110] DoE has been applied in numerous processes across science and engineering, [111–114] including enzyme electrode preparation.

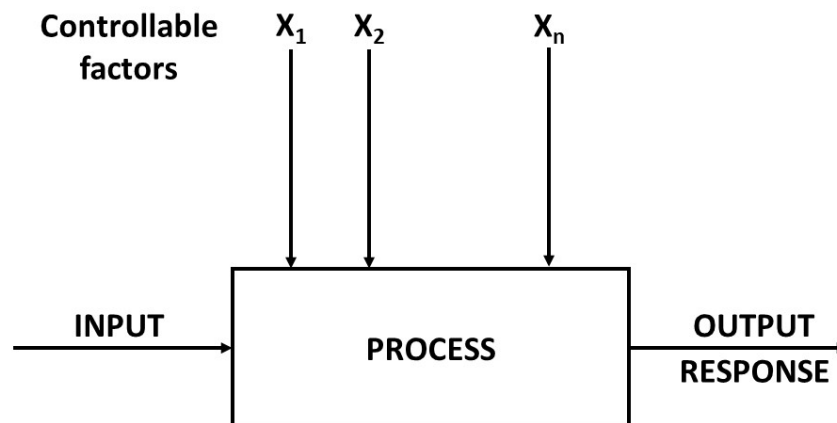


Figure 12: A model of an experimental process with controllable factors and a given output response which can be changed by manipulation of the controllable factors.

For example, Flexer *et al.* described the implementation of the relaxation method and a simplex algorithm to optimise experimental parameters from electrodes consisting of osmium redox polymer and GOx. The results obtained showed excellent correlation between experimental results and simulated results and allowed for optimisation of film thickness and redox mediator concentration. [115] Babanova *et al.* used DoE to improve the performance of an air-breathing bilirubin oxidase-based cathode. The major factors associated with improved performance were identified and an improved cathode was assembled based on DoE results. This cathode produced current densities 2-5 times higher than the previous highest reported current density from a similar cathode. [116] More recently Kumar and Leech described a DoE approach using a Box-Behnken design (BBD) for optimisation of current output of a glucose oxidising electrode based on GOx and an osmium redox complex. BBD is a type of response surface design using a three-level factorial design for each component; low, central and high. These factors can be estimated based on previous experiments using similar electrode assemblies. [109] Glucose oxidation currents were 32% higher than currents optimised through use of OFAT. [117] In Chapter 3 a Box-Behnken design is used for optimisation of current signal for glucose oxidising electrodes based on combination of redox polymer, FADGDH and MWCNTs.

1.8 Permselective membranes

Successful application of enzyme electrodes as implantable or semi-implantable devices face numerous challenges. One of the major challenges is the significant loss of performance due to

desorption from electrode surface and presence of interfering molecules when operated in physiological or pseudo-physiological solutions compared to operation in phosphate buffered saline (PBS). [118–122] Use of Nafion membranes is an attractive option for shielding glucose oxidising enzyme electrodes from physiological solutions as this decreases transport of bulky proteins and anionic compounds through the membrane while allowing glucose to permeate. [86] Nafion ionomers were first developed by DuPont and have been used extensively in sensing applications for their advantageous properties. [123–126] Nafion is an ionomer with a sulfonate group which gives the membrane its anionic nature and DuPont produces membranes of varying thickness suitable for a range of applications as well as Nafion solutions used to cast membranes on electrode assemblies (Fig. 13). [127]

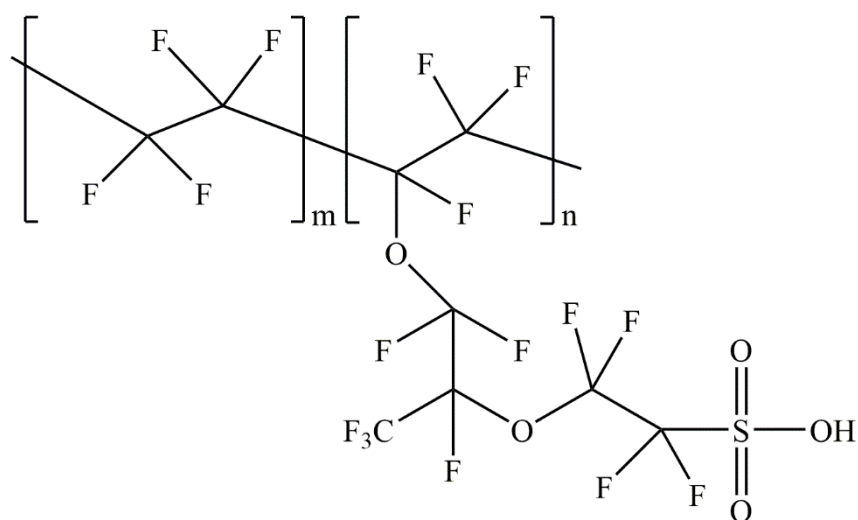


Figure 13: General structure of Nafion.

For example, Harrison *et al.* used Nafion as a membrane to protect enzyme electrodes used as glucose sensors in whole blood from interfering compounds such as ascorbic acid, uric acid and acetaminophen. The Nafion-coated electrodes were superior to cellulose dialysis membrane-coated electrodes and uncoated control electrodes, providing continuous measurement of glucose in blood for 6 days. [128] Bindra and Wilson reported a non-enzymatic glucose sensor using a Nafion membrane for improved selectivity and good limits of detection. [129] Vaidya *et al.* reported on Nafion membranes as a method of excluding interfering substances from enzymatic films at electrodes for glucose sensing and the extension of the linear range due to diffusion limitation of glucose. [130] Chapter 5 focuses on using Nafion membranes to improve operational stability of continuous use glucose oxidising electrodes in complex physiological and pseudo-physiological solutions.

1.9 Enzymatic fuel cells

From the breakthrough work of Yahrio *et al.* in the 1960s, with the report of an enzyme based glucose oxidising anode coupled to an oxygen reducing cathode, there have been significant developments in the field of EFCs up to now. [32] The main limitations to advancing EFC technology further are limited voltage output, low power density, poor operational stability, inability to fully oxidise fuels and biocompatibility issues for implantable and semi-implantable EFCs. [131] Research is being carried out to address each of these limitations crucial to achieving EFC advancements.

One route towards improved voltage output is the use of enzymes capable of DET, thus removing the need for mediators and the voltage losses associated with their use. CDH is an anodic enzyme capable of undergoing DET while laccase is a well-known cathodic enzyme capable of DET. Elouarzaki *et al.* reported on laccase electrode assemblies with DET and MET approaches as well as combined orientation and mediation strategies. [132] Current densities were recorded for mediated electrodes, electrodes using an orientation strategy, and electrodes using a combined orientation and mediation strategy. The highest current density recorded was 2.5 mA cm^{-2} for electrodes using a combined approach of orientation and inclusion of mediator. Tasca *et al.* compared anodic assemblies based on CDH and reported a higher voltage output for EFCs based on DET but with higher current densities recorded in the presence of redox polymer mediator. [133] There is therefore a trade-off between increasing the voltage output and producing higher current densities with the inclusion of mediators.

Current densities produced from enzyme electrodes are significantly lower compared to metal based electrodes of similar surface area resulting in lower power densities when assembled as part of a fuel cell. This is due to the density of active sites being lower as a result of the bulky protein shell surrounding the enzyme active site. [131] There are multiple strategies for increasing the current density of an electrode resulting in increased power densities when assembled in a fuel cell configuration. One method of increasing the current density is to increase the enzyme loading on an electrode through increasing the surface porosity. Deng *et al.* reported a power density of $178 \text{ } \mu\text{W cm}^{-2}$ compared to $12.6 \text{ } \mu\text{W cm}^{-2}$ in 30 mM glucose for a GDH/laccase fuel cell immobilised on highly ordered microporous gold electrodes compared to planar gold electrodes, respectively. [134] This increase in power density was due to increased enzyme loading as a result of the increase in surface porosity.

Most EFC assemblies use a single oxidising enzyme immobilised at the anode to oxidise a fuel. This only partially oxidises the fuel, with further enzymes required to further oxidise and

capture more of the energy available from the fuel. [135] Xu and Minteer demonstrated that complete oxidation of glucose to CO₂ is possible using an multi-enzyme electrode consisting of six enzymes that yields an enzyme cascade. [136] This highlights the potential for further efficiency gains using enzyme cascades in enzyme electrode assemblies.

While advances have been made in miniaturising EFCs and increasing power outputs, operational stability of EFCs remains a major barrier preventing deployment of EFCs. The loss of operational stability is due to numerous factors, with leaching of enzyme from the surface as well as enzyme deactivation some of the main reasons. One method of overcoming this loss of operational stability is the entrapment of enzyme at the surface. For example, Lojou and co-workers investigated recreating the physiological environment of the enzyme as a route towards improved stability. Here, O₂ resistant hydrogenases were inserted into liposomes with increased stability observed for hydrogenase inserted into liposomes compared to the free hydrogenase. [137,138]

1.10 Electroanalytical techniques

Electrochemical characterisation methodologies are the essential techniques required for studying performance of enzyme electrodes. Throughout this thesis various electroanalytical techniques are used to investigate the behaviour of enzyme electrodes. Therefore, a brief description of the techniques used is presented in the following sections.

During electrochemical investigations, a standard three cell electrode is typically used with no membranes present between electrodes. This consists of a working electrode, counter electrode and reference electrode. The working electrode is the electrode at which the redox process of interest occurs and is typically made of graphite, glassy carbon, platinum or gold. All work carried out in this thesis was performed using graphite working electrodes. The counter electrode is used to facilitate electron transfer in the electrolyte so current can be measured at the working electrode. Typical counter electrode materials are titanium or platinum, with a platinum mesh used for all experimental results generated in this thesis. This was used to ensure that the counter electrode was not limiting the current at the working electrode. The reference electrode is used to measure the potential applied at the working electrode. An Ag/AgCl (3M KCl) reference electrode was used throughout this thesis as it is inexpensive, simple to maintain and provides a consistently stable potential. [139–142]

If the working electrode is driven to more positive potentials, electrons will flow from an oxidisable species at the electrode/solution interface to the electrode, resulting in an anodic

process (Equation 1.5) as illustrated by consideration of electron energy levels in Fig. 14. Alternatively, if the working electrode is driven to more negative potentials, electrons will flow from the electrode to a reducible species at the electrode/solution interface, resulting in a cathodic process (Equation 1.5) (Fig. 14).

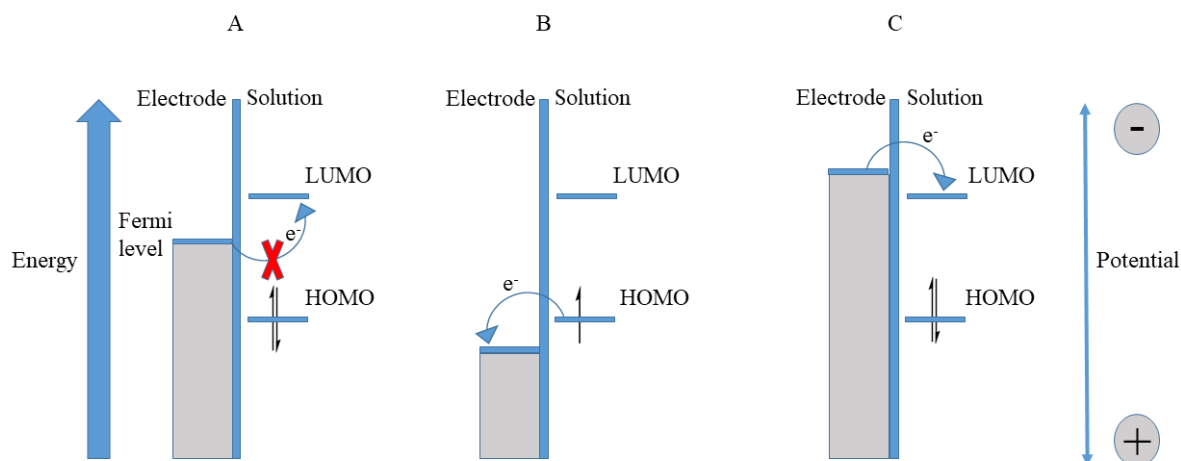


Figure 14: Simplified schematic showing electron transfer at the electrode/solution interface during an electrochemical process. A) This shows an example where no electron transfer is possible as the LUMO of the electrolyte species has a higher energy level than the electrode. B) This shows an example of oxidation of an electrolyte species where the electrode has a lower energy than the HOMO of the electrolyte species. C) This shows an example of reduction of an electrolyte species where the LUMO of the electrolyte species has a lower energy level than the electrode.

1.10.1 Voltammetric and amperometric techniques

One of the major electroanalytical techniques available to an electrochemist for studying redox processes is cyclic voltammetry. The technique works by applying an initial potential to the working electrode followed by the linear ramping of potential to a predetermined switching point where the potential is linearly ramped back across the same potential range at the same rate (Fig. 15). Throughout this process the electrochemical events resulting in current changes as a function of applied potential are recorded. This results in a cyclic voltammogram (CV) which is a plot of applied potential on the x axis with current flow at the working electrode on the y axis (Fig. 16). [141]

When the rate of heterogeneous electron transfer at the electrode surface is fast enough to ensure the concentrations of oxidised and reduced species are in equilibrium the redox reaction is deemed reversible and the Nernst equation is obeyed (Equation 1.6). [142] The key

parameters in a CV are seen in Fig. 16. On driving the electrode potential to positive potentials through the standard redox potential (E°) of a solution-phase redox species an oxidation peak is observed, with peak potential E_{pa} . Switching of the potential to scan in the reverse direction through the E° results in the formation of a reduction peak with peak potential E_{pc} , due to reduction of the previously oxidised species occurring.

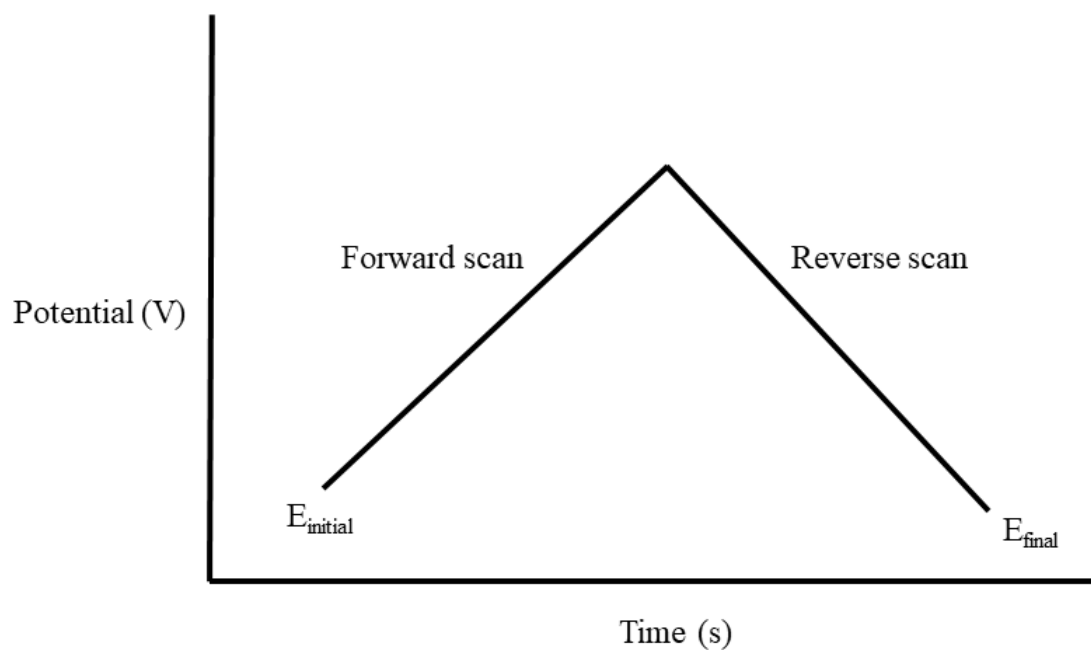


Figure 15: A typical linear waveform for a cyclic voltammogram.

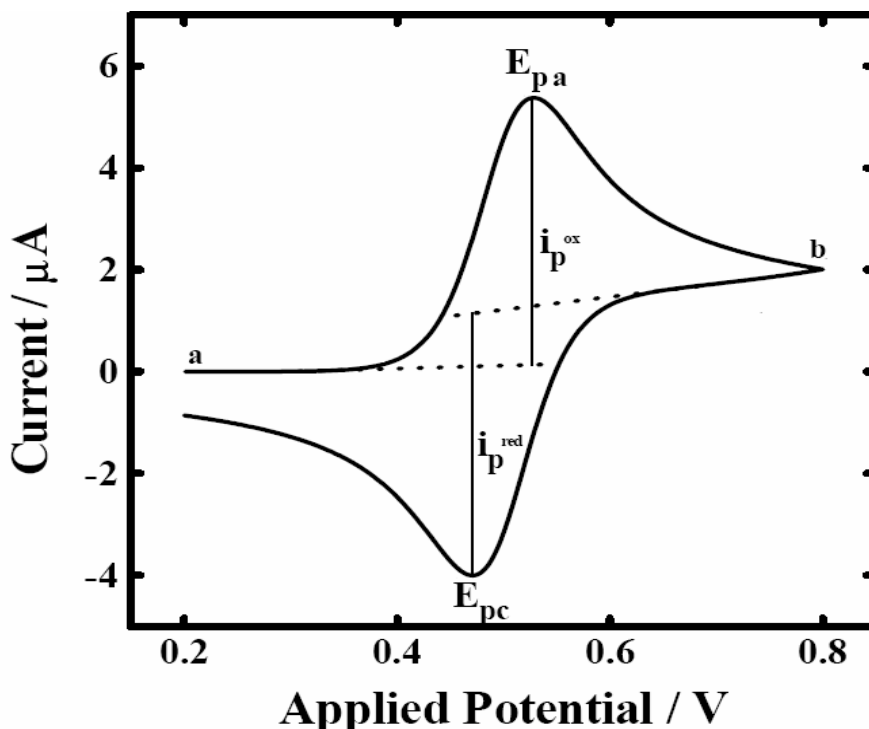


Figure 16: A typical cyclic voltammogram of a reversible solution-phase redox reaction. The initial potential applied is shown (a), the anodic peak potential and current (E_{pa} and i_{pa}), the switching potential (b) and the cathodic peak potential and current (E_{pc} and i_{pc}). [142]

The Nernst equation describes the relationship between the electrode potential (E), the standard electrode potential (E^o), the number of electrons involved in the process (n) and the concentration of the oxidised and reduced species, respectively (Ox), (Red).

$$E = E^o - \frac{0.059}{n} \log \frac{Red}{Ox} \quad \text{Equation 1.6}$$

For an electrochemically reversible process, when the heterogeneous electron transfer is faster than the rate of mass transport the separation of peak current potentials is given by:

$$\Delta E = E_{pa} - E_{pc} = \frac{59}{n} mV \quad \text{Equation 1.7}$$

Peak currents scale proportionally with the square root of scan rate. The peak oxidation or reduction current for an electrochemically reversible reaction is given by the Randles-Sevcik equation (Equation 1.8), where i_p is the peak current for an anodic or cathodic process (in Amps), n is the number of electrons transferring in the process, A is the area of the electrode (cm^2), D is the diffusion coefficient of the oxidised or reduced species ($cm^2 s^{-1}$), C is the concentration of the oxidised or reduced species ($mol cm^{-3}$) and v is the scan rate ($V s^{-1}$).

$$i_p = 0.4463 \cdot n \cdot F \sqrt{\frac{nF}{RT}} \cdot A \cdot D_2^1 \cdot C \cdot v_2^1 \quad \text{Equation 1.8}$$

Electrochemically irreversible or quasi-reversible behaviour occurs when the rate of electron transfer is slow relative to the applied scan rate. The Nernstian equilibrium is not maintained as the electron transfer is the rate determining step and the peak to peak separation is greater than $59/n$ mV. [142] For multilayer modified electrodes such as enzyme electrodes, the Randles-Sevcik equation may be used to model the CV once the scan rate is sufficiently quick to ensure semi-infinite diffusion. From this equation an estimation of the diffusion coefficient for charge transport through enzyme electrode multilayer films can be made.

For CV scans recorded using slow scan rates for monolayer or multilayer electrodes finite diffusion prevails due to extension of a depletion layer into the bulk solution. [142] In cases where finite diffusion prevails an estimation of surface coverage of redox active species confined to the electrode surface (Γ) can be made (Equation 1.9) by measuring the faradaic charge (Q) passed through the film during the electrolysis. This is quantified by measuring the area under the curve for either an anodic peak or cathodic peak on a CV.

$$\Gamma = \frac{Q}{nFA} \quad \text{Equation 1.9}$$

A CV for a surface confined species with an ideal Nernstian system behaviour with no lateral interactions between adjacent redox centres can be described by Equation 1.10 and Equation 1.11 where FWHM is the full width at half maximum of either the anodic or cathodic peak.

$$FWHM = \frac{3.53RT}{nF} = \frac{90.6}{n} mV \quad \text{Equation 1.10}$$

$$E_{pa} = E_{pc} \quad \text{Equation 1.11}$$

Each chapter of this thesis focuses on electron transfer at a modified electrode from an enzyme catalyst to an electrode surface. The process is known as an EC' mechanism and represents catalytic processes at electrodes. Catalysed electrochemical reactions including enzyme catalysed electrochemical processes have received widespread attention as they have numerous advantages including enhanced chemical reactivity and specificity. Typical cyclic

voltammograms for EC' processes show no catalytic current response in the absence of substrate. Catalytic processes show enhanced current response in the presence of increased substrate concentration at the same potential. [142] The transfer of electrons to the electrode which regenerates the enzyme catalyst for further electrocatalysis is discussed in detail in section 1.3. For this thesis the focus is on the electrocatalytic oxidation of glucose by glucose oxidising enzymes at graphite electrodes.

In addition to CV, amperometry is a commonly used technique for electrode characterisation and evaluation of electrode performance. Amperometry is used extensively in this thesis for investigating the performance of enzyme electrodes. The technique works through measurement of an anodic or cathodic current at a working electrode under a fixed applied potential. The current measured at the working electrode is plotted as a function of time. [142]

1.11 Thesis proposition

The aim of this thesis is to investigate routes towards improving glucose oxidising electrode performance for biosensing and biofuel cell applications. These investigations are detailed in the following 4 chapters with a concluding chapter to finish. Each chapter is based on the performance of glucose oxidising enzyme electrodes using novel methodologies or testing procedures and benchmarked against previously published methodologies.

Chapter 2 focuses on using the electropolymerisation of L-Dopa to poly(L-Dopa) as an immobilisation strategy to produce glucose oxidising enzyme electrodes. The poly(L-Dopa) film was used to immobilise enzyme, mediator and MWCNTs at the electrode surface. Chapter 3 addresses the use of a design of experiments approach towards optimisation of surface component amounts and compares the results with previously benchmarked electrodes optimised using a one factor at a time approach. The optimised electrodes showed a greater than 50 % increase in current density at 5 mM glucose levels when compared to previous electrodes optimised using an OFAT approach. Chapter 4 address the decrease in performance of glucose oxidising enzyme electrodes in complex human physiological solutions. Uric acid was successfully identified as the compound present in artificial plasma which resulted in the most significant drop-off in electrode performance for FADGDH electrodes. Chapter 5 aims to mitigate the effects of human physiological solutions on electrode performance by inclusion of Nafion membranes to diminish access of anionic components, such as uric acid, to the enzymatic film. Finally, chapter 6 is a summary of work completed to date during the thesis with suggestions of possible future directions to continue this research. As part of my PhD I have published first author research articles as well as receiving co-authorship on another

paper. A list of my publications, awards, oral and poster presentations to date is included in an appendix.

1.12 References

- [1] P.M. Zoll, Resuscitation of the Heart in Ventricular Standstill by External Electric Stimulation, *N. Engl. J. Med.* 247 (1952) 768–771.
doi:10.1056/NEJM195211132472005.
- [2] J.A. Johnson, FDA Regulation of Medical Devices, *Congr. Res. Serv.* (2016).
<https://fas.org/sgp/crs/misc/R42130.pdf>.
- [3] ISO 13485:2016 - Medical devices -- Quality management systems -- Requirements for regulatory purposes, (n.d.). <https://www.iso.org/standard/59752.html>
- [4] Z. Shlegr, A. Egorov, Implantable electric bladder stimulator used for neurogenic failures, *Biomed. Eng. (NY)*. 7 (1973) 382–383. doi:10.1007/BF00557586.
- [5] B.S. Wilson, M.F. Dorman, Cochlear implants: A remarkable past and a brilliant future, *Hear. Res.* 242 (2008) 3–21. doi:10.1016/j.heares.2008.06.005.
- [6] H. Beck, W.E. Boden, S. Patibandla, D. Kireyev, V. Gutpa, F. Campagna, M.E. Cain, J.E. Marine, 50th Anniversary of the first successful permanent pacemaker implantation in the United States: historical review and future directions., *Am. J. Cardiol.* 106 (2010) 810–8. <http://www.ncbi.nlm.nih.gov/pubmed/21391322>
- [7] O. Aquilina, A brief history of cardiac pacing., *Images Paediatr. Cardiol.* 8 (2006) 17–81. <http://www.ncbi.nlm.nih.gov/pubmed/22368662>
- [8] A. Heller, Miniature biofuel cells, *Phys. Chem. Chem. Phys.* 6 (2004) 209.
doi:10.1039/b313149a.
- [9] C.W. Simmons, Dry-cell battery., (1913).
<https://patents.google.com/patent/US1087612>
- [10] W. Greatbatch, C.F. Holmes, History of implantable devices, *IEEE Eng. Med. Biol. Mag.* 10 (1991) 38–41. doi:10.1109/51.84185.
- [11] O. Fiandra, The first pacemaker implant in America., *Pacing Clin. Electrophysiol.* 11 (1988) 1234–8. <http://www.ncbi.nlm.nih.gov/pubmed/2459678>
- [12] S. Sideris, S. Archontakis, P. Dilaveris, K.A. Gatzoulis, K. Trachanas, I. Sotiropoulos, P. Arsenos, D. Tousoulis, I. Kallikazaros, Leadless Cardiac Pacemakers: Current status of a modern approach in pacing, *Hell. J. Cardiol.* 58 (2017) 403–410.

- doi:10.1016/J.HJC.2017.05.004.
- [13] M.A. Miller, P. Neuzil, S.R. Dukkipati, V.Y. Reddy, Leadless Cardiac Pacemakers, *J. Am. Coll. Cardiol.* 66 (2015) 1179–1189. doi:10.1016/j.jacc.2015.06.1081.
- [14] J. Sperzel, H. Burri, D. Gras, F.V.Y. Tjong, R.E. Knops, G. Hindricks, C. Steinwender, P. Defaye, State of the art of leadless pacing, *Europace.* 17 (2015) 1508–1513. doi:10.1093/europace/euv096.
- [15] V.S. Mallela, V. Iankumaran, N.S. Rao, Trends in cardiac pacemaker batteries., *Indian Pacing Electrophysiol. J.* 4 (2004) 201–12. <http://www.ncbi.nlm.nih.gov/pubmed/16943934>
- [16] P. Ritter, G.Z. Duray, C. Steinwender, K. Soejima, R. Omar, L. Mont, L.V. Boersma, R.E. Knops, L. Chinitz, S. Zhang, C. Narasimhan, J. Hummel, M. Lloyd, T.A. Simmers, A. Voigt, V. Laager, K. Stromberg, M.D. Bonner, T.J. Sheldon, D. Reynolds, Early performance of a miniaturized leadless cardiac pacemaker: the Micra Transcatheter Pacing Study, *Eur. Heart J.* 36 (2015) 2510–2519. doi:10.1093/eurheartj/ehv214.
- [17] Y.-H. Joung, Development of Implantable Medical Devices: From an Engineering Perspective, *Int. Neurourol. J.* 17 (2013) 98. doi:10.5213/inj.2013.17.3.98.
- [18] S.C. Kelley, G.A. Deluga, W.H. Smyrl, A Miniature Methanol/Air Polymer Electrolyte Fuel Cell, *Electrochem. Solid-State Lett.* 3 (1999) 407. doi:10.1149/1.1391161.
- [19] M. Hayase, T. Fujii, J.G. Alves Brito-Neto, A Miniature Fuel Cell with Porous Pt Layer Formed on a Si Substrate, *J. Electrochem. Soc.* 158 (2011) B355. doi:10.1149/1.3545070.
- [20] T. Chen, S.C. Barton, G. Binyamin, Z. Gao, Y. Zhang, H.-H. Kim, A. Heller, A Miniature Biofuel Cell, *J. Am. Chem. Soc.* 123 (2001) 8630–8631. doi:10.1021/ja0163164.
- [21] W.R. Grove, LXXII. *On a gaseous voltaic battery*, London, Edinburgh, Dublin Philos. Mag. J. Sci. 21 (1842) 417–420. doi:10.1080/14786444208621600.
- [22] H. Davy, I. *The bakerian lecture, on some chemical agencies of electricity*, Philos. Mag. 28 (1807) 3–18. doi:10.1080/14786440708563473.

- [23] R.P. O'Hayre, S.-W. Cha, W.G. Colella, F.B. Prinz, *Fuel cell fundamentals*, n.d.
- [24] A.L. Dicks, D.A.J. Rand, *Fuel Cell Systems Explained*, John Wiley & Sons, Ltd, Chichester, UK, 2018. doi:10.1002/9781118706992.
- [25] S. Basu, ed., *Recent Trends in Fuel Cell Science and Technology*, Springer New York, New York, NY, 2007. doi:10.1007/978-0-387-68815-2.
- [26] P. Atkins, J. De Paula, *Elements of physical chemistry*, Oxford University Press, USA, 2013.
- [27] E. Katz, Biofuel Cells with Switchable Power Output, *Electroanalysis*. 22 (2010) 744–756. doi:10.1002/elan.200904648.
- [28] Z. Du, H. Li, T.G.-B. advances, undefined 2007, A state of the art review on microbial fuel cells: a promising technology for wastewater treatment and bioenergy, Elsevier. (n.d.).
- [29] R.A.S. Luz, A.R. Pereira, R.M. Iost, F.N. Crespilho, Biofuel Cells, in: *Nanoenergy*, Springer International Publishing, Cham, 2018: pp. 161–190. doi:10.1007/978-3-319-62800-4_5.
- [30] M.C. Potter, Electrical Effects Accompanying the Decomposition of Organic Compounds, *Proc. R. Soc. B Biol. Sci.* 84 (1911) 260–276. doi:10.1098/rspb.1911.0073.
- [31] B.E. Logan, *Microbial fuel cells*, Wiley-Interscience, 2008.
- [32] A.T. Yahiro, S.M. Lee, D.O. Kimble, Bioelectrochemistry: I. Enzyme utilizing bio-fuel cell studies, *Biochim. Biophys. Acta - Spec. Sect. Biophys. Subj.* 88 (1964) 375–383. doi:10.1016/0926-6577(64)90192-5.
- [33] M. Rasmussen, S. Abdellaoui, S.D. Minter, Enzymatic biofuel cells: 30 years of critical advancements, *Biosens. Bioelectron.* 76 (2016) 91–102. doi:10.1016/J.BIOS.2015.06.029.
- [34] S.D. Minter, B.Y. Liaw, M.J. Cooney, Enzyme-based biofuel cells, *Curr. Opin. Biotechnol.* 18 (2007) 228–234. doi:10.1016/J.COPBIO.2007.03.007.
- [35] D. Leech, P. Kavanagh, W. Schuhmann, Enzymatic fuel cells: Recent progress, *Electrochim. Acta.* 84 (2012) 223–234. doi:10.1016/j.electacta.2012.02.087.

- [36] A. Ben Amar, A.B. Kouki, H. Cao, Power Approaches for Implantable Medical Devices., *Sensors (Basel)*. 15 (2015) 28889–914. doi:10.3390/s151128889.
- [37] Y.-H. Joung, Development of Implantable Medical Devices: From an Engineering Perspective, *Int. Neurourol. J.* 17 (2013) 98. doi:10.5213/inj.2013.17.3.98.
- [38] D.C. Bock, A.C. Marschilok, K.J. Takeuchi, E.S. Takeuchi, Batteries used to power implantable biomedical devices, *Electrochim. Acta.* 84 (2012) 155–164. doi:10.1016/J.ELECTACTA.2012.03.057.
- [39] S. El Ichi-Ribault, J.-P. Alcaraz, F. Boucher, B. Boutaud, R. Dalmolin, J. Boutonnat, P. Cinquin, A. Zebda, D.K. Martin, Remote wireless control of an enzymatic biofuel cell implanted in a rabbit for 2 months, *Electrochim. Acta.* 269 (2018) 360–366. doi:10.1016/J.ELECTACTA.2018.02.156.
- [40] J.A. Cracknell, K.A. Vincent, F.A. Armstrong, Enzymes as Working or Inspirational Electrocatalysts for Fuel Cells and Electrolysis, *Chem. Rev.* 108 (2008) 2439–2461. doi:10.1021/cr0680639.
- [41] S. Calabrese Barton, J. Gallaway, P. Atanassov, Enzymatic Biofuel Cells for Implantable and Microscale Devices, *Chem. Rev.* 104 (2004) 4867–4886. doi:10.1021/cr020719k.
- [42] S. Cosnier, A. J. Gross, A. Le Goff, M. Holzinger, Recent advances on enzymatic glucose/oxygen and hydrogen/oxygen biofuel cells: Achievements and limitations, *J. Power Sources.* 325 (2016) 252–263. doi:10.1016/J.JPOWSOUR.2016.05.133.
- [43] S. Cosnier, A.J. Gross, F. Giroud, M. Holzinger, Beyond the hype surrounding biofuel cells: What’s the future of enzymatic fuel cells?, *Curr. Opin. Electrochem.* (2018). doi:10.1016/J.COEELEC.2018.06.006.
- [44] D.J. Caruana, S. Howorka, Biosensors and biofuel cells with engineered proteins, *Mol. Biosyst.* 6 (2010) 1548. doi:10.1039/c004951d.
- [45] O. Courjean, N. Mano, Recombinant glucose oxidase from *Penicillium amagasakiense* for efficient bioelectrochemical applications in physiological conditions, *J. Biotechnol.* 151 (2011) 122–129. doi:10.1016/J.JBIOTECH.2010.10.077.
- [46] M. Campàs, B. Prieto-Simón, J.-L. Marty, A review of the use of genetically engineered enzymes in electrochemical biosensors, *Semin. Cell Dev. Biol.* 20 (2009)

- 3–9. doi:10.1016/J.SEMCDB.2009.01.009.
- [47] P.R. Kommoju, Z.W. Chen, R.C. Bruckner, F.S. Mathews, M.S. Jorns, Probing oxygen activation sites in two flavoprotein oxidases using chloride as an oxygen surrogate., *Biochemistry*. 50 (2011) 5521–5534. doi:10.2210/PDB3QVP/PDB.
- [48] P.N. Bartlett, F.A. Al-Lolage, There is no evidence to support literature claims of direct electron transfer (DET) for native glucose oxidase (GOx) at carbon nanotubes or graphene, *J. Electroanal. Chem.* 819 (2018) 26–37. doi:10.1016/j.jelechem.2017.06.021.
- [49] R.D. Milton, F. Giroud, A.E. Thumser, S.D. Minter, R.C.T. Slade, Hydrogen peroxide produced by glucose oxidase affects the performance of laccase cathodes in glucose/oxygen fuel cells: FAD-dependent glucose dehydrogenase as a replacement, *Phys. Chem. Chem. Phys.* 15 (2013) 19371. doi:10.1039/c3cp53351d.
- [50] D. MacAodha, P. Ó Conghaile, B. Egan, P. Kavanagh, C. Sygmund, R. Ludwig, D. Leech, Comparison of Glucose Oxidation by Crosslinked Redox Polymer Enzyme Electrodes Containing Carbon Nanotubes and a Range of Glucose Oxidising Enzymes, *Electroanalysis*. 25 (2013) 94–100. doi:10.1002/elan.201200536.
- [51] G.G. Guilbault, G.J. Lubrano, An enzyme electrode for the amperometric determination of glucose, *Anal. Chim. Acta.* 64 (1973) 439–455. doi:10.1016/S0003-2670(01)82476-4.
- [52] J. Wang, Electrochemical Glucose Biosensors, *Chem. Rev.* 108 (2008) 814–825. doi:10.1021/cr068123a.
- [53] A.E.G. Cass, G. Davis, G.D. Francis, H.A.O. Hill, W.J. Aston, I.J. Higgins, E. V. Plotkin, L.D.L. Scott, A.P.F. Turner, Ferrocene-mediated enzyme electrode for amperometric determination of glucose, *Anal. Chem.* 56 (1984) 667–671. doi:10.1021/ac00268a018.
- [54] M.T. Meredith, D.-Y. Kao, D. Hickey, D.W. Schmidtke, D.T. Glatzhofer, High Current Density Ferrocene-Modified Linear Poly(ethylenimine) Bioanodes and Their Use in Biofuel Cells, *J. Electrochem. Soc.* 158 (2011) B166. doi:10.1149/1.3505950.
- [55] P. Kavanagh, D. Leech, Mediated electron transfer in glucose oxidising enzyme electrodes for application to biofuel cells: recent progress and perspectives, *Phys.*

- Chem. Chem. Phys. 15 (2013) 4859. doi:10.1039/c3cp44617d.
- [56] S.M. Zakeeruddin, D.M. Fraser, M.-K. Nazeeruddin, M. Grätzel, Towards mediator design: Characterization of tris-(4,4'-substituted-2,2'-bipyridine) complexes of iron(II), ruthenium(II) and osmium(II) as mediators for glucose oxidase of *Aspergillus niger* and other redox proteins, *J. Electroanal. Chem.* 337 (1992) 253–283. doi:10.1016/0022-0728(92)80542-C.
- [57] M.N. Zafar, N. Beden, D. Leech, C. Sygmund, R. Ludwig, L. Gorton, Characterization of different FAD-dependent glucose dehydrogenases for possible use in glucose-based biosensors and biofuel cells, *Anal. Bioanal. Chem.* 402 (2012) 2069–2077. doi:10.1007/s00216-011-5650-7.
- [58] A. Malinauskas, J. Kuzmarskyt, R. Meškys, A. Ramanavičius, Bioelectrochemical sensor based on PQQ-dependent glucose dehydrogenase, *Sensors Actuators B Chem.* 100 (2004) 387–394. doi:10.1016/J.SNB.2004.02.006.
- [59] R. Antiochia, L. Gorton, Development of a carbon nanotube paste electrode osmium polymer-mediated biosensor for determination of glucose in alcoholic beverages, *Biosens. Bioelectron.* 22 (2007) 2611–2617. doi:10.1016/J.BIOS.2006.10.023.
- [60] Y. Nihon Seikagakkai., *The Journal of biochemistry.*, Japanese Biochemical Society, 1951. https://www.jstage.jst.go.jp/article/biochemistry1922/38/1/38_1_75/_article/-char/ja/
- [61] S. Tsujimura, S. Kojima, K. Kano, T. Ikeda, M. Sato, H. Sanada, H. Omura, Novel FAD-Dependent Glucose Dehydrogenase for a Dioxygen-Insensitive Glucose Biosensor, *Biosci. Biotechnol. Biochem.* 70 (2006) 654–659. doi:10.1271/bbb.70.654.
- [62] J. Okuda-Shimazaki, N. Kakehi, T. Yamazaki, M. Tomiyama, K. Sode, Biofuel cell system employing thermostable glucose dehydrogenase, *Biotechnol. Lett.* 30 (2008) 1753–1758. doi:10.1007/s10529-008-9749-7.
- [63] K. Sode, W. Tsugawa, T. Yamazaki, M. Watanabe, N. Ogasawara, M. Tanaka, A novel thermostable glucose dehydrogenase varying temperature properties by altering its quaternary structures, *Enzyme Microb. Technol.* 19 (1996) 82–85. doi:10.1016/0141-0229(95)00170-0.
- [64] H. Yoshida, G. Sakai, K. Mori, K. Kojima, S. Kamitori, K. Sode, Structural analysis of

- fungus-derived FAD glucose dehydrogenase, *Sci. Rep.* 5 (2015) 13498.
doi:10.1038/srep13498.
- [65] S.C. Barton, Enzyme catalysis in biological fuel cells, in: *Handb. Fuel Cells*, John Wiley & Sons, Ltd, Chichester, UK, 2010. doi:10.1002/9780470974001.f500006.
- [66] F. Tasca, M.N. Zafar, W. Harreither, G. Nöll, R. Ludwig, L. Gorton, A third generation glucose biosensor based on cellobiose dehydrogenase from *Corynascus thermophilus* and single-walled carbon nanotubes, *Analyst.* 136 (2011) 2033–2036. doi:10.1039/C0AN00311E.
- [67] F. Tasca, R. Ludwig, L. Gorton, R. Antiochia, Determination of lactose by a novel third generation biosensor based on a cellobiose dehydrogenase and aryl diazonium modified single wall carbon nanotubes electrode, *Sensors Actuators B Chem.* 177 (2013) 64–69. doi:10.1016/J.SNB.2012.10.114.
- [68] W. Harreither, C. Sygmund, M. Augustin, M. Narciso, M.L. Rabinovich, L. Gorton, D. Haltrich, R. Ludwig, Catalytic Properties and Classification of Cellobiose Dehydrogenases from Ascomycetes, *Appl. Environ. Microbiol.* 77 (2011) 1804–1815. doi:10.1128/AEM.02052-10.
- [69] C. Sygmund, P. Staudigl, M. Klausberger, N. Pinotsis, K. Djinović-Carugo, L. Gorton, D. Haltrich, R. Ludwig, Heterologous overexpression of *Glomerella cingulata* FAD-dependent glucose dehydrogenase in *Escherichia coli* and *Pichia pastoris*., *Microb. Cell Fact.* 10 (2011) 106. doi:10.1186/1475-2859-10-106.
- [70] R.D. Milton, S.D. Minter, Direct enzymatic bioelectrocatalysis: differentiating between myth and reality, *J. R. Soc. Interface.* 14 (2017) 20170253. doi:10.1098/rsif.2017.0253.
- [71] M.W. Makinen, S.A. Schichman, S.C. Hill, H.B. Gray, Heme-heme orientation and electron transfer kinetic behavior of multisite oxidation-reduction enzymes., *Science.* 222 (1983) 929–31. doi:10.1126/science.6415814.
- [72] Y. Degani, A. Heller, Direct electrical communication between chemically modified enzymes and metal electrodes. I. Electron transfer from glucose oxidase to metal electrodes via electron relays, bound covalently to the enzyme, *J. Phys. Chem.* 91 (1987) 1285–1289. doi:10.1021/j100290a001.

- [73] A.L. Ghindilis, P. Atanasov, E. Wilkins, Enzyme-catalyzed direct electron transfer: Fundamentals and analytical applications, *Electroanalysis*. 9 (1997) 661–674. doi:10.1002/elan.1140090902.
- [74] J.M. Goran, S.M. Mantilla, K.J. Stevenson, Influence of Surface Adsorption on the Interfacial Electron Transfer of Flavin Adenine Dinucleotide and Glucose Oxidase at Carbon Nanotube and Nitrogen-Doped Carbon Nanotube Electrodes, *Anal. Chem.* 85 (2013) 1571–1581. doi:10.1021/ac3028036.
- [75] N. Mano, Engineering glucose oxidase for bioelectrochemical applications, *Bioelectrochemistry*. 128 (2019) 218–240. doi:10.1016/J.BIOELECTCHEM.2019.04.015.
- [76] D. Wang, L. Chen, Facile direct electron transfer in glucose oxidase modified electrodes, *Electrochim. Acta*. 54 (2009) 4316–4320. doi:10.1016/J.ELECTACTA.2009.02.096.
- [77] S. Boland, P. Kavanagh, D. Leech, Mediated Enzyme Electrodes for Biological Fuel Cell and Biosensor Applications, in: *ECS Trans.*, ECS, 2008: pp. 77–87. doi:10.1149/1.3036213.
- [78] R.A. Marcus, N. Sutin, Electron transfers in chemistry and biology, *Biochim. Biophys. Acta - Rev. Bioenerg.* 811 (1985) 265–322. doi:10.1016/0304-4173(85)90014-X.
- [79] F. Mao, N. Mano, A. Heller, Long Tethers Binding Redox Centers to Polymer Backbones Enhance Electron Transport in Enzyme “Wiring” Hydrogels, *J. Am. Chem. Soc.* 125 (2003) 4951–4957. doi:10.1021/ja029510e.
- [80] N. Mano, F. Mao, A. Heller, Characteristics of a Miniature Compartment-less Glucose–O₂ Biofuel Cell and Its Operation in a Living Plant, *J. Am. Chem. Soc.* 125 (2003) 6588–6594. doi:10.1021/ja0346328.
- [81] T. de Lumley-Woodyear, P. Rocca, J. Lindsay, Y. Dror, A. Freeman, A. Heller, Polyacrylamide-Based Redox Polymer for Connecting Redox Centers of Enzymes to Electrodes, *Anal. Chem.* 67 (1995) 1332–1338. doi:10.1021/ac00104a006.
- [82] P. O Conghaile, D. MacAodha, B. Egan, P. Kavanagh, D. Leech, Tethering Osmium Complexes within Enzyme Films on Electrodes to Provide a Fully Enzymatic Membrane-Less Glucose/Oxygen Fuel Cell, *J. Electrochem. Soc.* 160 (2013) G3165–G3170. doi:10.1149/2.026307jes.

- [83] D. MacAodha, P.Ó. Conghaile, B. Egan, P. Kavanagh, D. Leech, Membraneless Glucose/Oxygen Enzymatic Fuel Cells Using Redox Hydrogel Films Containing Carbon Nanotubes, *ChemPhysChem*. 14 (2013) 2302–2307. doi:10.1002/cphc.201300239.
- [84] R.J. Forster, J.G. Vos, Synthesis, characterization, and properties of a series of osmium- and ruthenium-containing metallopolymers, *Macromolecules*. 23 (1990) 4372–4377. doi:10.1021/ma00222a008.
- [85] S. Boland, F. Barrière, D. Leech, Designing Stable Redox-Active Surfaces: Chemical Attachment of an Osmium Complex to Glassy Carbon Electrodes Prefunctionalized by Electrochemical Reduction of an *In Situ* -Generated Aryldiazonium Cation, *Langmuir*. 24 (2008) 6351–6358. doi:10.1021/la7031972.
- [86] T.J. Ohara, R. Rajagopalan, A. Heller, Wired Enzyme Electrodes for Amperometric Determination of Glucose or Lactate in the Presence of Interfering Substances, *Anal. Chem*. 66 (1994) 2451–2457. doi:10.1021/ac00087a008.
- [87] D.N. Blauch, J.M. Saveant, Dynamics of electron hopping in assemblies of redox centers. Percolation and diffusion, *J. Am. Chem. Soc.* 114 (1992) 3323–3332. doi:10.1021/ja00035a025.
- [88] I. Ruff, V.J. Friedrich, Transfer diffusion. I. Theoretical, *J. Phys. Chem.* 75 (1971) 3297–3302. doi:10.1021/j100690a016.
- [89] H. Dahms, Electronic conduction in aqueous solution, *J. Phys. Chem.* 72 (1968) 362–364. doi:10.1021/j100847a073.
- [90] D. Macaodha, M.L. Ferrer, P. Conghaile, P. Kavanagh, D. Leech, Crosslinked redox polymer enzyme electrodes containing carbon nanotubes for high and stable glucose oxidation current, *Phys. Chem. Chem. Phys. Phys. Chem. Chem. Phys.* 14 (2012) 14667–14672. doi:10.1039/c2cp42089a.
- [91] S. Cosnier, Biosensors based on electropolymerized films: new trends, *Anal. Bioanal. Chem.* 377 (2003) 507–520. doi:10.1007/s00216-003-2131-7.
- [92] Y. Tan, W. Deng, Y. Li, Z. Huang, Y. Meng, Q. Xie, M. Ma, S. Yao, Polymeric Bionanocomposite Cast Thin Films with In Situ Laccase-Catalyzed Polymerization of Dopamine for Biosensing and Biofuel Cell Applications, *J. Phys. Chem. B*. 114 (2010)

- 5016–5024. doi:10.1021/jp100922t.
- [93] H. Lee, S.M. Dellatore, W.M. Miller, P.B. Messersmith, Mussel-Inspired Surface Chemistry for Multifunctional Coatings, *Science* (80-.). 318 (2007) 426–430. doi:10.1126/science.1147241.
- [94] M. Dai, L. Sun, L. Chao, Y. Tan, Y. Fu, C. Chen, Q. Xie, Immobilization of Enzymes by Electrochemical and Chemical Oxidative Polymerization of L-DOPA to Fabricate Amperometric Biosensors and Biofuel Cells, *ACS Appl. Mater. Interfaces*. 7 (2015) 10843–10852. doi:10.1021/acsami.5b01865.
- [95] B.A. Gregg, A. Heller, Cross-linked redox gels containing glucose oxidase for amperometric biosensor applications, *Anal. Chem.* 62 (1990) 258–263. doi:10.1021/ac00202a007.
- [96] J.W. Gallaway, S.A. Calabrese Barton, Effect of redox polymer synthesis on the performance of a mediated laccase oxygen cathode, *J. Electroanal. Chem.* 626 (2009) 149–155. doi:10.1016/j.jelechem.2008.12.004.
- [97] T.J. Ohara, R. Rajagopalan, A. Heller, Glucose electrodes based on cross-linked bis(2,2'-bipyridine)chloroosmium(+2+) complexed poly(1-vinylimidazole) films, *Anal. Chem.* 65 (1993) 3512–3517. doi:10.1021/ac00071a031.
- [98] D. MacAodha, M.L. Ferrer, P.Ó. Conghaile, P. Kavanagh, D. Leech, Crosslinked redox polymer enzyme electrodes containing carbon nanotubes for high and stable glucose oxidation current, *Phys. Chem. Chem. Phys.* 14 (2012) 14667. doi:10.1039/c2cp42089a.
- [99] X. Xiao, T. Siepenkoetter, P.Ó. Conghaile, D. Leech, E. Magner, Nanoporous Gold-Based Biofuel Cells on Contact Lenses, *ACS Appl. Mater. Interfaces*. 10 (2018) 7107–7116. doi:10.1021/acsami.7b18708.
- [100] M. Holzinger, A. Le Goff, S. Cosnier, Nanomaterials for biosensing applications: a review, *Front. Chem.* 2 (2014). doi:10.3389/fchem.2014.00063.
- [101] Y. Fu, P. Li, Q. Xie, X. Xu, L. Lei, C. Chen, C. Zou, W. Deng, S. Yao, One-Pot Preparation of Polymer-Enzyme-Metallic Nanoparticle Composite Films for High-Performance Biosensing of Glucose and Galactose, *Adv. Funct. Mater.* 19 (2009) 1784–1791. doi:10.1002/adfm.200801576.

- [102] A.J. Gross, M. Holzinger, S. Cosnier, Buckypaper bioelectrodes: emerging materials for implantable and wearable biofuel cells, *Energy Environ. Sci.* 11 (2018) 1670–1687. doi:10.1039/C8EE00330K.
- [103] I. Osadebe, D. Leech, Effect of Multi-Walled Carbon Nanotubes on Glucose Oxidation by Glucose Oxidase or a Flavin-Dependent Glucose Dehydrogenase in Redox-Polymer-Mediated Enzymatic Fuel Cell Anodes, *ChemElectroChem.* 1 (2014) 1988–1993. doi:10.1002/celec.201402136.
- [104] V. Švrček, C. Pham-Huu, J. Amadou, D. Begin, M.-J. Ledoux, F. Le Normand, O. Ersen, S. Joulié, Filling and capping multiwall carbon nanotubes with silicon nanocrystals dispersed in SiO₂-based spin on glass, *J. Appl. Phys.* 99 (2006) 064306. doi:10.1063/1.2181667.
- [105] P. Ó Conghaile, M. Falk, D. MacAodha, M.E. Yakovleva, C. Gonaus, C.K. Peterbauer, L. Gorton, S. Shleev, D. Leech, Fully Enzymatic Membraneless Glucose|Oxygen Fuel Cell That Provides 0.275 mA cm⁻² in 5 mM Glucose, Operates in Human Physiological Solutions, and Powers Transmission of Sensing Data, *Anal. Chem.* 88 (2016) 2156–2163. doi:10.1021/acs.analchem.5b03745.
- [106] C. Mercer, R. Bennett, P.Ó. Conghaile, J.F. Rusling, D. Leech, Glucose biosensor based on open-source wireless microfluidic potentiostat, *Sensors Actuators B Chem.* (2019). doi:10.1016/j.snb.2019.02.031.
- [107] P. Ó Conghaile, S. Pöller, D. MacAodha, W. Schuhmann, D. Leech, Coupling osmium complexes to epoxy-functionalised polymers to provide mediated enzyme electrodes for glucose oxidation, *Biosens. Bioelectron.* 43 (2013) 30–37. doi:10.1016/j.bios.2012.11.036.
- [108] S.A. Weissman, N.G. Anderson, Design of Experiments (DoE) and Process Optimization. A Review of Recent Publications, *Org. Process Res. Dev.* 19 (2015) 1605–1633. doi:10.1021/op500169m.
- [109] J. Antony, Design of experiments for engineers and scientists, n.d.
- [110] R. Leardi, Experimental design in chemistry: A tutorial, *Anal. Chim. Acta.* 652 (2009) 161–172. doi:10.1016/J.ACA.2009.06.015.
- [111] C.A. Griffiths, J. Howarth, G. De Almeida-Rowbotham, A. Rees, R. Kerton, A design

- of experiments approach for the optimisation of energy and waste during the production of parts manufactured by 3D printing, *J. Clean. Prod.* 139 (2016) 74–85. doi:10.1016/J.JCLEPRO.2016.07.182.
- [112] A.A. Giunta, V. Balabanov, D. Haim, B. Grossman, W.H. Mason, L.T. Watson, R.T. Haftka, Multidisciplinary optimisation of a supersonic transport using design of experiments theory and response surface modelling, *Aeronaut. J.* 101 (1997) 347–356. doi:10.1017/s0001924000066045.
- [113] F. Galvanin, E. Cao, N. Al-Rifai, V. Dua, A. Gavriilidis, Optimal design of experiments for the identification of kinetic models of methanol oxidation over silver catalyst, *Chim. Oggi-Chemistry Today*, 33 Pp. 51-56. (2015). <http://discovery.ucl.ac.uk/1469720/>
- [114] O. Levi, B. Tal, S. Hileli, A. Shapira, I. Benhar, P. Grabov, N. Eliaz, Optimization of EGFR high positive cell isolation procedure by design of experiments methodology, *Cytom. Part B Clin. Cytom.* 88 (2015) 338–347. doi:10.1002/cyto.b.21246.
- [115] V. Flexer, K.F.E. Pratt, F. Garay, P.N. Bartlett, E.J. Calvo, Relaxation and Simplex mathematical algorithms applied to the study of steady-state electrochemical responses of immobilized enzyme biosensors: Comparison with experiments, *J. Electroanal. Chem.* 616 (2008) 87–98. doi:10.1016/J.JELECHEM.2008.01.006.
- [116] S. Babanova, K. Artyushkova, Y. Ulyanova, S. Singhal, P. Atanassov, Design of experiments and principal component analysis as approaches for enhancing performance of gas-diffusional air-breathing bilirubin oxidase cathode, *J. Power Sources.* 245 (2014) 389–397. doi:10.1016/J.JPOWSOUR.2013.06.031.
- [117] R. Kumar, D. Leech, A glucose anode for enzymatic fuel cells optimized for current production under physiological conditions using a design of experiment approach., *Bioelectrochemistry.* 106 (2015) 41–6. doi:10.1016/j.bioelechem.2015.06.005.
- [118] V. Coman, R. Ludwig, W. Harreither, D. Haltrich, L. Gorton, T. Ruzgas, and S. Shleev, A Direct Electron Transfer-Based Glucose/Oxygen Biofuel Cell Operating in Human Serum, *Fuel Cells.* (2009) NA-NA. doi:10.1002/fuce.200900121.
- [119] T. Siepenkoetter, U. Salaj-Kosla, X. Xiao, P.Ó. Conghaile, M. Pita, R. Ludwig, E. Magner, Immobilization of Redox Enzymes on Nanoporous Gold Electrodes:

- Applications in Biofuel Cells, *Chempluschem*. 82 (2017) 553–560.
doi:10.1002/cplu.201600455.
- [120] R.D. Milton, K. Lim, D.P. Hickey, S.D. Minteer, Employing FAD-dependent glucose dehydrogenase within a glucose/oxygen enzymatic fuel cell operating in human serum, *Bioelectrochemistry*. 106 (2015) 56–63. doi:10.1016/J.BIOELECHEM.2015.04.005.
- [121] P. Ó Conghaile, M. Falk, D. MacAodha, M.E. Yakovleva, C. Gonaus, C.K. Peterbauer, L. Gorton, S. Shleev, D. Leech, Fully Enzymatic Membraneless Glucose|Oxygen Fuel Cell That Provides 0.275 mA cm⁻² in 5 mM Glucose, Operates in Human Physiological Solutions, and Powers Transmission of Sensing Data, *Anal. Chem.* 88 (2016) 2156–2163. doi:10.1021/acs.analchem.5b03745.
- [122] M. Cadet, S. Gounel, C. Stines-Chaumeil, X. Brilland, J. Rouhana, F. Louerat, N. Mano, Cadet, M., Gounel, S., Stines-Chaumeil, C., Brilland, X., Rouhana, J., Louerat, F., Mano, N., 2016. An enzymatic glucose/O₂ biofuel cell operating in human blood. *Biosens. Bioelectron.* 83, 60–67. <https://doi.org/10.1016/j.bios.2016.04.016>An enzymatic gluc, *Biosens. Bioelectron.* 83 (2016) 60–67.
doi:10.1016/j.bios.2016.04.016.
- [123] J. Lu, L.T. Drzal, R.M. Worden, I. Lee, Simple Fabrication of a Highly Sensitive Glucose Biosensor Using Enzymes Immobilized in Exfoliated Graphite Nanoplatelets Nafion Membrane, *Chem. Mater.* 19 (2007) 6240–6246. doi:10.1021/cm702133u.
- [124] E. Reitz, W. Jia, M. Gentile, Y. Wang, Y. Lei, CuO Nanospheres Based Nonenzymatic Glucose Sensor, *Electroanalysis*. 20 (2008) 2482–2486. doi:10.1002/elan.200804327.
- [125] D. Moatti-Sirat, V. Poitout, V. Thom□, M.N. Gangnerau, Y. Zhang, Y. Hu, G.S. Wilson, F. Lemonnier, J.C. Klein, G. Reach, Reduction of acetaminophen interference in glucose sensors by a composite Nafion membrane: demonstration in rats and man, *Diabetologia*. 37 (1994) 610–616. doi:10.1007/BF00403381.
- [126] J.-A. Ni, H.-X. Ju, H.-Y. Chen, D. Leech, Amperometric determination of epinephrine with an osmium complex and Nafion double-layer membrane modified electrode, *Anal. Chim. Acta.* 378 (1999) 151–157. doi:10.1016/S0003-2670(98)00569-8.
- [127] K.A. Mauritz, R.B. Moore, State of Understanding of Nafion, *Chem. Rev.* 104 (2004) 4535–4586. doi:10.1021/cr0207123.

- [128] D.J. Harrison, R.F.B. Turner, H.P. Baltes, Characterization of perfluorosulfonic acid polymer coated enzyme electrodes and a miniaturized integrated potentiostat for glucose analysis in whole blood, *Anal. Chem.* 60 (1988) 2002–2007.
doi:10.1021/ac00170a003.
- [129] D.S. Bindra, G.S. Wilson, Pulsed amperometric detection of glucose in biological fluids at a surface-modified gold electrode, *Anal. Chem.* 61 (1989) 2566–2570.
doi:10.1021/ac00197a022.
- [130] R. Vaidya, P. Atanasov, E. Wilkins, Effect of interference on the performance of glucose enzyme electrodes using Nafion® coatings, *Med. Eng. Phys.* 17 (1995) 416–424. doi:10.1016/1350-4533(94)00006-U.
- [131] X. Xiao, H. Xia, R. Wu, L. Bai, L. Yan, E. Magner, S. Cosnier, E. Lojou, Z. Zhu, A. Liu, Tackling the Challenges of Enzymatic (Bio)Fuel Cells, *Chem. Rev.* (2019) acs.chemrev.9b00115. doi:10.1021/acs.chemrev.9b00115.
- [132] K. Elouarzaki, D. Cheng, A.C. Fisher, J.-M. Lee, Coupling orientation and mediation strategies for efficient electron transfer in hybrid biofuel cells, *Nat. Energy.* 3 (2018) 574–581. doi:10.1038/s41560-018-0166-4.
- [133] F. Tasca, L. Gorton, M. Kujawa, I. Patel, W. Harreither, C.K. Peterbauer, R. Ludwig, G. Nöll, Increasing the coulombic efficiency of glucose biofuel cell anodes by combination of redox enzymes., *Biosens. Bioelectron.* 25 (2010) 1710–6.
doi:10.1016/j.bios.2009.12.017.
- [134] L. Deng, F. Wang, H. Chen, L. Shang, L. Wang, T. Wang, S. Dong, A biofuel cell with enhanced performance by multilayer biocatalyst immobilized on highly ordered macroporous electrode, *Biosens. Bioelectron.* 24 (2008) 329–333.
doi:10.1016/J.BIOS.2008.04.006.
- [135] M.J. Cooney, V. Svoboda, C. Lau, G. Martin, S.D. Minteer, Enzyme catalysed biofuel cells, *Energy Environ. Sci.* 1 (2008) 320. doi:10.1039/b809009b.
- [136] S. Xu, S.D. Minteer, Enzymatic Biofuel Cell for Oxidation of Glucose to CO₂, *ACS Catal.* 2 (2012) 91–94. doi:10.1021/cs200523s.
- [137] P. Infossi, E. Lojou, J.-P. Chauvin, G. Herbette, M. Brugna, M.-T. Giudici-Ortoni, Aquifex aeolicus membrane hydrogenase for hydrogen biooxidation: Role of lipids

- and physiological partners in enzyme stability and activity, *Int. J. Hydrogen Energy*. 35 (2010) 10778–10789. doi:10.1016/J.IJHYDENE.2010.02.054.
- [138] E. Lojou, Hydrogenases as catalysts for fuel cells: Strategies for efficient immobilization at electrode interfaces, *Electrochim. Acta*. 56 (2011) 10385–10397. doi:10.1016/J.ELECTACTA.2011.03.002.
- [139] F. Marken, A. Neudeck, A.M. Bond, Cyclic Voltammetry, in: *Electroanal. Methods*, Springer Berlin Heidelberg, Berlin, Heidelberg, 2010: pp. 57–106. doi:10.1007/978-3-642-02915-8_4.
- [140] Z. Stojek, Experimental Setup, in: *Electroanal. Methods*, Springer Berlin Heidelberg, Berlin, Heidelberg, 2010: pp. 331–335. doi:10.1007/978-3-642-02915-8_17.
- [141] N. Elgrishi, K.J. Rountree, B.D. McCarthy, E.S. Rountree, T.T. Eisenhart, J.L. Dempsey, A Practical Beginner's Guide to Cyclic Voltammetry, *J. Chem. Educ.* 95 (2018) 197–206. doi:10.1021/acs.jchemed.7b00361.
- [142] A.J. Bard, L.R. Faulkner, *Electrochemical methods : fundamentals and applications*, Wiley, 2001.

Chapter 2: Bio-inspired strategy for surface immobilisation of enzyme and osmium redox centres using poly(L-Dopa).

Introduction

Catecholamine based chemistry has received increased attention in recent years due to the importance of molecules such as dopamine (DA) and noradrenaline. [1,2] Catecholamines are produced within the human body and act as neurological signalling compounds. They have been previously studied due to their electrochemical activity[3–5] and have been used to modify electrodes through electropolymerisation of DA to form polymer films of polydopamine (PDA). [6] Films consisting of coated PDA are advantageous as they are biocompatible for biosensing and biopower applications. [7]

A structurally similar but far less studied molecule amenable to electropolymerisation for immobilisation on films on electrodes is L-Dopa. L-Dopa is found in high concentrations in an adhesive protein in mussels. This discovery resulted in increased interest in bio-inspired adhesive compounds. [8]:[9] While L-Dopa has been extensively studied in other capacities such as the treatment of Parkinson's disease, it has not received much attention to date for use in electrode immobilisation strategies. [10]:[11] L-Dopa is self-polymerised to form poly(L-Dopa) (PLD) in a similar route to that for PDA. This is achieved by one of three methods; chemical, enzymatic or electrochemical polymerisation. Chemical oxidation is achieved using NaAuCl_4 and enzymatic oxidation is achieved using horseradish peroxidase. [12–14] Electropolymerisation of L-Dopa to produce thin films of PLD is an attractive route towards formation of redox active biofilms for application as either anodic or cathodic electrodes for enzymatic based fuel cells (EFCs) or biosensing applications. This is due to the ease at which these films can be created at an electrode surface as well as their highly controllable nature when synthesised electrochemically. [15]

Enzyme electrodes for biosensing and biofuel cell applications operate by converting chemical reactions with an enzyme into an electrical signal. [16–18] Enzymes capable of electrolysing a fuel/oxidant present in the human body such as glucose and oxygen make them suitable for *in-vivo* power or biosensor development. [19–22] Enzymes offer numerous advantages over traditional metal catalysts such as platinum as they are highly specific, operate under physiological conditions (pH 7.4, 37 °C) and do not require a membrane, all of which allows for device miniaturisation. [23–25]

Improved shuttling of electrons between the active site of an enzyme and the electrode surface is achieved by inclusion of a redox mediator complex. Osmium based metal centres have been

well studied for this application due to their stability in the Os(II)/Os(III) states, fast electron transfer rate and their tuneable redox potential by using coordinating ligands attached to the metal centre. [26–28] Enhanced current densities are achieved on inclusion of nanomaterials on the electrode surface such as multi-walled carbon nanotubes (MWCNTs). [29–31] This is attributed to increased surface area for immobilisation. Immobilisation strategies used to date rely on crosslinking agents such as glutaraldehyde or PEGDGE. [32–34] These require long curing times (~24 hours) before the electrode is ready for operation. It is proposed that PLD electrodes can be prepared in a shorter time frame with a fall in time for immobilisation from 24 hours to under 4 hours.

This chapter focuses on immobilisation of glucose oxidising enzyme electrode components using PLD. A flavin adenine dinucleotide dependent glucose dehydrogenase (FADGDH) was co-immobilised with $[\text{Os}(2,2'\text{-bipyridine})_2(4\text{-aminomethyl pyridine})\text{Cl}]\cdot\text{PF}_6$ ($\text{Os}(\text{bpy})_2(4\text{-AMP})\text{Cl}$) or $[\text{Os}(2,2'\text{-bipyridine})_2(\text{poly-vinylimidazole})_{10}\text{Cl}]^+$ ($\text{Os}(\text{bpy})\text{PVI}$) and with MWCNTs using PLD. Characterisation of the electrodes was undertaken by electrochemical methods and scanning electron microscopy (SEM).

Experimental

Materials and reagents

All chemicals were purchased from Sigma Aldrich. The flavin adenine dinucleotide dependent glucose dehydrogenase was from *Aspergillus sp.* (Sekisui Diagnostics). The multi walled carbon nanotubes (MWCNTs) were purchased from Sigma Aldrich and acid treated (conc. nitric acid) under reflux for 6 hours before being filtered and washed with deionised water until neutral. This was determined by monitoring the pH of the washings passing through the column. All aqueous solutions were prepared using HPLC grade deionised water from Sigma Aldrich unless otherwise stated (18 M Ω cm). The $(\text{Os}(\text{bpy})_2(4\text{-AMP})\text{Cl})$ and $(\text{Os}(\text{bpy})\text{PVI})$ were synthesised as previously reported in the literature. [35,36]

Enzyme electrode preparation

Graphite rods (3 mm diameter) were purchased from the Graphite store. The cylinder of these rods was insulated with heat shrink tubing with the exposed tip creating an electrode surface. This surface was polished using p-400 and p-1200 grit silicon carbide paper (Buehler) with a final washing in deionised water and subsequent drying. The finished electrode surface had a defined geometric surface area of 0.0707 cm². Aqueous solutions of enzyme (10 mg ml⁻¹),

redox polymer/complex (5 mg ml⁻¹), acid treated MWCNTs (46.25 mg ml⁻¹), PEGDGE (15 mg ml⁻¹) and L-Dopa (1.97 mg ml⁻¹) were prepared. The electrodes were modified by depositing 10 µl of the FADGDH solution, 10 µl of the osmium solution, 10 µl of the MWCNTs dispersion and either 20 µl of the L-Dopa solution or 2 µl of the PEGDGE solution onto the exposed electrode disk area. The L-Dopa electrodes were allowed to stand for 3 hours to ensure the electrodes are dry prior to initiating the electropolymerisation process. For the electrochemical polymerisation of the L-Dopa on the modified electrode, cyclic voltammetry was performed from -0.5 V to 0.5V (vs. Ag/AgCl) for 20 sweeps at a scan rate of 50 mV s⁻¹. The PEGDGE electrodes were allowed to crosslink and dry for 24 hours prior to testing in accordance with established procedures. [37]

Electrochemical measurements

Electrochemical testing was carried out using a 1030 multichannel potentiostat from CH Instruments. All testing was performed in a custom designed electrochemical cell permitting use of 8 working electrodes. The electrolyte was phosphate buffered saline (PBS) prepared by inclusion of 150 mM NaCl in a solution of 50 mM phosphate buffer, pH adjusted to 7.4. Testing was carried out at 37 °C unless otherwise stated. The graphite rods were used as working electrode electrodes, with a common Ag/AgCl reference electrode and either a Pt mesh or Ti counter electrode (Goodfellow) in the cell.

Results

Polymerisation of L-dopamine or L-dopa to form Polydopamine (PDA) or Poly(L-dopa) (PLD) respectively by electrochemical or chemical means, has previously been reported as an immobilisation strategy for preparation of modified electrode surfaces.[15] [38] Dai *et al.* reported on electrodes assembled using electropolymerised PLD to immobilise glucose oxidase and gold nanoparticles for biosensing and biofuel cell applications. [15] The first step in the proposed mechanism for the electrochemical polymerisation of L-Dopa to PLD is through the oxidation of L-Dopa to give dopaquinone. This cyclises to form leucodopachrome which is oxidised to dopachrome. The dopachrome undergoes further electropolymerisation to give PLD at the electrode surface, see Fig. 1. [15]

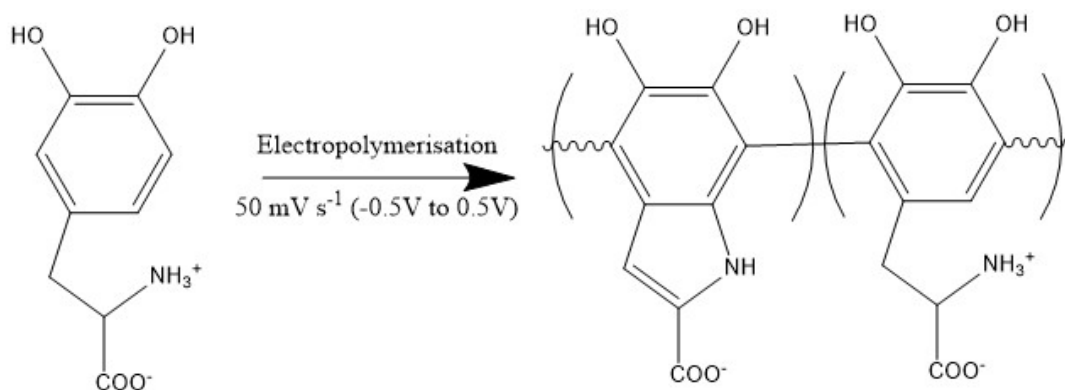


Figure 1: Schematic showing the conversion of L-Dopa to poly(L-Dopa) through electropolymerisation.

This research targets co-immobilisation of a glucose oxidising enzyme (FADGDH) and an osmium redox centre (polymer or complex) with MWCNTs using PLD.

The immobilisation of components at the electrode was achieved through electropolymerisation of L-Dopa at the electrode surface. Figure 2 below shows the initial CV scan recorded showing the presence of L-Dopa at the electrode surface. This is in agreement with work previously carried out. [41] The continued electropolymerisation of L-Dopa to form PLD, a non-conducting polymer can be seen with the only remaining redox peak showing the presence of the osmium complex at the electrode surface at the end of the process.

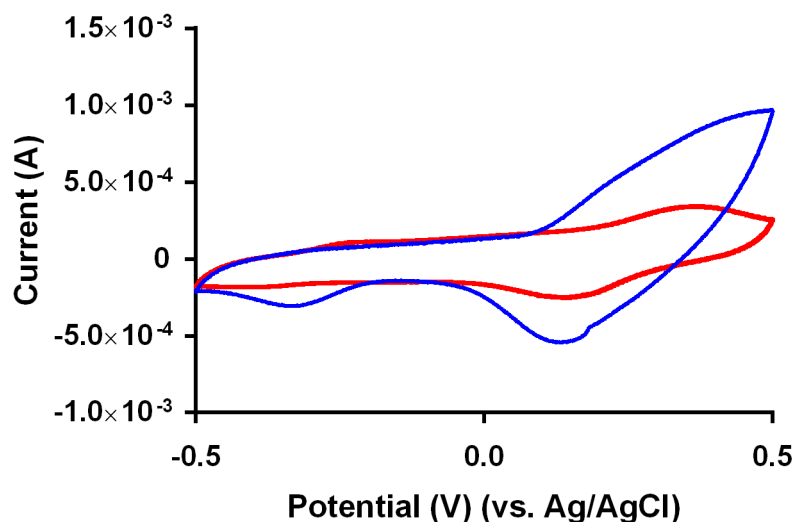


Figure 1: CV scans taken during the electropolymerisation process for films containing FADGDH, Os(bpy)₂(4-AMP)Cl and MWCNTs. Scans taken at 50 mV s⁻¹ (PBS @pH 7.4, 37°C). The blue line shows the first sweep of the process with the red line showing the final sweep.

Scanning electron microscopy was used to verify the presence of PLD films on the electrode surface. Fig.3 and Fig.4 below show the modified electrodes prepared with PLD. The images

indicate the presence of PLD within the film. The images were taken of electrode surfaces after testing and are identical to those mentioned in the experimental section. Figure 5 shows an electrode drop coated with MWCNTs and no PLD to compare with electrodes modified with both MWCNTs and PLD (Fig. 3 and Fig. 4).

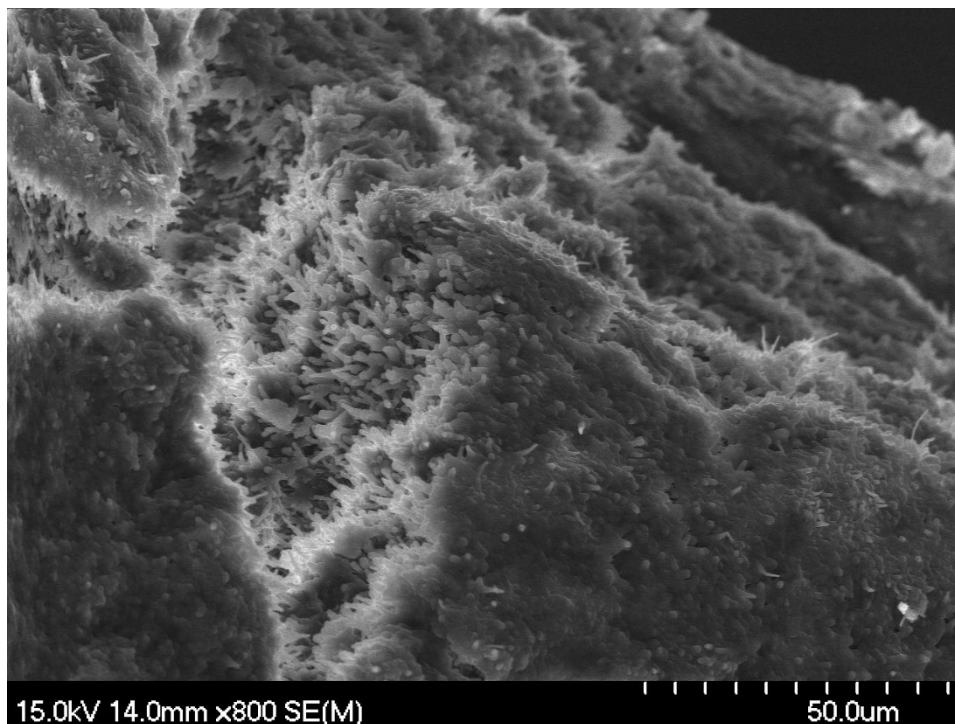


Figure 2: SEM image taken of the modified electrode using electropolymerisation to give PLD immobilised surfaces. The biofilm contains FADGDH, $\text{Os}(\text{bpy})_2(4\text{-AMP})\text{Cl}$, MWCNTs and PLD. The structures visible are a combination of MWCNTs and the PLD.

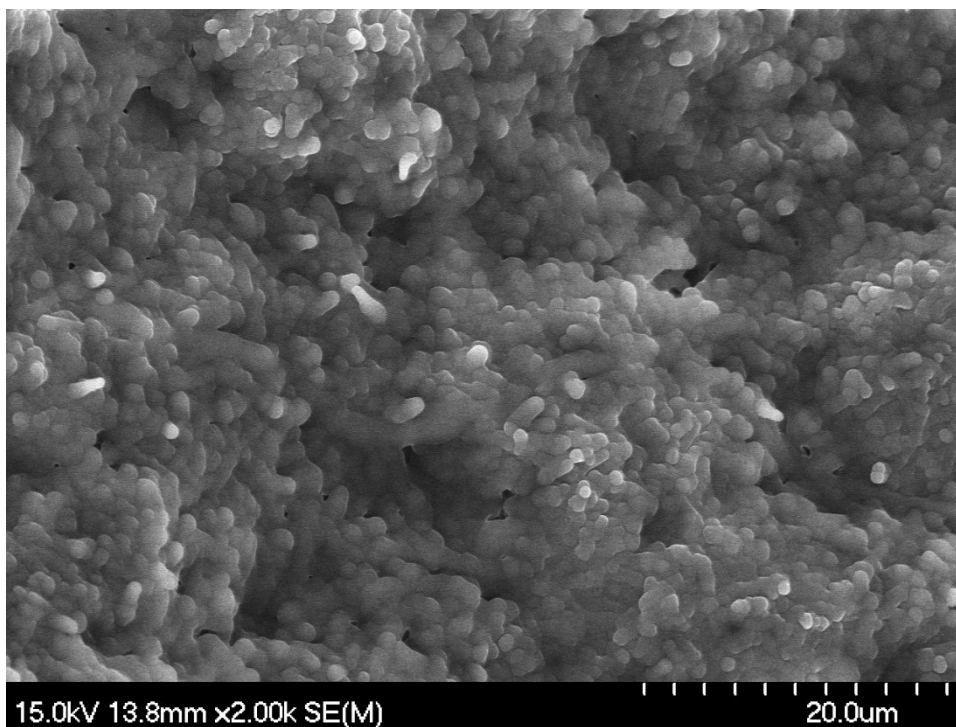


Figure 3: SEM image taken of the modified electrode using electropolymerisation to give PLD immobilised surfaces. The biofilm contains FADGDH, $\text{Os}(\text{bpy})_2(4\text{-AMP})\text{Cl}$, MWCNTs and PLD. The structures visible are a combination of MWCNTs and the PLD.

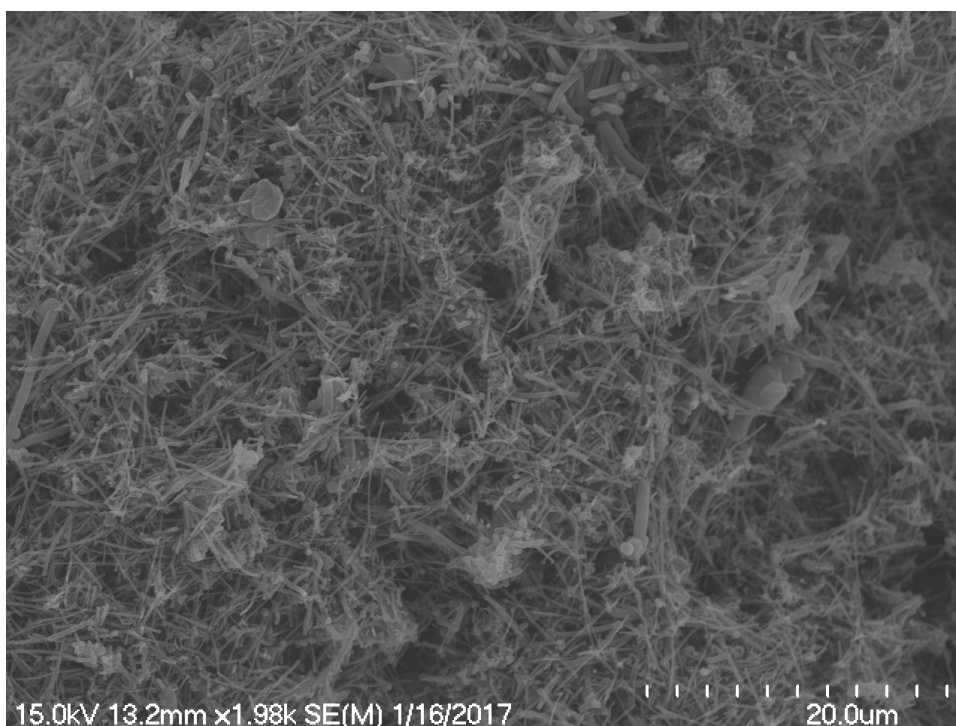


Figure 4: SEM image taken of an electrode surface modified with MWCNTs with no PLD present, to highlight the difference between electrodes modified with and without PLD.

The performance of these electrodes is assessed through comparison with electrodes prepared using a PEGDGE crosslinker. Verification of the presence of $\text{Os}(\text{bpy})_2(4\text{-AMP})\text{Cl}$ and

(Os(bpy)PVI) and of the enzyme at the surface was accomplished by recording cyclic voltammograms in the presence and absence of glucose substrate. The redox potential for the complex and polymer estimated from the midpoint between oxidation and reduction potentials in the absence of substrate at slow scan rates (1 mV s^{-1}) were confirmed to be 250 mV and 220 mV, respectively, versus an Ag/AgCl (3M KCl) reference electrode, in agreement with previously quoted redox potentials for these materials. [39] Cyclic voltammograms measured in the absence of glucose at slow scan rates ($<20 \text{ mV s}^{-1}$) have peak currents that scale linearly with scan rate, indicative of a surface-confined redox response. [40] At higher scan rates the measured peak currents scale linearly with the square root of the scan rate, which is indicative of semi-infinite diffusion within the films. [40]

Electrodes containing PLD were compared to electrodes that did not have PLD present but were otherwise identical ($n=3$). Figure 6 shows the inclusion of L-Dopa in the electrode preparation step results in higher current for the enzyme electrodes for CVs recorded in the presence of 10 mM glucose. A comparison of current density response as a function of increasing glucose concentration for electrodes prepared with PDA versus those without is presented in Fig. 7. The increase in glucose oxidation current at low concentrations for electrodes prepared without PLD is most likely due to the presence of residual unbound enzyme and redox complex dissolving from the electrode surface over the experimental timeframe. This current drops off upon increasing the glucose concentration when detachment of the enzyme/redox centre couple from the electrode surface occurs.

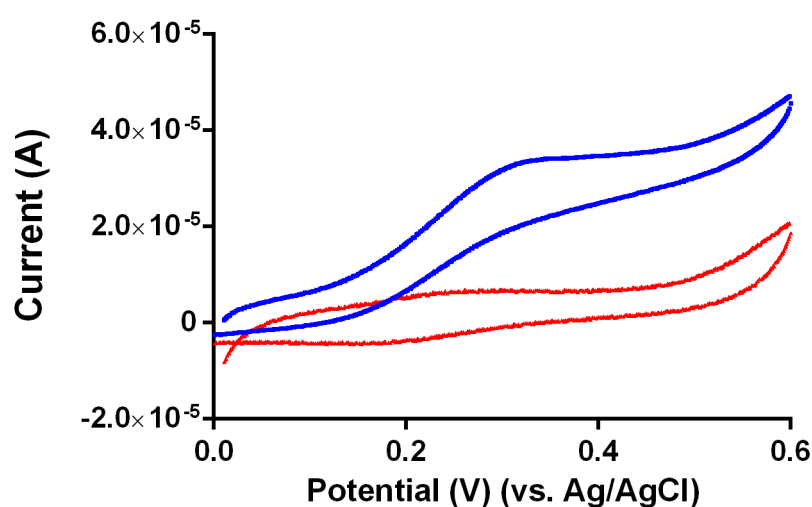


Figure 5: CV scans (1 mV s^{-1}) recorded in quiescent solution (PBS @ pH 7.4, $37 \text{ }^\circ\text{C}$) of electrodes with FADGDH, Os(bpy)₂(4-AMP)Cl, MWCNTs with PLD present (blue) and absent (red) in 10 mM glucose.

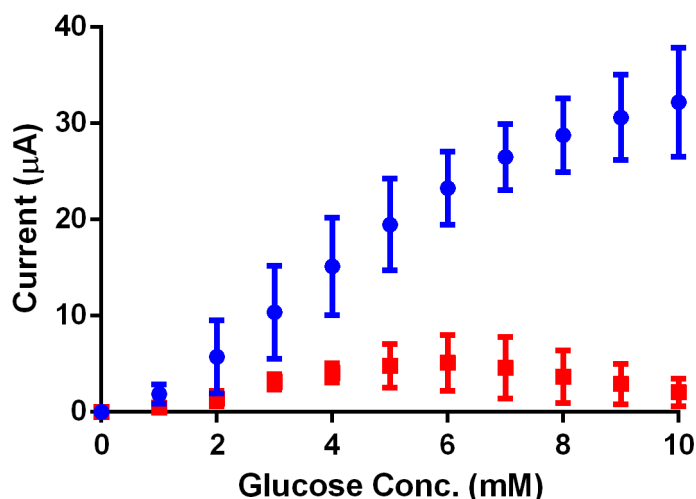


Figure 6: Current responses for glucose oxidation in PBS (pH 7.4 @ 37 °C) stirring at 150 rpm at an applied potential of 0.45 V (vs. Ag/AgCl), for electrodes containing FADGDH, Os(bpy)₂(4-AMP)Cl, MWCNTs with PLD present (blue) and absent (red) (n=3).

These results suggest that electropolymerisation of PLD is effective for immobilising the enzyme/redox complex at the electrode surface. Further testing was carried out by comparison of the response recorded for two types of enzyme electrodes: one group containing the redox centre and the second group without. The results shown below in Fig. 8 and 9 show that the redox centre is required to shuttle electrons from enzymatic active site to the electrode surface. The results above are in agreement with previous research carried out using FADGDH for glucose oxidation at an electrode surface. [42,43]

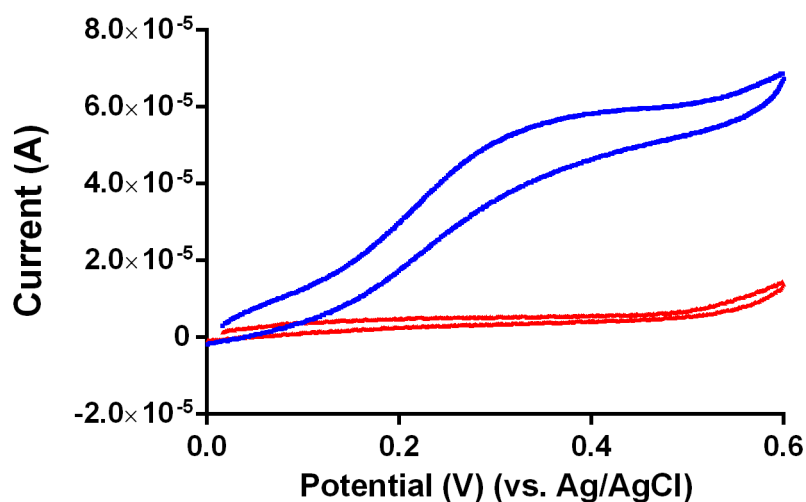


Figure 7: CV scans (1 mV s^{-1}) recorded in quiescent solution (PBS @ pH 7.4, 37 °C containing 10 mM glucose) for electrodes prepared with FADGDH, MWCNTs, immobilised in the presence (blue) and absence (red) of Os(bpy)₂(4-AMP)Cl in PLD films.

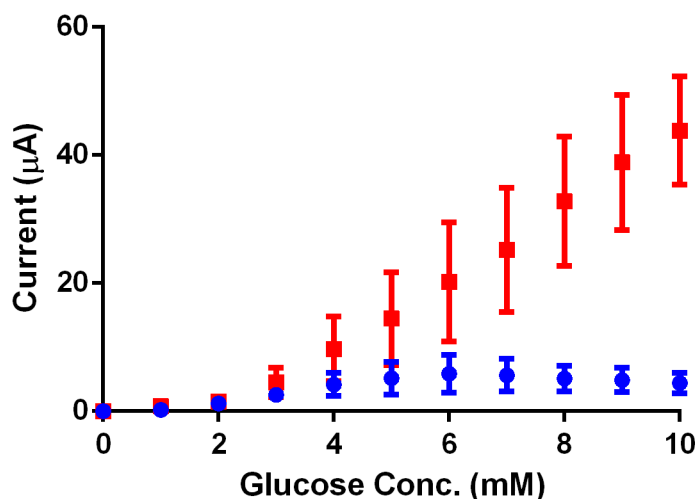


Figure 8: Current responses for glucose oxidation in PBS (pH 7.4 @ 37 °C) stirring at 150 rpm at an applied potential of 0.45 V (vs. Ag/AgCl), for electrodes prepared with FADGDH, MWCNTs, immobilised in the presence (red) and absence (blue) of Os(bpy)₂(4-AMP)Cl (n=4) in PLD films.

Testing of electrodes over a longer time frame is performed to assess the operational stability in PBS given the importance of signal stability for application to continuous use enzyme electrodes as biosensors or EFC assembly. Amperometry is performed at 0.45 V vs. Ag/AgCl in solutions containing 100 mM glucose with stirring at 150 rpm (pH 7.4 @ 37 °C). Comparison of the current obtained after a 24-hour timeframe is used to assess stability of signal. The current remaining after 24 hours is used to report on the performance of enzyme electrodes.

The PLD modified electrodes were compared to PEGDGE crosslinked electrodes to benchmark their suitability for biosensing and EFC applications over a 24-hour timeframe. Amperometry was performed at 0.45V (vs. Ag/AgCl) in 100 mM glucose allowing for comparison of signal stability throughout the experiment for each electrode assembly. Fig. 10 shows that electrodes assembled with PEGDGE as crosslinker produced higher current densities consistently over the 24-hours of testing when compared to electrodes modified with electropolymerised PLD.

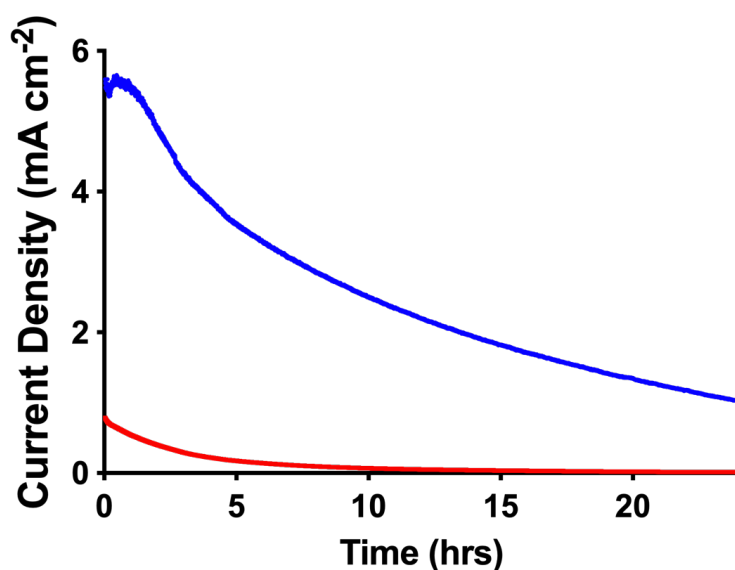


Figure 10: Mean current response ($n=3$) over 24-hours in PBS (pH 7.4 @ 37 °C) stirring at 150 rpm with an applied potential of 0.45 V (vs. Ag/AgCl). The graph shows the decrease in current for electrodes with FADGDH, MWCNTs, Os(bpy)PVI with PEGDGE as crosslinker (blue) and electropolymerised PLD as immobilisation strategy (red).

Both electrode groups showed a significant decrease in operational stability over 24-hours of continuous operation. The PLD coated electrodes had significantly less current signal at the beginning of testing and produced less current throughout testing when compared to the crosslinked electrodes.

Conclusions

Enzyme electrode components were immobilised at the electrode surface through electropolymerisation of L-Dopa. Electrodes prepared with PLD were compared with a control group prepared using no immobilisation strategy. The PLD electrodes achieved current values in the presence of 10 mM glucose ($n=3$) of $32.2 \pm 5.6 \mu\text{A}$ compared to $2.73 \pm 0.5 \mu\text{A}$ for electrodes prepared without using PLD. This suggests that electropolymerisation of L-Dopa successfully immobilised the enzyme and redox polymer at the electrode surface. The combination of osmium redox centre with the enzyme and PLD provided higher currents than the control group containing no enzyme showing the requirement for a mediator. The PLD electropolymerisation process was effective at immobilising the surface components at the electrode surface. When compared with electrodes prepared using PEGDGE, the current signal was much lower. This suggests that PLD as an immobilisation strategy is not a suitable replacement for crosslinker based strategies. Further work is required to provide enzyme electrodes that produce higher current densities and maintain high operational stabilities over their lifetime. Crosslinking of components co-deposited at the electrode surface using

PEGDGE is used as an immobilisation strategy in the subsequent chapters of this thesis as it produced higher current densities and maintained higher current signal after continuous operation over 24 hours compared to electropolymerised PLD.

References

- [1] H. Lee, J. Rho, P.B. Messersmith, Facile Conjugation of Biomolecules onto Surfaces via Mussel Adhesive Protein Inspired Coatings, *Adv. Mater.* 21 (2009) 431–434. doi:10.1002/adma.200801222.
- [2] C. Xu, K. Xu, H. Gu, R. Zheng, H. Liu, X. Zhang, Z. Guo, B. Xu, Dopamine as A Robust Anchor to Immobilize Functional Molecules on the Iron Oxide Shell of Magnetic Nanoparticles, *J. Am. Chem. Soc.* 126 (2004) 9938–9939. doi:10.1021/ja0464802.
- [3] Y. Chen, Y. Li, D. Deng, H. He, X. Yan, Z. Wang, C. Fan, L. Luo, Effective immobilization of Au nanoparticles on TiO₂ loaded graphene for a novel sandwich-type immunosensor, *Biosens. Bioelectron.* 102 (2018) 301–306. doi:10.1016/j.bios.2017.11.009.
- [4] C.-H. Yeh, Y.-W. Chen, M.-Y. Shie, H.-Y. Fang, Poly(Dopamine)-Assisted Immobilization of Xu Duan on 3D Printed Poly(Lactic Acid) Scaffolds to Up-Regulate Osteogenic and Angiogenic Markers of Bone Marrow Stem Cells, *Materials (Basel)*. 8 (2015) 4299–4315. doi:10.3390/ma8074299.
- [5] C. Chen, Y. Fu, C. Xiang, Q. Xie, Q. Zhang, Y. Su, L. Wang, S. Yao, Electropolymerization of preoxidized catecholamines on Prussian blue matrix to immobilize glucose oxidase for sensitive amperometric biosensing, *Biosens. Bioelectron.* 24 (2009) 2726–2729. doi:10.1016/j.bios.2008.12.016.
- [6] Q. Yue, M. Wang, Z. Sun, C. Wang, C. Wang, Y. Deng, D. Zhao, A versatile ethanol-mediated polymerization of dopamine for efficient surface modification and the construction of functional core–shell nanostructures, *J. Mater. Chem. B*. 1 (2013) 6085. doi:10.1039/c3tb21028f.
- [7] M.E. Lynge, P. Schattling, B. Städler, Recent developments in poly(dopamine)-based coatings for biomedical applications, *Nanomedicine*. 10 (2015) 2725–2742. doi:10.2217/nmm.15.89.
- [8] J.H. Waite, M.L. Tanzer, Polyphenolic Substance of *Mytilus edulis*: Novel Adhesive

- Containing L-Dopa and Hydroxyproline, *Science* (80-.). 212 (1981) 1038–1040. doi:10.1126/science.212.4498.1038.
- [9] H. Lee, S.M. Dellatore, W.M. Miller, P.B. Messersmith, Mussel-inspired surface chemistry for multifunctional coatings., *Science*. 318 (2007) 426–430. doi:10.1126/science.1147241.
- [10] L. Curtis, A.J. Lees, G.M. Stern, M.G. Marmot, Effect of L-Dopa on Course of Parkinson's Disease, *Lancet*. 324 (1984) 211–212. doi:10.1016/S0140-6736(84)90493-8.
- [11] N. Mercuri, G. Bernardi, The ‘magic’ of -dopa: why is it the gold standard Parkinson’s disease therapy?, *Trends Pharmacol. Sci.* 26 (2005) 341–344. doi:10.1016/j.tips.2005.05.002.
- [12] Y. Tan, W. Deng, Y. Li, Z. Huang, Y. Meng, Q. Xie, M. Ma, S. Yao, Polymeric Bionanocomposite Cast Thin Films with In Situ Laccase-Catalyzed Polymerization of Dopamine for Biosensing and Biofuel Cell Applications, *J. Phys. Chem. B*. 114 (2010) 5016–5024. doi:10.1021/jp100922t.
- [13] H. Lee, S.M. Dellatore, W.M. Miller, P.B. Messersmith, Mussel-Inspired Surface Chemistry for Multifunctional Coatings, *Science* (80-.). 318 (2007) 426–430. doi:10.1126/science.1147241.
- [14] Y. Li, M. Liu, C. Xiang, Q. Xie, S. Yao, Electrochemical quartz crystal microbalance study on growth and property of the polymer deposit at gold electrodes during oxidation of dopamine in aqueous solutions, *Thin Solid Films*. 497 (2006) 270–278. doi:10.1016/J.TSF.2005.10.048.
- [15] M. Dai, L. Sun, L. Chao, Y. Tan, Y. Fu, C. Chen, Q. Xie, Immobilization of Enzymes by Electrochemical and Chemical Oxidative Polymerization of L-DOPA to Fabricate Amperometric Biosensors and Biofuel Cells, *ACS Appl. Mater. Interfaces*. 7 (2015) 10843–10852. doi:10.1021/acsami.5b01865.
- [16] A. Heller, B. Feldman, Electrochemical Glucose Sensors and Their Applications in Diabetes Management, *Chem. Rev.* 108 (2008) 2482–2505. doi:10.1021/cr068069y.
- [17] A. Heller, Electrical wiring of redox enzymes, *Acc. Chem. Res.* 23 (1990) 128–134. doi:10.1021/ar00173a002.

- [18] A. Heller, Miniature biofuel cells, *Phys. Chem. Chem. Phys.* 6 (2004) 209. doi:10.1039/b313149a.
- [19] T. Chen, S.C. Barton, G. Binyamin, Z. Gao, Y. Zhang, H.-H. Kim, A. Heller, A Miniature Biofuel Cell, *J. Am. Chem. Soc.* 123 (2001) 8630–8631. doi:10.1021/ja0163164.
- [20] S. Calabrese Barton, J. Gallaway, P. Atanassov, Enzymatic Biofuel Cells for Implantable and Microscale Devices, *Chem. Rev.* 104 (2004) 4867–4886. doi:10.1021/cr020719k.
- [21] A.A. Babadi, S. Bagheri, S.B.A. Hamid, Progress on implantable biofuel cell: Nano-carbon functionalization for enzyme immobilization enhancement, *Biosens. Bioelectron.* 79 (2016) 850–860. doi:10.1016/j.bios.2016.01.016.
- [22] C.N. Kotanen, F.G. Moussy, S. Carrara, A. Guiseppi-Elie, Implantable enzyme amperometric biosensors, *Biosens. Bioelectron.* 35 (2012) 14–26. doi:10.1016/j.bios.2012.03.016.
- [23] S. Tsujimura, M. Fujita, H. Tatsumi, K. Kano, T. Ikeda, Bioelectrocatalysis-based dihydrogen/dioxygen fuel cell operating at physiological pH, *Phys. Chem. Chem. Phys.* 3 (2001) 1331–1335. doi:10.1039/b009539g.
- [24] P. Ó Conghaile, M. Falk, D. MacAodha, M.E. Yakovleva, C. Gonaus, C.K. Peterbauer, L. Gorton, S. Shleev, D. Leech, Fully Enzymatic Membraneless Glucose|Oxygen Fuel Cell That Provides 0.275 mA cm⁻² in 5 mM Glucose, Operates in Human Physiological Solutions, and Powers Transmission of Sensing Data, *Anal. Chem.* 88 (2016) 2156–2163. doi:10.1021/acs.analchem.5b03745.
- [25] M.J. González-Guerrero, F.J. del Campo, J.P. Esquivel, D. Leech, N. Sabaté, Paper-based microfluidic biofuel cell operating under glucose concentrations within physiological range, *Biosens. Bioelectron.* 90 (2017) 475–480. doi:10.1016/j.bios.2016.09.062.
- [26] D. Leech, P. Kavanagh, W. Schuhmann, Enzymatic fuel cells: Recent progress, *Electrochim. Acta.* 84 (2012) 223–234. doi:10.1016/j.electacta.2012.02.087.
- [27] I. Osadebe, P.Ó. Conghaile, P. Kavanagh, D. Leech, Glucose oxidation by osmium redox polymer mediated enzyme electrodes operating at low potential and in oxygen,

- for application to enzymatic fuel cells, *Electrochim. Acta.* 182 (2015) 320–326. doi:10.1016/j.electacta.2015.09.088.
- [28] P. O Conghaile, D. MacAodha, B. Egan, P. Kavanagh, D. Leech, Tethering Osmium Complexes within Enzyme Films on Electrodes to Provide a Fully Enzymatic Membrane-Less Glucose/Oxygen Fuel Cell, *J. Electrochem. Soc.* 160 (2013) G3165–G3170. doi:10.1149/2.026307jes.
- [29] D. MacAodha, P. Ó Conghaile, B. Egan, P. Kavanagh, C. Sygmund, R. Ludwig, D. Leech, Comparison of Glucose Oxidation by Crosslinked Redox Polymer Enzyme Electrodes Containing Carbon Nanotubes and a Range of Glucose Oxidising Enzymes, *Electroanalysis.* 25 (2013) 94–100. doi:10.1002/elan.201200536.
- [30] B. Reuillard, A. Le Goff, C. Agnès, M. Holzinger, A. Zebda, C. Gondran, K. Elouarzaki, S. Cosnier, High power enzymatic biofuel cell based on naphthoquinone-mediated oxidation of glucose by glucose oxidase in a carbon nanotube 3D matrix, *Phys. Chem. Chem. Phys.* 15 (2013) 4892. doi:10.1039/c3cp50767j.
- [31] J. Wang, Carbon-Nanotube Based Electrochemical Biosensors: A Review, *Electroanalysis.* 17 (2005) 7–14. doi:10.1002/elan.200403113.
- [32] A. Killyéni, M.E. Yakovleva, D. MacAodha, P.Ó. Conghaile, C. Gonaus, R. Ortiz, D. Leech, I.C. Popescu, C.K. Peterbauer, L. Gorton, Effect of deglycosylation on the mediated electrocatalytic activity of recombinantly expressed *Agaricus meleagris* pyranose dehydrogenase wired by osmium redox polymer, *Electrochim. Acta.* 126 (2014) 61–67. doi:10.1016/j.electacta.2013.08.069.
- [33] Kaushik Sirkar, and Alexander Revzin, M. V. Pishko, Glucose and Lactate Biosensors Based on Redox Polymer/Oxidoreductase Nanocomposite Thin Films, (2000). doi:10.1021/AC991041K.
- [34] S. Nardecchia, M.C. Serrano, M.C. Gutiérrez, M.T. Portolés, M.L. Ferrer, F. del Monte, Osteoconductive Performance of Carbon Nanotube Scaffolds Homogeneously Mineralized by Flow-Through Electrodeposition, *Adv. Funct. Mater.* 22 (2012) 4411–4420. doi:10.1002/adfm.201200684.
- [35] C. Danilowicz, E. Cortón, F. Battaglini, Osmium complexes bearing functional groups: building blocks for integrated chemical systems, *J. Electroanal. Chem.* 445 (1998) 89–

94. doi:10.1016/S0022-0728(97)00484-1.
- [36] E.M. Kober, J. V. Caspar, B.P. Sullivan, T.J. Meyer, Synthetic routes to new polypyridyl complexes of osmium(II), *Inorg. Chem.* 27 (1988) 4587–4598. doi:10.1021/ic00298a017.
- [37] T. de Lumley-Woodyear, P. Rocca, J. Lindsay, Y. Dror, A. Freeman, A. Heller, Polyacrylamide-Based Redox Polymer for Connecting Redox Centers of Enzymes to Electrodes, *Anal. Chem.* 67 (1995) 1332–1338. doi:10.1021/ac00104a006.
- [38] Y. Guan, L. Liu, C. Chen, X. Kang, Q. Xie, Effective immobilization of tyrosinase via enzyme catalytic polymerization of l-DOPA for highly sensitive phenol and atrazine sensing, *Talanta*. 160 (2016) 125–132. doi:10.1016/J.TALANTA.2016.07.003.
- [39] S. Boland, P. Kavanagh, D. Leech, Mediated Enzyme Electrodes for Biological Fuel Cell and Biosensor Applications, in: *ECS Trans.*, ECS, 2008: pp. 77–87. doi:10.1149/1.3036213.
- [40] A.J. Bard, L.R. Faulkner, *Electrochemical methods : fundamentals and applications*, Wiley, 2001.
- [41] M. Eslami, H.R. Zare, M. Namazian, *Thermodynamic Parameters of Electrochemical Oxidation of L-DOPA: Experimental and Theoretical Studies*, (n.d.). doi:10.1021/jp3054229.
- [42] I. Osadebe, D. Leech, Effect of Multi-Walled Carbon Nanotubes on Glucose Oxidation by Glucose Oxidase or a Flavin-Dependent Glucose Dehydrogenase in Redox-Polymer-Mediated Enzymatic Fuel Cell Anodes, *ChemElectroChem.* 1 (2014) 1988–1993. doi:10.1002/celec.201402136.
- [43] M. Hatada, N. Loew, Y. Inose-Takahashi, J. Okuda-Shimazaki, W. Tsugawa, A. Mulchandani, K. Sode, Development of a glucose sensor employing quick and easy modification method with mediator for altering electron acceptor preference, *Bioelectrochemistry.* 121 (2018) 185–190. doi:10.1016/j.bioelechem.2018.02.001.
- [44] A. PrévotEAU, N. Mano., Oxygen reduction on redox mediators may affect glucose biosensors based on “wired” enzymes, *Electrochim. Acta.* 68(2012) 128-133. doi:10.1016/j.electacta.2012.02.053.
- [45] A. PrévotEAU, N. Mano, How the reduction of O₂ on enzymes and/or redox mediators

affects the calibration curve of “wired” glucose oxidase and glucose dehydrogenase biosensors, *Electrochim. Acta.* 112 (2013) 318–326.

doi:10.1016/J.ELECTACTA.2013.08.173.

- [46] R. Bennett, I. Osadebe, R. Kumar, P.Ó. Conghaile, D. Leech, Design of Experiments Approach to Provide Enhanced Glucose-oxidising Enzyme Electrode for Membrane-less Enzymatic Fuel Cells Operating in Human Physiological Fluids, *Electroanalysis.* 30 (2018) 1438–1445. doi:10.1002/elan.201600402.

Chapter 3: Design of Experiments Approach to Provide Enhanced Glucose-Oxidising Enzyme Electrode for Membrane-Less Enzymatic Fuel Cells Operating in Human Physiological Fluids

Published as:

Design of Experiments Approach to Provide Enhanced Glucose-Oxidising Enzyme Electrode for Membrane-Less Enzymatic Fuel Cells Operating in Human Physiological Fluids

Richard Bennett, Isioma Osadebe, Rakesh Kumar, Peter Ó Conghaile and Dónal Leech. *Electroanalysis*, (2018) 30(7), 1438-1445.

Co-author contributions:

I wrote the adapted draft of the publication and performed lab work and the analysis required for the publication.

Isioma Osadebe synthesised the PVI-bound Os polymer and contributed through her initial involvement in the publication.

Rakesh Kumar and Peter Ó Conghaile contributed advice and guidance throughout the laboratory work and analysis.

Dónal Leech, as the project supervisor, contributed through advice and guidance throughout the work and wrote the final version of the publication.

Design of experiments approach to provide enhanced glucose-oxidising enzyme electrode for membrane-less enzymatic fuel cells operating in human physiological fluids

Richard Bennett, Isioma Osadebe, Rakesh Kumar, Peter Ó Conghaile, Dónal Leech*

School of Chemistry & Ryan Institute, National University of Ireland Galway, University Road, Galway, Ireland

DOI: 10.1002/elan.201600402

Abstract

Graphite electrodes are modified with a redox polymer, $[\text{Os}(4,4'\text{-dimethoxy-2,2'\text{-bipyridine})}_2(\text{polyvinylimidazole})_{10}\text{Cl}]^+$ ($E^{\circ'} = -0.02\text{ V vs Ag/AgCl (3M KCl)}$), crosslinked with a flavin adenine dinucleotide glucose dehydrogenase and multi-walled carbon nanotubes for electrocatalytic oxidation of glucose. The enzyme electrodes provide 52% higher current density, $1.22 \pm 0.1\text{ mA cm}^{-2}$ in 50 mM phosphate-buffered saline at 37 °C containing 5 mM glucose, when component amounts are optimised using a design of experiments approach compared to one-factor-at-a-time. Current densities of $0.84 \pm 0.15\text{ mA cm}^{-2}$ were achieved in the presence of oxygen for these enzyme electrodes. Further analysis of the model allowed for altering of the electrode components while maintaining similar current densities, $0.78 \pm 0.11\text{ mA cm}^{-2}$ with 34% less enzyme. Application of the cost-effective anodes in membrane-less enzymatic fuel cells is demonstrated by connection to cathodes prepared by co-immobilisation of $[\text{Os}(2,2'\text{-bipyridine})}_2(\text{polyvinylimidazole})_{10}\text{Cl}^+$ redox polymer, *Myrothecium verrucaria* bilirubin oxidase and multi-walled carbon nanotubes on graphite electrodes. Power densities of up to $285\text{ }\mu\text{W cm}^{-2}$, $146\text{ }\mu\text{W cm}^{-2}$ and $60\text{ }\mu\text{W cm}^{-2}$ are achieved in pseudo-physiological buffer, artificial plasma and human plasma respectively, showing promise for *in vivo* or *ex vivo* power generation under these conditions depending on power requirements for prototype devices.

Introduction

Enzymatic fuel cells (EFCs) are electrochemical devices that utilise biocatalysts for conversion of chemical energy to electrical energy [1-3]. In EFCs, enzymes replace the conventional metal catalyst providing improved specificity towards reactions they catalyse [1, 4, 5] allowing for development of miniaturised, potentially implantable or portable, membrane-less EFCs

through the elimination of the need for half-cell compartments and separating membranes [2-4, 6]. Enzyme catalysts operate under relatively mild conditions (20-40 °C, neutral pH), making them attractive for power generation *in vivo* utilising fuels and oxidants such as glucose and oxygen present in the bloodstream [7-9].

Redox polymer matrices for enzyme electrodes improve shuttling of electrons between active site and electrode surface, making electron transfer independent of orientation or proximity of the enzyme active site to the electrode surface, in comparison to that for direct electron-transfer mechanisms between enzyme and electrode [5, 10]. Current output from enzyme electrodes depends on selection of mediator with appropriate structure and suitable redox potential for rapid electron transfer between enzyme active site and electrode surface [11, 12]. Osmium-based mediators have been widely used [2, 13-15] owing to the ability to modulate the mediator redox potential of the central Os metal by using coordinating ligands, the relative stability of the resulting complexes in the Os(II)/Os(III) states, and because the hydrogel characteristics of redox-polymer films permit rapid mass and charge transport, thus generating substantial current signals [2, 16, 17]. The inclusion of multi-walled carbon nanotubes (MWCNTs) is one route towards improving glucose oxidation currents for enzyme electrodes prepared by crosslinking the nanomaterial with enzymes and osmium-based redox mediators [8, 18-20], attributed to improved retention of enzyme activity [21, 22]. Tsujimura *et al.* reported on similar bio anodes with magnesium oxide-templated mesoporous carbon as a support structure for hydrogels consisting of FADGDH and redox polymer [23].

We here report on optimisation of an enzyme electrode for glucose oxidation based on co-immobilisation of an $[\text{Os}(4,4'\text{-dimethoxy-2,2'}\text{-bipyridine})_2(\text{poly-vinyl imidazole})_{10}\text{Cl}]^+$ (Os(dmobpy)PVI) polymer, selected due to its lower redox potential, $-0.02\text{ V vs Ag/AgCl (3 M KCl)}$, compared to our previous studies using $[\text{Os}(4,4'\text{-dimethyl-2,2'}\text{-bipyridine})_2(\text{poly-vinylimidazole})_{10}\text{Cl}]^+$ (Os(dmbpy)PVI), and an enzyme [22]. A flavin adenine dinucleotide dependent glucose dehydrogenase (FADGDH) enzyme is selected over glucose oxidase due to its lack of reactivity with oxygen as co-substrate, for operation of an EFC in a membrane-less glucose/oxygen solution. Tremey *et al.* have shown improved performance of glucose oxidase in the presence of oxygen through mutation of the enzyme [24].

Enzyme electrode current output is dependent on the relative amount of components (osmium redox polymer, enzyme and MWCNTs) and optimisation is usually undertaken by varying one factor at a time. Kumar *et al.* [25] used a response surface design of experiment (DoE) methodology to optimise components used to construct enzyme electrodes. They reported a

32% increase in glucose oxidation current in comparison to that observed for enzyme electrodes optimised by varying of one factor at a time [25, 26].

Here we develop and validate a DoE methodology to optimise the enzyme electrode performance for current output under pseudo-physiological conditions (5 mM glucose, 50 mM phosphate buffered saline, PBS, pH 7.4, 37 °C). The DoE-optimised enzyme electrodes provide >50% improvement of glucose oxidation current density in absence of oxygen compared to previously reported values with the same components optimised using one-factor-at-a-time approach (OFAT) [22]. Tailoring of dropcoat amounts guided by contour plots from DoE software to include a lower amount of enzyme provides similar current density at 5 mM glucose concentrations while saving on enzyme amount required. Application of the selected anodes in membrane-less enzymatic fuel cells is demonstrated by connection to an oxygen-reducing *Myrothecium verrucaria* bilirubin oxidase-based cathode, operating in pseudo-physiological buffer, artificial plasma and human plasma respectively, showing promise for *in vivo* or *ex vivo* power generation under these conditions.

Experimental

Materials

All chemicals and biochemicals were purchased from Sigma-Aldrich, unless otherwise stated. The flavin dependent glucose dehydrogenase is from *Aspergillus sp.* (FADGDH 1.1.99.10, Sekisui, Cambridge, USA; product GLDE-70-1192). The *Myrothecium verrucaria* bilirubin oxidase (MvBOd) is provided by Amano Enzyme Inc. (Product BO-3, Nagoya, Japan). The MWCNTs (product 659258; Sigma-Aldrich) were pre-treated under reflux in concentrated nitric acid for 6 h and isolated by filtration. Polyethylene glycol diglycidyl ether (PEGDGE) was purchased from Sigma-Aldrich (average Mn ~ 526). All aqueous solutions unless otherwise stated were prepared in Milli-Q water (18 MΩ cm). The [Os(4,4'-dimethoxy-2,2'-bipyridine)₂(polyvinylimidazole)₁₀Cl]⁺ (Os(dmobpy)PVI) and [Os(2,2'-bipyridine)₂(polyvinylimidazole)₁₀Cl]⁺ (Os(bpy)PVI) redox polymers were synthesised according to literature procedures [27, 28].

Methods

Anode enzyme electrode preparation

Electrodes were prepared from graphite rods (Graphite store, USA, 3.0 mm diameter, NC001295) insulated with heat shrink tubing and the exposed disk polished on fine grit paper to create a geometric working surface area of 0.0707 cm². Enzyme electrode assembly was achieved by depositing appropriate volumes from 5 mg mL⁻¹ redox polymer aqueous solution, 10 mg mL⁻¹ FADGDH aqueous solution, 46 mg mL⁻¹ aqueous dispersion of acid-treated MWCNTs and 2 μL of a 15 mg mL⁻¹ PEGDGE aqueous solution on the surface of the graphite working electrode and allowing the deposition to dry for 24 h. The amount of each component of MWCNTs, Os(dmobpy)PVI and FADGDH added in the enzyme electrode preparation step is determined by the Design Expert Software (version 9, STAT-EASE Inc., Minneapolis, USA) using the low, central and high levels selected in Table 5.1.

Electrochemical measurements

Electrochemical tests were conducted using a CH Instrument 1030 multichannel potentiostat in a three electrode cell containing 50 mM phosphate buffer saline (PBS, 150 mM NaCl) pH 7.4, at 37 °C as electrolyte and a Ag/AgCl (3 M KCl) reference electrode, a graphite working electrode and a platinum mesh counter electrode (Goodfellow).

Fuel cell assembly and testing

The EFCs were constructed by combining anode enzyme electrodes with a previously described cathode [29], prepared as described for anode enzyme electrodes except using *MvBOd* as enzyme, Os(bpy)PVI as redox polymer and a volume of the 46 mg mL⁻¹ aqueous dispersion of acid-treated MWCNTs to provide 78 % w/w MWCNTs in the coating procedure. The EFC current and power densities were estimated from linear sweep voltammetry (LSV) obtained at 1 mV s⁻¹ and normalised to the geometric area of the current-limiting electrode. Oxygen saturation was estimated, by using a dissolved oxygen electrode and meter (EUTech Instruments), to occur at approximately 0.22 mM O₂, achieved by bubbling oxygen into the solution. The artificial plasma contained uric acid (68.5 mg L⁻¹), ascorbic acid (9.5 mg L⁻¹), fructose (36 mg L⁻¹), lactose (5.5 mg L⁻¹), urea (267 mg L⁻¹), glucose (916.5 mg L⁻¹), cysteine (18 mg L⁻¹), sodium chloride (6.75 g L⁻¹), sodium bicarbonate (2.138 g L⁻¹), calcium sulfate (23.8 mg L⁻¹), magnesium sulfate (104.5 mg L⁻¹) and bovine serum albumin (7 g L⁻¹) [30].

Results and Discussion

Enzyme electrodes were initially modified through the co-immobilisation of Os(dmobpy)PVI redox polymer, FADGDH and MWCNTs, using a PEGDGE di-epoxide cross-linker on graphite electrode. Cyclic voltammetry (CV) is used to characterise the Os(II/III) transition for the Os(dmobpy)PVI in the enzyme electrode for the presence and absence of substrate. CVs recorded at 1 mV s^{-1} scan rate in the absence of glucose display oxidation and reduction peaks centred at $-0.02 \text{ V vs Ag/AgCl}$, which is similar to the redox potential previously reported for the osmium polymer in solution and on electrode surface [16, 19, 31]. In the absence of substrate, peak currents vary linearly with scan rate at slow scan rates ($< 20 \text{ mV s}^{-1}$), thereby indicating a surface-confined response. At high scan rates ($> 20 \text{ mV s}^{-1}$), CVs display peak currents that scale linearly to the square roots of scan rates, which indicates semi-infinite diffusion control as expected for the formation of multi-layered films on electrode surface. The osmium surface coverage (Γ_{Os}) for the redox polymer is calculated by integrating the area under the peak for CVs recorded at slow scan rates, the Γ_{Os} is comparable to previously reported values in the presence of MWCNTs [19]. CV upon addition of glucose to the electrochemical cells, measured at slow scan rates, resulted in a sigmoidal-shaped response for enzyme electrodes (Figure 1), which is characteristic of an electrocatalytic (EC') process. A shift of $\sim 100 \text{ mV}$ for the half-wave potential ($E_{1/2}$) of the sigmoidal-shaped catalytic wave for enzyme electrodes in the presence of glucose in comparison to that observed in the absence of glucose is observed. Others have reported that a shift indicates glucose substrate transport limitation and occurs for a mixed-case between kinetic- and substrate-limited conditions [32, 33].

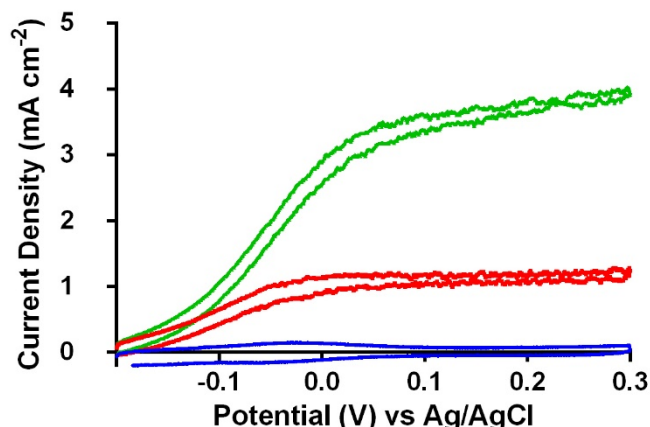


Figure 1 Slow scan rate, 1 mV s^{-1} , CV of Os(dmobpy)PVI ($80 \mu\text{g}$) films co-immobilised with FADGDH ($100 \mu\text{g}$) and MWCNTs ($410 \mu\text{g}$) in oxygen-free PBS containing no glucose (blue), 5 mM glucose (red) and 100 mM glucose (green) concentrations.

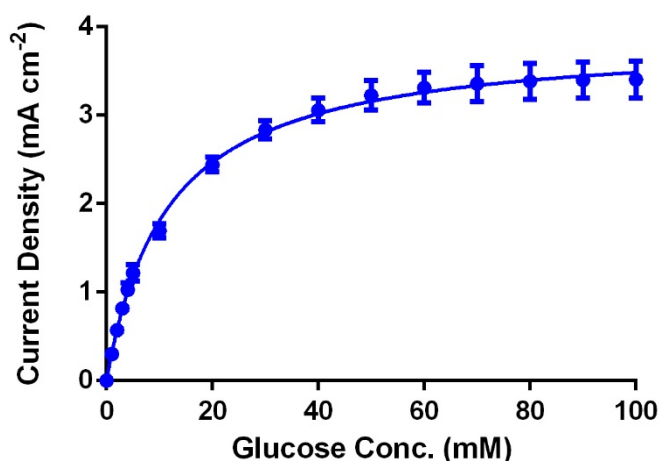


Figure 2: Glucose oxidation current densities as a function of glucose concentration, measured in oxygen-free PBS at $37 \text{ }^\circ\text{C}$ with stirring at 150 rpm at an applied potential of 0.15 V, for enzyme electrodes using Os(dmobpy)PVI ($80 \mu\text{g}$) co-immobilised with FADGDH ($100 \mu\text{g}$) and MWCNTs ($410 \mu\text{g}$).

Catalytic current densities for all anodes are extracted from steady state amperometry at an applied potential of 0.15 V, a potential selected to be in the region of the plateau current in the CV in the presence of 100 mM glucose (Figure 1) to ensure steady state current is achieved. Amperometric glucose oxidation current density is measured as a function of glucose concentrations (Figure 2). Amperometric current densities obtained are similar in magnitude to the catalytic plateau current densities observed with the slow-scan CV, thereby confirming steady state. An increase in glucose oxidation current density as a function of glucose concentration is observed, with substrate saturation at concentrations greater than 50 mM

glucose for all enzyme electrodes. Apparent Michaelis-Menten constants, K_M^{app} , and maximum current densities j_{max} can be estimated using non-linear least squares to fit the amperometric plots to the Michaelis-Menten equation. The K_M^{app} of 16 ± 1 mM is obtained for enzyme electrodes co-immobilised with Os(dmobpy)PVI, MWCNTs and FADGDH and is similar to values obtained from previous report [19, 21].

Design of Experiment

For the optimisation of bioanodes, a DoE based on response surface factorial Box–Behnken Design (BBD) with a three level factorial design is used to evaluate the main effect and interaction between the MWCNTs, osmium redox polymer and FADGDH components required to prepare glucose-oxidising enzyme electrodes. The Box-Behnken design requires an experiment number according to $N = 2k(k - 1) + C_0$ [34], where k is the number of factors, and C_0 is the number of central points. The 16 run (with n=3 electrodes used to determine the current density for each run) experimental design is used to demonstrate the relative significance of the bioanode components and seek to enhance current density in pseudo-physiological conditions, compared to OFAT approach. The range and level of components investigated is given in Table 1 and runs and results used to build the model given in Table 2.

Table 1: The factors and levels selected to vary for DoE optimisation of performance of enzyme electrode.

Factor/Level	Low (-1)	Central (0)	High (+1)
MWCNTs (μg)	0	300	600
Os(dmobpy)PVI (μg)	10	55	100
FADGDH (μg)	20	60	100

Table 2 Design layout showing the run number, component level and the response (current densities in mA cm⁻² measured amperometrically at 0.15 V vs Ag/AgCl in 5 mM glucose solution) and standard deviation (SD, n=3)

Run	Os(dmobpy)PVI	MWCNTs	FADGDH	Response	SD
1	-1	0	1	0.36	0.10
2	0	0	0	0.75	0.13
3	1	1	0	0.77	0.08
4	0	1	-1	0.58	0.04
5	0	0	0	0.85	0.10
6	-1	-1	0	0.23	0.08
7	0	-1	1	0.58	0.12
8	1	0	-1	0.63	0.14
9	-1	0	-1	0.21	0.07
10	0	0	0	0.70	0.10
11	0	-1	-1	0.39	0.05
12	1	0	1	0.79	0.11
13	1	-1	0	0.49	0.05
14	0	0	0	0.83	0.15
15	-1	1	0	0.14	0.05
16	0	1	1	0.87	0.24

The low levels of FADGDH and Os(dmobpy)PVI in this design are selected to be 20 µg and 10 µg respectively as a minimum level requirement for the production of glucose oxidation current density based on previous reports [2, 10, 14, 25, 35]. The high levels selected for each component are to eliminate difficulties in co-immobilisation and retention of higher amounts on electrode surface. For example, if higher amounts of the components are added, it is difficult to control the drop-coat on the electrode surface. The four runs for electrodes prepared using the central (0) component level, runs 2, 5, 10 and 14 in Table 2, achieve responses of 0.75 ± 0.13 , 0.85 ± 0.10 , 0.70 ± 0.10 and 0.83 ± 0.15 mA cm⁻², respectively, which, when all 12 electrode responses are considered together yield an average response of 0.77 ± 0.16 mA cm⁻² for the central component level. Replication of the central levels strengthens the model. The response can be presented by a quadratic equation,

$$y = b_0 + b_1x_1 + b_2x_2 + b_3x_3 + b_{11}x_1^2 + b_{22}x_2^2 + b_{33}x_3^2 + b_{12}x_1x_2 + b_{13}x_1x_3 + b_{23}x_2x_3 \quad (1)$$

where y is the predicted current response value in mA cm^{-2} , x_1 , x_2 and x_3 are the MWCNTs, redox polymer and enzyme amounts in μg used in the enzyme electrode preparation, b_0 is the constant coefficient (intercept), b_1 , b_2 , b_3 and b_{12} , b_{13} , b_{23} are linear and cross product coefficients, respectively, and the quadratic coefficients are b_{11} , b_{22} and b_{33} . The resulting response model from the 16 runs is

$$y = -0.15634 + 0.015719x_1 + 6.85648 \times 10^{-4}x_2 + 5.14236 \times 10^{-3}x_3 - 1.17901 \times 10^{-4}x_1^2 - 1.48611 \times 10^{-6}x_2^2 - 2.73438 \times 10^{-5}x_3^2 + 6.85185 \times 10^{-6}x_1x_2 + 1.38889 \times 10^{-6}x_1x_3 + 1.875 \times 10^{-6}x_2x_3 \quad (2)$$

In this response model, analysis of variance (ANOVA) is used for statistical testing and the data extracted demonstrates whether or not the model is statistically significant [36]. The low F -value (19.43) and p -value (0.0009) evaluated suggests that the model is statistically significant, as the higher the values, the more likely the rejection of the null hypothesis that the data show no variation. Furthermore, a coefficient of determination (R^2) between predicted and observed responses was evaluated to be 0.97, and when the amount of variation in the model was adjusted the measure of the adjusted R^2 (Adj R^2) value is 0.92, thereby suggesting significant correlation. These results are similar to those observed previously by Kumar *et al.* [25] for enzyme electrodes prepared by co-immobilisation of MWCNTs, GOx, osmium redox complex and carboxymethylated dextran on graphite and current measured in physiological conditions.

Model Validation and Optimised Enzyme Electrode

In order for a system to be optimised, it is imperative to demonstrate that the model is a reasonable representation of the actual system and that it reproduces system behaviour with enough fidelity to satisfy analysis objectives. Model validation was tested based on values randomised by the model together with their predicted results under pseudo-physiological conditions (5 mM glucose, 50 mM phosphate buffered saline, PBS, pH 7.4, 37 °C), with the results presented in Table 3. A plot of predicted current density versus observed current density delivers a correlation (R^2) of 0.87 suggesting that the model is valid.

Table 3: Model validation comparing predicted versus actual (at 0.15 V) amperometric current density response for enzyme electrodes under pseudo-physiological conditions. Conditions as in Table 2. Errors are from the predicted standard deviation from the model for the predicted current density or from the standard deviation of 4 electrodes for the actual current density.

Os(dmoby) PVI (μg)	MWCNTs (μg)	FADGDH (μg)	Predicted Current density mA cm^{-2}	Actual Current density mA cm^{-2}
56	316	63	0.80 ± 0.07	0.81 ± 0.05
100	316	63	0.78 ± 0.07	0.89 ± 0.04
100	600	63	0.81 ± 0.07	0.88 ± 0.07
100	600	97	0.88 ± 0.07	1.07 ± 0.13
100	600	26	0.67 ± 0.07	0.96 ± 0.09
100	291	26	0.64 ± 0.07	0.78 ± 0.15
54	600	26	0.59 ± 0.07	0.60 ± 0.09
100	600	100	0.89 ± 0.07	1.06 ± 0.27

Following the response achieved from enzyme electrodes prepared using this model, the FADGDH and MWCNTs amounts were shown to be the main factors contributing to the enhanced current densities (see Figure 3). A previous report has shown that the addition of MWCNTs on the enzyme electrode increased the amount of redox polymer that is co-immobilised and electronically coupled within the enzyme films leading to greater current response [21]. Variation in the amount of the Os(dmoby)PVI, once added, have the smallest effect of the three components.

The DoE optimum component amounts, based on maximising the predicted current density using equation 2, are $80 \mu\text{g}$ redox polymer, $410 \mu\text{g}$ MWCNTs and $100 \mu\text{g}$ FADGDH, predicted to deliver a current density of $0.93 \pm 0.07 \text{ mA cm}^{-2}$ in PBS containing 5 mM glucose. An actual measured current density of $1.22 \pm 0.1 \text{ mA cm}^{-2}$ ($n=4$) is obtained for the enzyme electrodes prepared using the DoE determined optimum component amounts. This represents a 52% increase on the response, under similar conditions, for enzyme electrodes (0.8 mA cm^{-2}) using the same components and a OFAT method of optimisation of response [22].

The electrochemical response for the optimised enzyme electrodes is shown in Figure 1 and 2, demonstrating a maximum current density j_{max} of $3.41 \pm 0.21 \text{ mA cm}^{-2}$ for the electrode under glucose saturation (100 mM) conditions in comparison to previously reported j_{max} of $2.30 \pm 0.31 \text{ mA cm}^{-2}$ for the same enzyme electrode using the OFAT optimised component amounts.

Prior to incorporation of the optimised anode in a fuel cell setup a further round of testing was conducted based on consideration of the contour plot generated for FADGDH versus MWCNTs levels (Figure 3). The consideration of the contour plots and predicted response by variation in FADGDH and MWCNT amounts (Table 4) demonstrates that little variation in current density is observed in the region of 0.5 to 1.0 FADGDH and MWCNT levels (Figure 4). Thus the selected amounts for each of these factors can be altered depending on other factors to be considered in manufacturing enzyme electrodes, such as cost of materials or ease of electrode preparation.

Table 4: Predicted current densities from the model upon altering the amount of enzyme and MWCNTs on the electrode surface, using 80 μg for Os polymer. The errors are the predicted errors from the model.

MWCNTs (μg)	FADGDH (μg)	Predicted Current Density (mA cm^{-2})
410	100	0.93 ± 0.07
500	100	0.93 ± 0.07
600	100	0.91 ± 0.07
410	80	0.90 ± 0.07
500	64	0.87 ± 0.07
540	64	0.86 ± 0.07
600	64	0.86 ± 0.07

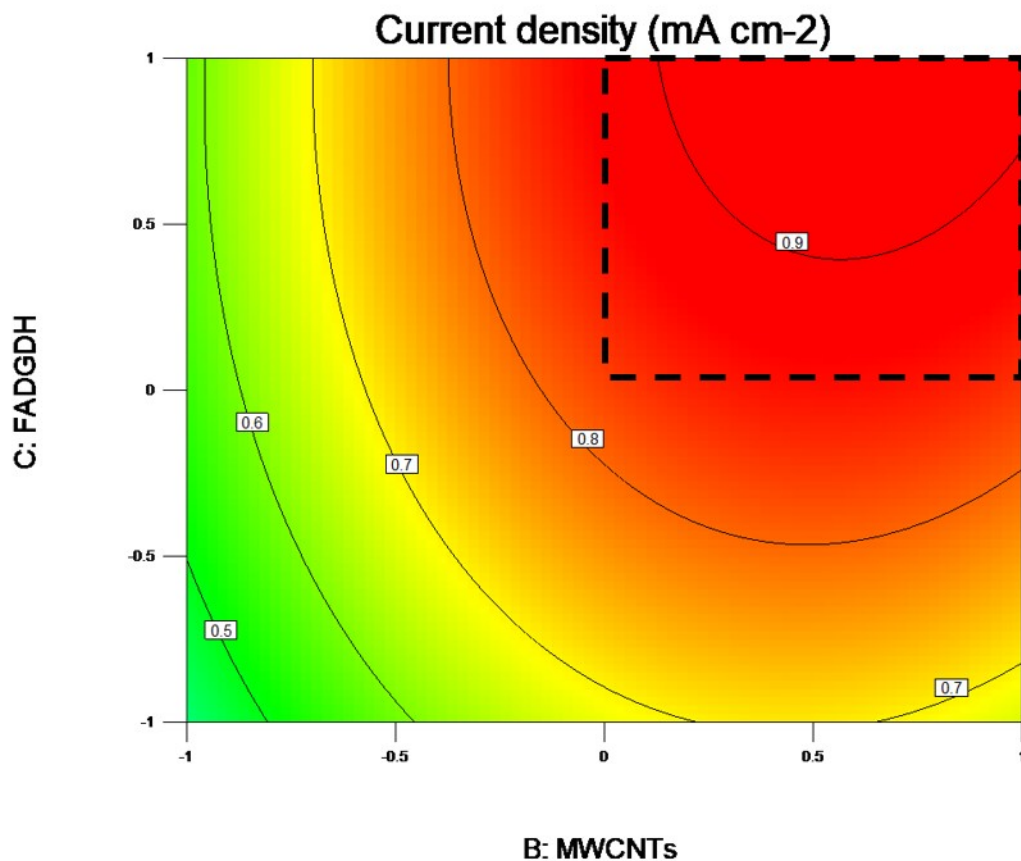


Figure 3: Contour plot for FADGDH vs MWCNTs showing glucose oxidation current density values predicted from the model (equation 2) attributed for each contour in mA cm⁻². The area outlined by the dotted black line shows relative component amounts that predict high current responses.

For example, use of lower amounts of enzyme makes the anode less expensive to produce while maintaining a high current response. A compromise amount of FADGDH of 64 μg and 540 μg of MWCNT is selected to maintain a high current response. This selected anode was used for fuel cell testing with component amounts of Os(dmobpy)PVI (80 μg), FADGDH (64 μg) and MWCNTs (540 μg) which is predicted to deliver $0.86 \pm 0.07 \text{ mA cm}^{-2}$. Testing of the enzyme electrode anodes generated a current density of $1.0 \pm 0.1 \text{ mA cm}^{-2}$ ($n=3$) in 5 mM glucose solutions. These enzyme electrode anodes produce a maximum current density j_{max} of $2.63 \pm 0.73 \text{ mA cm}^{-2}$ in solutions of 100 mM glucose concentrations.

Operation in Oxygen

The selected bioanodes were further tested in the presence of oxygen in order to evaluate the effect of oxygen on these enzyme electrodes for eventual application in membrane-less EFCs. A 17% decrease in current density is observed for the enzyme electrode operating in 5 mM

glucose concentration in the presence of oxygen, compared to the absence of oxygen, Figure 4. The decrease in glucose currents in the presence of oxygen suggests that molecular oxygen is reduced by the osmium redox polymer, which in turn decreases the amount of osmium redox centres that can be accessed by the electrons from glucose substrate, thus decreasing current density in the presence of oxygen, as reported on recently [16, 22, 37].

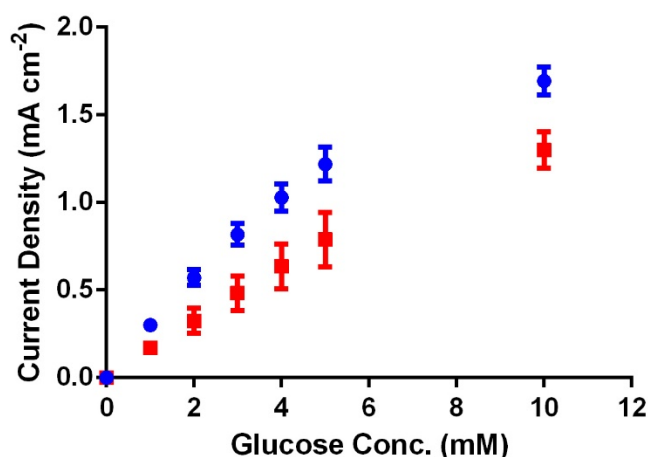


Figure 4: Glucose oxidation current density observed as a function of glucose concentration for the selected enzyme electrode (Os(dmobpy)PVI (80 μg) co-immobilised with FADGDH (100 μg) and MWCNTs (410 μg) measured in PBS at 37 $^{\circ}\text{C}$ with stirring at 150 rpm at an applied potential of 0.15 V, for enzyme electrodes in the presence (red) and absence of oxygen (blue).

Enzymatic Fuel Cell Testing

Enzymatic fuel cells were assembled based on the utilisation of glucose as fuel and oxygen as oxidant for testing under pseudo-physiological conditions using anodes prepared by co-immobilisation of Os(dmobpy)PVI redox polymers with FADGDH and MWCNTs using amounts optimised from the DoE approach. Enzyme electrodes chosen as cathodes are based on previous reports [22, 29] of Os(bpy)PVI redox polymer co-immobilised with *Mv*BOd and 78% w/w MWCNTs on graphite electrodes of the same geometric area as the anodes.

A potential application for EFC system is to power implantable medical devices via the oxidation of glucose as fuel and the reduction of oxygen as oxidant available in the bloodstream. Assembled EFC were therefore first tested in pseudo-physiological buffer conditions containing 0.2 mM O_2 . For these EFCs, average power density of $270 \pm 15 \mu\text{W cm}^{-2}$ is achieved (Figure 5) with a maximum power output of $285 \mu\text{W cm}^{-2}$. The polarisation curves

(Figure 6) for enzyme electrodes and the assembled EFC indicate that the cathode current density limits power produced. The maximum power density is observed at ~ 0.3 V similar to that obtained previously [22]. Others have reported on a membrane-less EFC operating at higher cell voltages. For example, Kim *et al.* [38] report on an EFC producing a power density of $50 \mu\text{W cm}^{-2}$ at a 0.5 V cell voltage under physiological conditions (air saturated pH 7.4, 140 mM NaCl, 37.5°C in 15 mM glucose concentration) with the increased voltage due to the differences in redox potential of the osmium redox polymers selected. Due to differences in operating conditions, such as pH, glucose concentrations and also electrode preparation methodologies, comparison with other EFC results has proven difficult. Nonetheless our results compare well with those reported on for similar systems. For example, Soukharev *et al.* [39] report an EFC using GOx and a fungal laccase, co-immobilised with osmium redox polymers on $7 \mu\text{m}$ diameter, 2 cm long carbon fibres, produces a power density of $350 \mu\text{W cm}^{-2}$ in 15 mM glucose solutions. However, when the same EFC is tested for operation in 5 mM glucose solutions and using GOx sourced from *Penicillium pinophilum*, a power density of $280 \mu\text{W cm}^{-2}$ is achieved [40] similar to the maximum power density obtained in Figure 6. More recently MacAodha *et al.* [29] report on an EFC operating in pseudo-physiological conditions using a GDH enzyme but co-immobilised with Os(dmbpy)PVI redox polymer at the anode while *Myceliophthora thermophila* laccase enzyme was used at the biocathode that produced a power density in 5 mM glucose solutions of $145 \mu\text{W cm}^{-2}$.

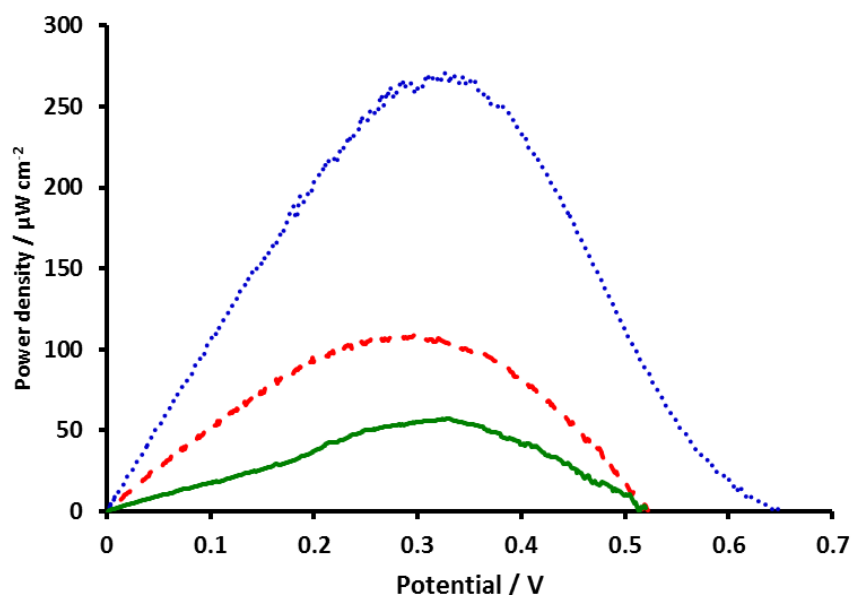


Figure 5: Power curves recorded for membrane-less enzymatic fuel cells using 1 mV s^{-1} linear sweep voltammetry in 50 mM PBS, at 37°C , containing 5 mM glucose (blue dots), artificial plasma (red dash) and human plasma (green solid) for optimised bioanodes prepared by co-immobilisation of Os(dmoby)PVI $80 \mu\text{g}$ with FADGDH $64 \mu\text{g}$ and MWCNTs $540 \mu\text{g}$. Cathode enzyme electrodes prepared by co-immobilisation of Os(bpy)PVI, MWCNT and *MvBOd*. Power densities normalised to the geometric area of the current-limiting electrode.

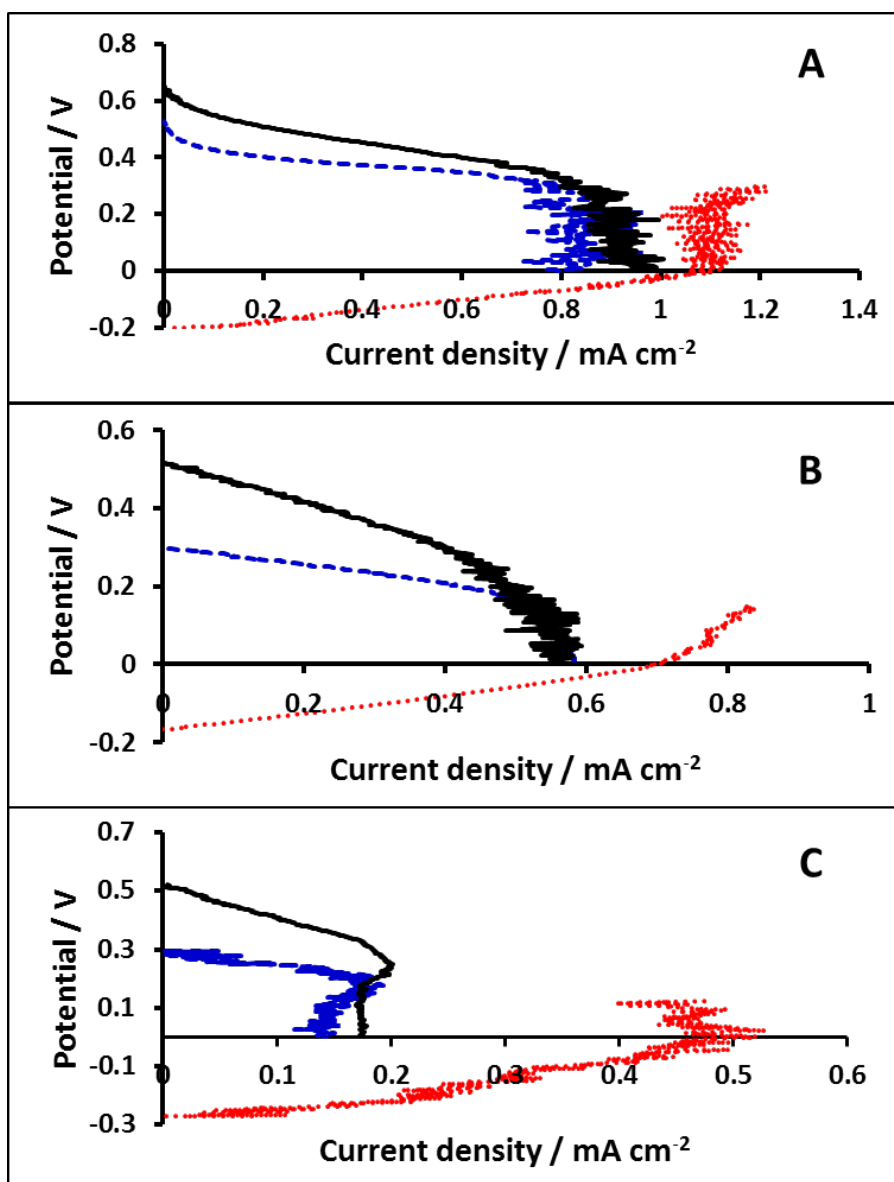


Figure 6: Polarisation curves from 1 mV s^{-1} linear sweep voltammetry recorded in 5 mM glucose and O_2 at $37 \text{ }^\circ\text{C}$ for optimised enzyme electrodes prepared by co-immobilisation of $\text{Os}(\text{dmbpy})\text{PVI}$ $80 \text{ }\mu\text{g}$ co-immobilised with FADGDH $64 \text{ }\mu\text{g}$ and MWCNTs $540 \text{ }\mu\text{g}$ (red dotted line) as anodes and a cathode enzyme electrode prepared by co-immobilisation of $Mv\text{BOd}$ and $\text{Os}(\text{bpy})\text{PVI}$ (blue dashed line) reported vs Ag/AgCl , and for the enzyme electrodes assembled as a membrane-less fuel cell (black solid line) operating in PBS (A), artificial plasma (B) and human plasma (C). Current densities normalised to electrode geometric area for anode and cathode and to the geometric area of the current-limiting electrode for the EFC.

To verify that EFC can produce power under more realistic sample conditions the assembled EFCs were operated in an artificial plasma recipe solution [30], providing an average power density of $109 \pm 37 \text{ }\mu\text{W cm}^{-2}$ (Figure 5) with a maximum power output of $146 \text{ }\mu\text{W cm}^{-2}$. Maximum power output produced in artificial plasma is approximately half that observed for the same EFC operating in PBS: a similar change has been reported by MacAodha *et al.* achieving a power density of $60 \text{ }\mu\text{W cm}^{-2}$ [29]. This difference in power output observed

between artificial plasma and PBS is probably due to the presence of antioxidants and enzyme-inhibiting compounds in the artificial plasma solutions [41-43]. In addition, an oxygen concentration of only 0.06 mM was measured in the plasma, achieved by oxygen sparging through the solution, compared to 0.125 mM measured in the PBS. To evaluate the factors limiting the power output for the EFCs, polarisation curves at the anode and cathode enzyme electrodes from the 1 mV s^{-1} slow scan CVs can be combined to model cell polarisation curves for each EFC (see Figure 6). The polarisation curves indicate that the current at the cathode (as cathode and anode areas are the same) limits power produced at the assembled fuel cell under these conditions.

Further experiments were conducted to test for EFC operation in human plasma in an attempt to evaluate the effect of the deployment in real solutions. The human plasma sample was used as purchased. An average power density of $53 \pm 9 \mu\text{W cm}^{-2}$ (Figure 6) with a maximum power output of $60 \mu\text{W cm}^{-2}$ is achieved for the EFC this sample. The maximum power output observed for human plasma is approximately half of that observed in artificial plasma. This difference is possibly due to the fact that blood plasma contains additional components such as blood clotting factors, lipids, hormones, enzymes, antibodies, and other proteins/components not present in artificial plasma, some of which are enzyme-inhibiting [44]. Although the oxygen concentration measured in human plasma is 0.1 mM and similar to a previous reported value [43, 45], the power density achieved is lower in comparison to that observed in artificial plasma which is most likely due to the effect that additional components in the plasma have on the cathode as the polarisation curves for the EFC (Figure 6) indicate that the cathode still limits the power produced in the EFC.

Others have reported on EFC operation in real samples. For example, an EFC based on direct electron transfer by cellobiose dehydrogenase enzyme at the anode and *Mv*BOD enzyme at the cathode was operated in human serum, human plasma and human blood samples [42], where no significant change in power output between PBS and real physiological solutions were observed, but a maximum power density of only $4 \mu\text{W cm}^{-2}$ obtained. A recent study on an EFC utilising FADGDH with a ferrocene redox hydrogel as bioanode and direct electron transfer at the biocathode using *Mv*BOD immobilised onto multi-walled carbon nanotubes modified with anthracene moieties reported power densities of $\sim 58 \mu\text{W cm}^{-2}$ and $\sim 45 \mu\text{W cm}^{-2}$ in human serum and citrate/phosphate buffer respectively at $37 \text{ }^\circ\text{C}$ [7]. Ó Conghaile *et al.* [45] report on an EFC constructed using enzyme electrodes of Os(dmbpy)PVI, MWCNTs, and a de-glycosylated pyranose dehydrogenase at anodes and *Mv*BOD on a gold-nanoparticle modified electrode substrate as cathode. Power densities of up to $275 \pm 50 \mu\text{W cm}^{-2}$ were

achieved in pseudo physiological conditions, and $73 \pm 7 \mu\text{W cm}^{-2}$ when tested in whole human blood [45, 46].

Conclusions

Enzyme electrode components were optimised using DoE methodology for application in physiologically relevant glucose solutions. Current densities of $1.22 \pm 0.1 \text{ mA cm}^{-2}$ were achieved at 5 mM glucose concentration in the absence of oxygen with $0.84 \pm 0.15 \text{ mA cm}^{-2}$ produced in the presence of oxygen. This represents a >50% increase on previously reported enzyme electrodes optimised using OFAT approach in absence of oxygen. Consideration of the model allowed for altering the electrode components to minimise cost while providing high current outputs. This suggests that at biologically relevant concentrations there is no precise optimal surface concentration but a range of values where high current outputs are achievable in the presence of oxygen. Further testing is required to provide a more robust model for current response. EFCs were assembled and tested for power generation to compare performances in oxygenated PBS, artificial plasma and human plasma using the optimised anode coupled to a cathode containing *Mv*BOD co-immobilised with Os(bpy)₃PVI and MWCNTs. The fuel cells were cathode limiting showing the need for further cathodic improvement to increase power output from the EFC. The assembled membrane-less EFCs produced power densities of $285 \mu\text{W cm}^{-2}$, $146 \mu\text{W cm}^{-2}$ and $60 \mu\text{W cm}^{-2}$ in PBS, artificial plasma and human plasma respectively.

Acknowledgements

RB acknowledges support through an NUI Galway College of Science fellowship and an Irish Research Council postgraduate scholarship. IO acknowledges support through an NUI Galway College of Science fellowship. RK acknowledges support from the Earth and Natural Science Doctoral Studies Programme funded by the Higher Education Authority (HEA) through the Programme for Research at Third-Level Institutions, Cycle 5 (PRTL-5) and co-funded by the European Regional Development Fund (ERDF). POC acknowledges support through a Science Foundation Ireland Technology Innovation Development Award.

References

- [1] A. Heller, *Phys. Chem. Chem. Phys.* **2004**, *6*, 209.
- [2] A. Heller, B. Feldman, *Acc. Chem. Res.* **2010**, *43*, 963.
- [3] A. Heller, *AIChE J.* **2005**, *51*, 1054.
- [4] S.C. Barton, J. Gallaway, P. Atanassov, *Chem. Rev.* **2004**, *104*, 4867.
- [5] D. Leech, P. Kavanagh, W. Schuhmann, *Electrochim. Acta* **2012**, *84*, 223.
- [6] T. Chen, S.C. Barton, G. Binyamin, Z. Gao, Y. Zhang, H.-H. Kim, A. Heller, *J. Am. Chem. Soc.* **2001**, *123*, 8630.
- [7] R.D. Milton, K. Lim, D.P. Hickey, S.D. Minter, *Bioelectrochem.* **2015**, *106*, 56.
- [8] P. Ó Conghaile, D. MacAodha, B. Egan, P. Kavanagh, D. Leech, *J. Electrochem. Soc.* **2013**, *160*, G3165.
- [9] S. Tsujimura, M. Fujita, H. Tatsumi, K. Kano, T. Ikeda, *Phys. Chem. Chem. Phys.* **2001**, *3*, 1331.
- [10] A. Heller, *Phys. Chem. Chem. Phys.* **2004**, *6*, 209.
- [11] A.E.G. Cass, G. Davis, G.D. Francis, H.A.O. Hill, W.J. Aston, I.J. Higgins, E.V. Plotkin, L.D.L. Scott, A.P.F. Turner, *Anal. Chem.* **1984**, *56*, 667.
- [12] S.M. Zakeeruddin, D.M. Fraser, M.K. Nazeeruddin, M. Grätzel, *J. Electroanal. Chem.* **1992**, *337*, 253.
- [13] Y. Ackermann, D.A. Guschin, K. Eckhard, S. Shleev, W. Schuhmann, *Electrochem. Comm.* **2010**, *12*, 640.
- [14] F. Mao, N. Mano, A. Heller, *J. Am. Chem. Soc.* **2003**, *125*, 4951.
- [15] M.D. Scanlon, U. Salaj-Kosla, S. Belochapkine, D. MacAodha, D. Leech, Y. Ding, E. Magner, *Langmuir* **2011**, *28*, 2251.
- [16] A. Prévot, N. Mano, *Electrochim. Acta* **2013**, *112*, 318.
- [17] D. MacAodha, M.L. Ferrer, P. O'Conghaile, P. Kavanagh, D. Leech, *Phys. Chem. Chem. Phys.* **2012**, *14*, 14667.
- [18] B. Reuillard, A. Le Goff, C. Agnes, M. Holzinger, A. Zebda, C. Gondran, K. Elouarzaki, S. Cosnier, *Phys. Chem. Chem. Phys.* **2013**, *15*, 4892.
- [19] D. MacAodha, P. Ó Conghaile, B. Egan, P. Kavanagh, C. Sygmund, R. Ludwig, D. Leech, *Electroanalysis* **2013**, *25*, 94.
- [20] P. Kavanagh, D. Leech, *Phys. Chem. Chem. Phys.* **2013**, *15*, 4859.
- [21] I. Osadebe, D. Leech, *ChemElectroChem* **2014**, *1*, 1988.
- [22] I. Osadebe, P. Ó Conghaile, P. Kavanagh, D. Leech, *Electrochim. Acta* **2015**, *182*, 320.
- [23] S. Tsujimura, K. Murata, W. Akatsuka, *J. Am. Chem. Soc.* **2014**, *136*, 14432.

- [24] E. Tremey, C. Stines-Chaumeil, S. Gounel, N. Mano, *ChemElectroChem*, **2017**, *4*, 2520.
- [25] R. Kumar, D. Leech, *Bioelectrochem.* **2015**, *106*, 41.
- [26] R. Kumar, D. Leech, *J. Electrochem. Soc.* **2014**, *161*, H3005.
- [27] E.M. Kober, J.V. Caspar, B.P. Sullivan, T.J. Meyer, *Inorg. Chem.* **1988**, *27*, 4587.
- [28] R.J. Forster, J.G. Vos, *Macromolecules* **1990**, *23*, 4372.
- [29] D. MacAodha, P.Ó Conghaile, B. Egan, P. Kavanagh, D. Leech, *ChemPhysChem* **2013**, *14*, 2302.
- [30] C. A. Burtis and E. R. Ashwood (eds.), *Tietz Fundamentals of Clinical Chemistry* W. B. Saunders Co., Philadelphia, Pennsylvania, 4th ed., **1996**.
- [31] C. Taylor, G. Kenausis, I. Katakis, A. Heller, *J. Electroanal. Chem.* 1995, 396, 511.
- [32] P.N. Bartlett, K.F.E. Pratt, *J. Electroanal. Chem.* 1995, 397, 61.
- [33] B.T. Limoges, J. Moiroux, J.-M. Savéant, *J. Electroanal. Chem.* 2002, 521, 8.
- [34] B. Qi, X. Chen, F. Shen, Y. Su, Y. Wan, *Ind. & Eng. Chem. Res.* **2009**, *48*, 7346.
- [35] E.J. Calvo, C. Danilowicz, L. Diaz, *J. Chem. Soc., Faraday Trans.* **1993**, *89*, 377.
- [36] G. Chen, J. Chen, C. Srinivasakannan, J. Peng, *Appl. Surf. Sci.* **2012**, *258*, 3068.
- [37] A. PrévotEAU, N. Mano, *Electrochim. Acta* **2012**, *68*, 128.
- [38] H.-H. Kim, N. Mano, Y. Zhang, A. Heller, *J. Electrochem. Soc.* **2003**, *150*, A209.
- [39] V. Soukharev, N. Mano, A. Heller, *J. Am. Chem. Soc.* **2004**, *126*, 8368.
- [40] N. Mano, *Chem. Comm.* **2008**, 2221.
- [41] E. Magner, *Analyst* **2001**, *126*, 861.
- [42] V. Coman, R. Ludwig, W. Harreither, D. Haltrich, L. Gorton, T. Ruzgas, S. Shleev, *Fuel Cells* **2010**, *10*, 9.
- [43] C. Kang, H. Shin, Y. Zhang, A. Heller, *Bioelectrochem.* **2004**, *65*, 83.
- [44] A.C. Guyton, J.E. Hall, *Textbook of Medical Physiology*, 11th ed., Elsevier Saunders, Philadelphia, PA, **2006**.
- [45] P. Ó Conghaile, M. Falk, D. MacAodha, M.E. Yakovleva, C. Gonaus, C.K. Peterbauer, L. Gorton, S. Shleev, D. Leech, *Anal. Chem.* **2016**, *88*, 2156.
- [46] M. Cadet, S. Gounel, C. Stines-Chaumeil, X. Brilland, J. Rouhana, F. Louerat, N. Mano, *Biosens. & Bioelectron.*, **2016**, *83*, 60.

Chapter 4: Effect of individual plasma components on the performance of a glucose enzyme electrode based on redox polymer mediation of a flavin adenine dinucleotide-dependent glucose dehydrogenase

Published as:

Effect of individual plasma components on the performance of a glucose enzyme electrode based on redox polymer mediation of a flavin adenine dinucleotide-dependent glucose dehydrogenase

Richard Bennett, Estelle Blochouse and Dónal Leech. *Electrochimica Acta* (2019) 302, 270-276.

Co-author contributions:

I synthesised the PVI-bound osmium redox polymer, performed the lab work, the analysis and wrote the first draft of the publication.

Estelle Blochouse contributed to the publication through involvement in performing the lab work.

Dónal Leech, as the project supervisor, contributed through advice and guidance and wrote the final draft of the publication.

Effect of individual plasma components on the performance of a glucose enzyme electrode based on redox polymer mediation of a flavin adenine dinucleotide-dependent glucose dehydrogenase

*Richard Bennett, Estelle Blochouse, Dónal Leech**

School of Chemistry & Ryan Institute, National University of Ireland Galway, University Road, Galway, Ireland

DOI: 10.1016/j.electacta.2019.02.039

Abstract

The performance of glucose enzyme electrodes, consisting of crosslinked flavin adenine dinucleotide glucose dehydrogenase (FADGDH), an osmium redox polymer and multi-walled carbon nanotubes on graphite electrodes, was tested in phosphate buffered saline, artificial plasma and the individual components of artificial plasma to assess the effect of each component on current response and operational stability of the response to better understand the decrease in electrode performance observed in blood. Electrodes tested in artificial plasma show a significant decrease in current response in 5 mM glucose, and operational stability of the response in 100 mM glucose, compared to electrodes tested in buffer. The lowest current response for the enzyme electrodes was observed in the presence of physiological level of uric acid although the largest alteration to enzyme affinity, as estimated from the apparent Michaelis-Menten constant, occurred upon addition of physiological level of sodium bicarbonate. The operational stability observed in the presence of uric acid was the lowest of all components tested, with only 46 % of initial current response after 12 hours and was comparable to the 27% of current remaining after 12 hours for electrodes operating in artificial plasma. The effect of uric acid on glucose oxidation by enzyme electrodes prepared using both glucose oxidase (GOx) and a recombinant cellobiose dehydrogenase (CDH) was assessed. The maximum current decreased for both FADGDH and GOx enzyme electrodes in the presence of uric acid, with no significant change to the enzyme affinity, suggesting non-competitive inhibition. The CDH based electrodes provided highest stability of current signal in buffer, with 86 % of the initial signal present after 12 hours, but display significant change enzyme affinity, maximum current and operational stability, dropping to only 33%, in the presence of

uric acid. In contrast the operational stability of the GOx-based enzyme electrodes was unaffected by the presence of physiological level of uric acid. As uric acid and sodium bicarbonate are present in blood, these results highlight the importance of enzyme selection for *in vivo* biosensing and biofuel cell applications. Further work is required to understand the mechanism of uric acid inhibition on each of the enzymes.

Introduction

A fuel cell couples the electrocatalytic oxidation of a fuel at an electrode with the reduction of an oxidant at a separate electrode to generate power. These reactions occur readily at electrodes using traditional metal-based catalysts. However, numerous disadvantages are associated with implementation of non-specific transition metals as catalysts: the electrode can be easily poisoned, lacks specificity, operates most efficiently under harsh conditions (temperature and pH) and requires a membrane to separate the electrode compartments.[1–4] The use of enzymes as catalysts immobilised at electrode surfaces offers solutions to these drawbacks. Enzyme electrodes are specific, operate under physiological conditions and do not require a membrane to operate, allowing for miniaturisation of enzymatic fuel cells (EFCs). EFCs operate by using enzymes to oxidise a fuel at the anode such as glucose while reducing an oxidant, such as molecular oxygen, at the cathode.[5–10] As the fuel and oxidant are readily available in the human body, powering of implantable or semi-implantable devices by miniaturised EFCs using immobilised enzyme biofilms is one potential application.[1,11–15]

Efficient electron transfer from the enzyme active site to the electrode surface is required in order for sufficient current generation by the electrode. Direct electron transfer (DET) and mediated electron transfer (MET) are the two routes of electron transfer between enzyme and electrode. If the active site of the enzyme is greater than 2 nm from the electrode surface DET becomes difficult to achieve. [16–18] For this reason, redox centres are immobilised in the biofilm as mediators to shuttle electrons from the active site to the surface. Osmium based redox polymers co-immobilised at the electrode surface are widely used mediators as they are relatively stable in the Os(II)/Os(III) states, have tunable redox potentials and the polymer films allow fast charge and mass transport resulting in high current generation.[19–22]

Inclusion of a multifunctional crosslinker such as poly(ethylene glycol) diglycidyl ether (PEGDGE) and nano-supports such as multi-walled carbon nanotubes (MWCNTs) in the biofilm improves the stability and magnitude of current signal generated from the glucose oxidising electrodes.[21,23] The MWCNTs provide a larger surface area for the electrode,

leading to higher production of current density.[24,25] Electrodes consisting of co-immobilised osmium-based redox centres with nano-supports and enzyme to form enzymatic fuel cells have been widely reported.[26–30]

We recently reported on a design of experiments-based optimisation process for maximising current generation from glucose oxidising electrodes prepared using a flavin adenine dinucleotide dependent glucose dehydrogenase (FADGDH), osmium based redox polymer, MWCNTs and PEGDGE. Current densities of $1.2 \pm 0.1 \text{ mAcm}^{-2}$ in 5 mM glucose in the absence of oxygen and $0.8 \pm 0.2 \text{ mAcm}^{-2}$ in the presence of oxygen were achieved. For fuel cell testing, oxygen reducing cathodes consisting of *Myrothecium verrucaria* bilirubin oxidase, MWCNTs and osmium redox polymer were coupled to the glucose oxidising electrodes yielding power densities of $285 \mu\text{Wcm}^{-2}$ in phosphate buffered saline (PBS), and $146 \mu\text{Wcm}^{-2}$ in artificial plasma.[31] The poor long term stability, coupled to the low power output, from EFC remain major roadblocks towards continuous use implantable and semi-implantable EFC devices.[32–35] One of the major reasons for low current output and lack of stability is the impact that interfering molecules have on performance of the electrodes.[36–42]

Here we report on testing of glucose oxidising enzyme electrodes in PBS, artificial plasma and stability of the glucose oxidation current over a 12-hour window in the presence of each interfering molecule present in artificial plasma is measured to assess the impact on enzyme electrode performance. In addition, FADGDH was replaced as glucose oxidising enzyme by glucose oxidase (GOx) or cellobiose dehydrogenase (CDH) in the presence of an interfering molecule to gain greater understanding of the importance of enzyme catalyst on the deterioration of current response and stability of the biofilms.

Experimental

Materials

The redox polymer $[\text{Os}(2,2'\text{-bipyridine})_2(\text{poly-vinylimidazole})_{10}\text{Cl}]^+$ (Os(bpy)PVI), was synthesised by modification of procedures found in the literature. [43,44] All chemicals were purchased from Sigma-Aldrich, unless otherwise stated. The flavin dependent glucose dehydrogenase is from *Aspergillus sp.* (FADGDH 1.1.99.10, Sekisui, Cambridge, USA; product GLDE-70-1192). The glucose oxidase is from *Aspergillus niger* (GOx, EC 1.1.3.4., Sigma-Aldrich). The flavodehydrogenase domain of *Corynascus thermophilus* CDH (rCtCDH) was heterologously expressed in the methylotrophic yeast *Pichia pastoris* and purified as previously described. [45] The MWCNTs (Sigma-Aldrich) were pretreated in

concentrated nitric acid under reflux for 6 hours followed by washing and filtration. The PEGDGE was purchased from Sigma-Aldrich (average Mn~526). Milli-Q water (18 MΩcm) was used to prepare all aqueous solutions unless otherwise stated.

Methods

Graphite electrodes were prepared to give a geometric working surface area of 0.0707 cm² by insulating graphite rods (Graphite store, USA, 3.0 mm diameter, NC001295) with heat shrink tubing and polishing the exposed surface on fine grit paper. Enzyme electrodes were prepared through deposition of 16 μL of a 5 mg mL⁻¹ redox polymer aqueous solution, 2 μL of a 15 mg mL⁻¹ PEGDGE aqueous solution, 8.88 μL of a 46.25 mg mL⁻¹ MWCNT aqueous dispersion and sufficient quantity of enzyme (aqueous solution) to achieve a deposition of 0.1 mg of enzyme per electrode. All electrodes were allowed to stand for 24 hours to ensure the biofilm had cured.

Electrochemical testing was performed using a CH Instrument 1030a multichannel potentiostat with a three electrode cell containing 50 mM PBS (150 mM NaCl, pH 7.4, 37°C). Graphite rods were used as working electrodes with a platinum mesh as counter electrode (Goodfellow) and a custom-built Ag/AgCl (3M KCl) as reference electrode. All electrochemical responses are an average of the response obtained for 4 separate electrodes.

The artificial plasma contained uric acid (68.5 mg L⁻¹), ascorbic acid (9.5 mg L⁻¹), fructose (36 mg L⁻¹), lactose (5.5 mg L⁻¹), urea (267 mg L⁻¹), cysteine (18 mg L⁻¹), sodium chloride (6.75 g L⁻¹), sodium bicarbonate (2.138 g L⁻¹), calcium sulfate (23.8 mg L⁻¹), magnesium sulfate (104.5 mg L⁻¹) and bovine serum albumin (7 g L⁻¹). [46]

Results and Discussion

Previous studies wiring FADGDH with osmium redox polymers at electrode surfaces have focused on optimising current density for application as anodes in EFCs. [28,31,47–49] Substantial changes to current density, or EFC power, responses are observed when anodes or EFCs are operated in physiological fluids, compared to operation in buffer solutions. [31,38,50–52] We report the effect of selected blood plasma components on the performance of wired glucose oxidising electrodes, in an attempt to understand and hence mitigate against any effect. The performance of the electrodes is assessed by measuring current response in the presence of increasing concentration of glucose as well as the stability of the signal over a 12-hour timeframe. Control testing is carried out in PBS with no other plasma component present.

Enzyme electrodes are produced by coating graphite electrodes with an amount of enzyme, redox polymer, MWCNTs and crosslinker, with amounts selected based on results from previous work.[31] Slow-scan cyclic voltammetry (CV) in the presence and absence of glucose substrate is used to monitor the response of the enzyme electrodes (Figure 1). In the absence of glucose, oxidation and reduction peaks for Os(bpy)PVI centre at ~ 0.22 V vs Ag/AgCl, in agreement with previously reported values for the Os(II/III) redox transition for this redox polymer at an electrode surface.[53,54] Peak currents vary linearly with scan rate at slow scan rates (<20 mVs $^{-1}$) in the absence of substrate which indicates a surface confined response. At higher scan rates (>20 mVs $^{-1}$) peak currents vary linearly with the square root of scan rate indicative of semi-infinite diffusion which is expected from multi-layer biofilms at an electrode surface. Slow scan CV recorded in the presence of glucose shows a sigmoidal response for the enzyme electrodes (Figure 1), characteristic of an electrocatalytic process (EC'). The half-wave potential ($E_{1/2}$) of the catalytic response is negatively shifted by approx. 100 mV when compared to the response in the absence of substrate. At low substrate concentration a separation of the response between the plateau-shaped catalytic wave and a reversible mediator wave is also evident. This shift and separation may be due to transport limitation of the glucose and occurs for a mixed case between substrate-limited and kinetic-limited conditions, particularly for high local mediator concentrations relative to the Michaelis-Menten kinetics for the enzyme-mediator interaction, as is the case for these redox polymer films. [55–57].

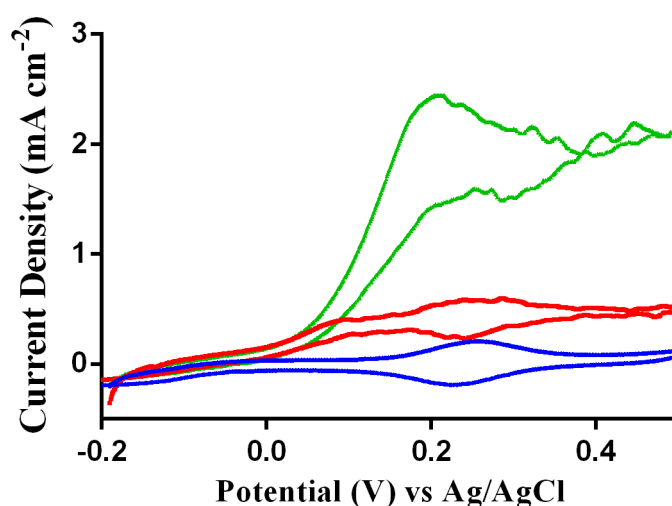


Figure 1: Slow scan (1 mVs $^{-1}$) cyclic voltammograms of electrodes in quiescent 50 mM PBS solution (150 mM NaCl, pH 7.4 , 37°C). Electrode biofilms consisted of FADGDH (100 μg), Os(bpy)PVI (80 μg), MWCNTs (410 μg) and PEGDGE (30 μg). CV scans were recorded in the absence of glucose (blue), 5 mM glucose (red) and 100 mM glucose (green).

Plateau currents observed in 100 mM glucose concentrations in Figure 1 are used to select an electrode potential of 0.45 V to be applied for steady state amperometry measurements. The amperometric response of enzyme electrodes is then measured as a function of increasing glucose concentration (Figure 2). Current densities observed in steady state amperometry are slightly higher than those for the same potential in slow scan CVs, due to the stirring of the solution during amperometric measurements implemented to avoid depletion of the substrate at the electrode surface, as reported previously.[49]

Parallel amperometric responses of enzyme electrodes are measured in PBS, in artificial plasma as well as in PBS containing only one of the components of artificial plasma. Oxidation current responses increase with increasing glucose concentrations for all enzyme electrodes, with some variation in magnitude of current response in the presence of plasma components. Representative current vs concentration plots are shown in Figure 2 and the response in the presence of 5 mM and 100 mM glucose, representing response under typical human physiological and under typical substrate saturated conditions, shown in Table 1.

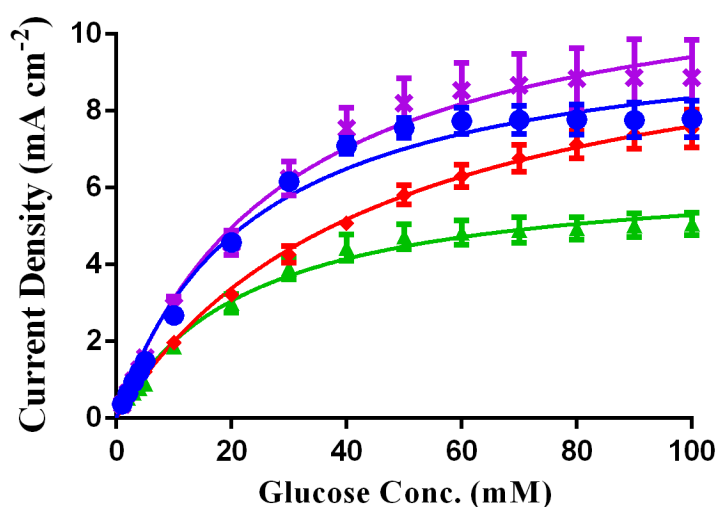


Figure 2: Current response at 0.45 V (37 °C) with stirring at 150 rpm for enzyme electrodes (n=4) consisting of FADGDH (100 μ g), Os(bpy)PVI (80 μ g), MWCNTs (410 μ g) and PEGDGE (30 μ g) in PBS, pH 7.4 (blue circle), artificial plasma (red diamond) and in the presence of magnesium sulfate (purple star), or uric acid (green triangle) at the level expected for plasma (see experimental section).

Electrodes tested in artificial plasma show a significant decrease in performance compared to electrodes tested in PBS, as reported previously. [31,50,51] Testing of electrodes in PBS containing magnesium sulfate, cysteine and calcium sulfate produced marginally higher glucose oxidation current densities at 5 mM and 100 mM glucose when compared with testing

in PBS. The observed increase in current density is in agreement with work published previously on the effect of cations in solution on glucose oxidising enzymes, such as calcium. [58–60] The effect of individual plasma components on biosensor or bioanode performance has been reported previously, although not extensively studied. [61–64] Current densities recorded for enzyme electrodes in the individual presence of either urea, fructose, lactose, ascorbic acid, BSA, sodium bicarbonate or uric acid are lower than responses in PBS, Table 1. Nonlinear least-squares fitting of the data points obtained to the Michaelis-Menten equation is used to estimate K_m^{app} and j_{max} values for the enzyme electrode, to permit comparison of performance, Table 1. The estimated K_m^{app} values obtained in the presence of individual plasma components are similar to that obtained in PBS, with the exception of that obtained in the presence of sodium bicarbonate which is significantly higher than the value obtained in PBS. This suggests that the significant increase in K_m^{app} observed for FADGDH enzyme electrodes in artificial plasma, compared to buffer, is due to the presence of sodium bicarbonate. It is unclear as yet if the observed change in K_m^{app} is due to a specific effect of sodium bicarbonate on the enzyme or on the redox polymer. The estimated j_{max} value in the presence of uric acid is significantly lower than values for enzyme electrodes tested in PBS, and in all other plasma components. Uric acid and ascorbic acid are capable of undergoing direct oxidation at electrodes. [65,66] There is evidence of direct oxidation of uric acid at these physiological concentrations at the enzyme electrode, but not of ascorbic acid. Although oxidation of uric acid should provide for increased enzyme electrode response in its presence it is possible that the allantoin product of uric acid oxidation is accumulated within the enzyme electrode, and therefore decreases enzyme electrode response.

Further testing of the enzyme electrodes is performed to assess the operational stability in buffer, artificial plasma, and the individual components of artificial plasma, given the importance of stability of signal for application to continuous enzyme electrode operation as a biosensor or EFC. Amperometry was performed at 0.45 V vs. Ag/AgCl in solutions containing 100 mM glucose with stirring at 150 rpm (pH 7.4 @ 37 °C), immediately following recording of the slow-scan CV (see Figure 1). Comparison of the current obtained 10 min after testing was commenced with that after a 12-hour timeframe is used to assess stability of signal. The percentage of current remaining after 12 hours is used to report on the performance of enzyme electrodes in the presence of plasma components (Table 2).

Table 1: The current densities observed at 5 mM and 100 mM for electrodes consisting of FADGDH (100 μg), Os(bpy)PVI (80 μg), MWCNTs (410 μg) and PEGDGE (30 μg) tested in the presence of an individual plasma component ($n=4$). Apparent Michaelis-Menten constants (K_m^{app}) and j_{max} values for each experimental run is included below. Amperometry performed at 0.45V vs. Ag/AgCl in PBS with stirring at 150 rpm (pH 7.4 @ 37 $^{\circ}\text{C}$).

Plasma component	Current density at 5 mM glucose (mA cm ⁻²)	Current density at 100 mM glucose (mA cm ⁻²)	K_m^{app} (mM)	j_{max} (mA cm ⁻²)
Magnesium sulfate	1.6 \pm 0.2	8.9 \pm 1.0	28.9 \pm 2.8	12.1 \pm 0.4
Cysteine	1.5 \pm 0.1	8.8 \pm 0.6	28.4 \pm 1.9	11.8 \pm 0.3
Calcium sulfate	1.5 \pm 0.2	9.2 \pm 2.0	25.3 \pm 4.3	12.3 \pm 0.7
None (PBS)	1.5 \pm 0.1	7.8 \pm 0.5	23.4 \pm 1.8	10.3 \pm 0.3
Urea	1.3 \pm 0.1	7.8 \pm 0.6	25.7 \pm 2.5	10.5 \pm 0.3
Fructose	1.3 \pm 0.1	8.0 \pm 0.7	26.9 \pm 3.3	10.7 \pm 0.5
Lactose	1.3 \pm 0.1	7.9 \pm 0.6	28.5 \pm 1.8	10.8 \pm 0.3
Ascorbic acid	1.2 \pm 0.1	7.4 \pm 0.4	29.7 \pm 1.8	9.9 \pm 0.2
Artificial plasma	1.2 \pm 0.1	7.5 \pm 0.5	45.5 \pm 2.8	11.1 \pm 0.3
BSA	1.2 \pm 0.2	7.0 \pm 0.8	24.4 \pm 2.7	9.3 \pm 0.3
Sodium bicarbonate	1.2 \pm 0.2	9.5 \pm 1.3	48.9 \pm 6.1	14.4 \pm 0.8
Uric acid	0.9 \pm 0.1	5.1 \pm 0.3	22.4 \pm 1.7	6.5 \pm 0.2

Table 2: Current densities recorded for electrodes consisting of FADGDH (100 μg), Os(bpy)PVI (80 μg), MWCNTs (410 μg) and PEGDGE (30 μg) in PBS (pH 7.4 @ 37 $^{\circ}\text{C}$) containing 100 mM glucose and in the presence of an individual plasma component after 10 minutes and after 12 hours of continuous operation. Amperometry performed at 0.45V vs. Ag/AgCl with stirring at 150 rpm.

Plasma component	Initial current after 10 minutes (mA cm^{-2})	Current after 12 hours (mA cm^{-2})	% current after 12 hours
Fructose	7.7 ± 0.6	7.1 ± 0.5	92
Urea	8.3 ± 0.8	6.8 ± 0.6	82
Lactose	7.5 ± 0.6	5.9 ± 0.5	80
BSA	7.3 ± 0.7	5.8 ± 0.4	79
Calcium sulfate	9.2 ± 2.1	7.1 ± 0.7	77
Magnesium sulfate	8.7 ± 0.9	6.5 ± 0.4	75
Sodium bicarbonate	8.5 ± 1.3	6.3 ± 1.0	74
None (PBS)	8.2 ± 0.3	5.9 ± 0.2	72
Cysteine	8.5 ± 0.5	5.3 ± 0.3	63
Ascorbic acid	7.3 ± 0.5	4.6 ± 0.4	62
Uric acid	4.7 ± 0.2	2.2 ± 0.4	46
Artificial plasma	7.0 ± 0.2	1.9 ± 0.1	27

Enzyme electrodes tested in PBS, with no additional plasma component, retain 72 % of initial current after 12 hours. This performance is in agreement with that reported previously for similar enzyme electrodes.[49] However, enzyme electrodes tested in artificial plasma retain only 27% of initial current after 12 hours of continuous operation. Previous work carried out on EFC response in complex solutions, such as artificial tears, report a similar decrease in operational stability over time. [63] Interestingly, highest operational stability for glucose oxidation, 92 % of initial current remaining after 12 hours, is achieved for enzyme electrodes operating in PBS and fructose at physiological levels (36 mg L^{-1}). It is unclear why the presence of fructose in solution stabilises the current response over this time period. For example, the FADGDH enzyme shows no activity towards fructose. [67,68] Of all the individual

components present in artificial plasma, the presence of uric acid at physiological levels (68.5 mg L^{-1}) results in the greatest % decrease in current over 12 hours operation, as well as the lowest initial current response in the presence of 5 mM or 100 mM glucose, and lowest j_{max} . It is known that uric acid is responsible for interfering signals to *in-vivo* electrochemical sensing as a result of direct oxidation of uric acid at electrodes (0.59 V vs. NHE) [41,42,69] If the effect of uric acid on these enzyme electrodes was due to direct oxidation, an increase in current in its presence is anticipated, not a decrease. The results obtained in this study suggest that uric acid inhibits enzyme electrode performance resulting in decreased current production and operational stability (Table 1 and Table 2).

In order to determine whether uric acid affects the FADGDH enzyme, or any of the other components in the enzyme electrode, enzyme electrodes prepared using alternate glucose oxidising enzymes (glucose oxidase or recombinant cellobiose dehydrogenase at a loading of $0.1 \text{ mg per electrode}$) within otherwise identical biofilms of osmium polymer, MWCNTs and PEGDGE are tested. Steady state amperometry is used to record current responses as a function of increasing glucose concentration, with testing in the presence and absence of uric acid at physiological level (Figure 3), with K_m^{app} and j_{max} values estimated as before, Table 3.

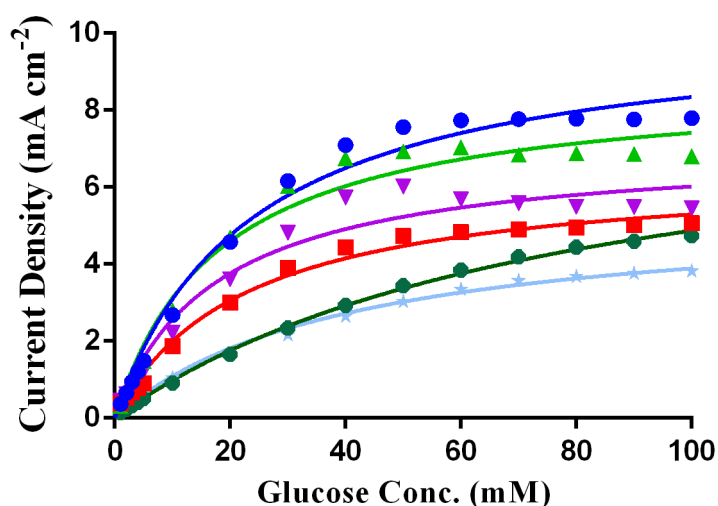


Figure 3: Average current response ($n=4$) generated for each electrode consisting of glucose oxidising enzyme ($100 \mu\text{g}$), $\text{Os}(\text{bpy})\text{PVI}$ ($80 \mu\text{g}$), MWCNTs ($410 \mu\text{g}$) and PEGDGE ($30 \mu\text{g}$). Amperometry performed at $0.45 \text{ V vs. Ag/AgCl}$ in PBS with stirring at 150 rpm ($\text{pH } 7.4 @ 37 \text{ }^\circ\text{C}$). Uric acid concentration was 68.5 mg L^{-1} . FADGDH electrodes tested in the presence (red) and absence (blue) of uric acid. GOx electrodes tested in the presence (green) and absence (pink) of uric acid. CDH electrodes tested in the presence (dark green) and absence (light blue) of uric acid.

Table 3: Apparent Michaelis-Menten constants (K_m^{app}), j_{max} values, initial current, remaining current and percentage remaining current for enzyme electrodes (n=4) prepared using a glucose oxidising enzyme (100 μg), Os(bpy)PVI (80 μg), MWCNTs (410 μg) and PEGDGE (30 μg) from currents in the presence of glucose recorded under steady state amperometry at 0.45V vs. Ag/AgCl in PBS with stirring at 150 rpm (pH 7.4 @ 37 °C). Uric acid concentration was 68.5 mg L⁻¹.

Enzyme	K_m^{app} (mM)	j_{max} (mA cm ⁻²)	Initial current after 10 minutes (mA cm ⁻²)	Remaining current after 12 hours (mA cm ⁻²)	Remaining current (%)
FADGDH	23.4 ± 1.8	10.3 ± 0.3	8.2 ± 0.3	5.9 ± 0.2	72
in uric acid	22.4 ± 1.7	6.5 ± 0.2	4.7 ± 0.2	2.2 ± 0.4	46
GOx	18.0 ± 4.2	8.8 ± 0.6	6.0 ± 1.1	4.3 ± 1.1	70
in uric acid	17.7 ± 4.9	7.1 ± 0.6	4.5 ± 1.3	3.1 ± 1.0	70
CDH	80.0 ± 5.8	8.8 ± 0.4	4.3 ± 0.2	3.7 ± 0.1	86
in uric acid	40.1 ± 5.2	5.5 ± 0.3	3.5 ± 0.4	1.2 ± 0.1	33

K_m^{app} values are similar for enzyme electrodes produced using FADGDH or GOx when operated in the presence or absence of uric acid. The j_{max} value for enzyme electrodes using GOx is 20% lower in the presence of uric acid than that in PBS buffer alone. This difference is not as significant as the 37% decrease observed for enzyme electrodes based on FADGDH in the presence of uric acid. A decrease in j_{max} while maintaining a similar K_m^{app} is indicative of non-competitive enzyme inhibition [70–72] thus uric acid inhibits non-competitively both FADGDH and GOx activity although GOx is not as badly affected as the FADGDH enzyme. For comparison, both K_m^{app} and j_{max} values decrease significantly for enzyme electrodes produced using a CDH enzyme when operated in the presence of uric acid instead of PBS buffer alone. The decrease in both K_m^{app} and j_{max} suggests uncompetitive inhibition [70] occurs for the CDH based enzyme electrode in the presence of uric acid. The effect of interfering compounds on the CDH enzyme has been reported on previously, although uric acid was not investigated. [73]

The proportion of initial current remaining after 12 hr operation dropped from 72 % to 46 % in the presence of uric acid, compared to operation in PBS buffer alone, for the FADGDH based electrodes. The stability of the current response is unaltered in the presence of uric acid for the GOx based enzyme electrodes, although the initial current density, in the absence of uric acid, is lower than that observed for FADGDH based enzyme electrodes. As reported on previously

CDH electrodes, in the absence of uric acid, produce the most stable current, retaining 86% of initial current after 12 hr operation in PBS. [49,74] However, in the presence of uric acid, CDH based enzyme electrodes retain only 33 % of initial current after 12 hr operation. Again, the results, in combination with the observed changes to K_m^{app} and j_{max} , suggest that the uric acid acts as an uncompetitive inhibitor of the CDH enzyme for the oxidation of glucose. From the three glucose oxidising enzymes tested, the operational stability of GOx based electrodes in the presence of uric acid was least affected by the presence of uric acid, with however significant changes to estimated maximum current density of all three enzyme electrodes in the presence of uric acid. One possible explanation is that uric acid acts as an inhibitor of the enzyme however further testing is required to test this hypothesis.

Conclusion

Enzyme electrodes consisting of co-immobilised FADGDH, Os(bpy)PVI, MWCNTs and PEGDGE were tested in PBS, artificial plasma and the individual components of the artificial plasma to gain a better understanding of the reason for a decrease in electrode performance observed in artificial serum and human serum.[31,38,50–52] The lowest current response for these electrodes was observed in the presence of physiological level of uric acid although the largest change to K_m^{app} occurred upon addition of physiological level of sodium bicarbonate. The lowest operational stability observed in the presence of a single plasma component was recorded in the presence of uric acid, with only 46 % of initial current response after 12 hours: this compares to only 27% of current remaining after 12 hours for electrodes operating in artificial plasma. Electrodes were prepared using alternate glucose oxidising enzymes, GOx and CDH, and tested in the presence of uric acid. For both FADGDH and GOx enzyme electrodes, j_{max} decreased significantly with no significant change to the K_m^{app} suggesting non-competitive inhibition. The CDH based electrodes provide highest stability of current signal in PBS, with 86 % of the initial signal present after 12 hours, but demonstrate significant change to the K_m^{app} and j_{max} values as well as operational stability dropping to only 33% in the presence of uric acid. In contrast the operational stability of the GOx based enzyme electrodes was unaffected by the presence of physiological level of uric acid. As uric acid and sodium bicarbonate are present in blood, careful consideration is required in choosing a glucose oxidising enzyme for both glucose sensing and EFC device assembly. Further work is required to understand the mechanism of uric acid inhibition on each of the FADGDH, GOx and CDH enzymes.

Acknowledgments

R. Bennett acknowledges support through an NUI Galway College of Science fellowship and an Irish Research Council Postgraduate Scholarship (GOIPG/2016/505). Donation of recombinant CDH produced with financial support from the European Commission (“Bioenergy” PEOPLE-2013-ITN-607793) by Roland Ludwig (University of Boku) is gratefully acknowledged.

References

- [1] S. Calabrese Barton, J. Gallaway, P. Atanassov, Enzymatic Biofuel Cells for Implantable and Microscale Devices, *Chem. Rev.* 104 (2004) 4867–4886. doi:10.1021/cr020719k.
- [2] D. Leech, P. Kavanagh, W. Schuhmann, Enzymatic fuel cells: Recent progress, *Electrochim. Acta.* 84 (2012) 223–234. doi:10.1016/j.electacta.2012.02.087.
- [3] M. Rasmussen, S. Abdellaoui, S.D. Minter, Enzymatic biofuel cells: 30 years of critical advancements, *Biosens. Bioelectron.* 76 (2016) 91–102. doi:10.1016/J.BIOS.2015.06.029.
- [4] A. Heller, Miniature biofuel cells, *Phys. Chem. Chem. Phys.* 6 (2004) 209–216. doi:10.1039/b313149a.
- [5] S.D. Minter, B.Y. Liaw, M.J. Cooney, Enzyme-based biofuel cells, *Curr. Opin. Biotechnol.* 18 (2007) 228–234. doi:10.1016/J.COPBIO.2007.03.007.
- [6] A.T. Yahiro, S.M. Lee, D.O. Kimble, Bioelectrochemistry: I. Enzyme utilizing bio-fuel cell studies, *Biochim. Biophys. Acta - Spec. Sect. Biophys. Subj.* 88 (1964) 375–383. doi:10.1016/0926-6577(64)90192-5.
- [7] T. Chen, S.C. Barton, G. Binyamin, Z. Gao, Y. Zhang, H.-H. Kim, A. Heller, A Miniature Biofuel Cell, *J. Am. Chem. Soc.* 123 (2001) 8630–8631. doi:10.1021/ja0163164.
- [8] J.A. Cracknell, K.A. Vincent, F.A. Armstrong, Enzymes as Working or Inspirational Electrocatalysts for Fuel Cells and Electrolysis, *Chem. Rev.* 108 (2008) 2439–2461. doi:10.1021/cr0680639.
- [9] S. Tsujimura, From fundamentals to applications of bioelectrocatalysis: bioelectrocatalytic reactions of FAD-dependent glucose dehydrogenase and bilirubin oxidase, *Biosci. Biotechnol. Biochem.* (2018) 1–10. doi:10.1080/09168451.2018.1527209.
- [10] I. Mazurenko, A. de Poulpiquet, E. Lojou, Recent developments in high surface area

- bioelectrodes for enzymatic fuel cells, *Curr. Opin. Electrochem.* 5 (2017) 74–84. doi:10.1016/j.coelec.2017.07.001.
- [11] R.F.B. Turner, D.J. Harrison, R.V. Rajotte, H.P. Baltes, A biocompatible enzyme electrode for continuous in vivo glucose monitoring in whole blood, *Sensors Actuators B Chem.* 1 (1990) 561–564. doi:10.1016/0925-4005(90)80273-3.
- [12] C.A. Quinn, R.E. Connor, A. Heller, Biocompatible, glucose-permeable hydrogel for in situ coating of implantable biosensors., *Biomaterials.* 18 (1997) 1665–1670. <http://www.ncbi.nlm.nih.gov/pubmed/9613815> (accessed April 9, 2018).
- [13] C.N. Kotanen, F.G. Moussy, S. Carrara, A. Guiseppi-Elie, Implantable enzyme amperometric biosensors, *Biosens. Bioelectron.* 35 (2012) 14–26. doi:10.1016/j.bios.2012.03.016.
- [14] P. Cinquin, C. Gondran, F. Giroud, S. Mazabrard, A. Pellissier, F. Boucher, J.-P. Alcaraz, K. Gorgy, F. Lenouvel, S. Mathé, P. Porcu, S. Cosnier, A Glucose BioFuel Cell Implanted in Rats, *PLoS One.* 5 (2010) e10476. doi:10.1371/journal.pone.0010476.
- [15] S. Cosnier, A.J. Gross, F. Giroud, M. Holzinger, Beyond the hype surrounding biofuel cells: What’s the future of enzymatic fuel cells?, *Curr. Opin. Electrochem.* (2018). doi:10.1016/J.COEELEC.2018.06.006.
- [16] A.L. Ghindilis, P. Atanasov, E. Wilkins, Enzyme-catalyzed direct electron transfer: Fundamentals and analytical applications, *Electroanalysis.* 9 (1997) 661–674. doi:10.1002/elan.1140090902.
- [17] P. Kavanagh, D. Leech, Mediated electron transfer in glucose oxidising enzyme electrodes for application to biofuel cells: recent progress and perspectives, *Phys. Chem. Chem. Phys.* 15 (2013) 4859–4869. doi:10.1039/c3cp44617d.
- [18] J.C. Pickup, G.W. Shaw, D.J. Claremont, Potentially-implantable, amperometric glucose sensors with mediated electron transfer: improving the operating stability., *Biosensors.* 4 (1989) 109–119. <http://www.ncbi.nlm.nih.gov/pubmed/2719726> (accessed October 5, 2018).
- [19] N. Mano, F. Mao, A. Heller, Characteristics of a Miniature Compartment-less Glucose–O₂ Biofuel Cell and Its Operation in a Living Plant, *J. Am. Chem. Soc.* 125 (2003) 6588–6594. doi:10.1021/ja0346328.
- [20] F. Mao, N. Mano, A. Heller, Long Tethers Binding Redox Centers to Polymer Backbones Enhance Electron Transport in Enzyme “Wiring” Hydrogels, *J. Am. Chem. Soc.* 125 (2003) 4951–4957. doi:10.1021/ja029510e.

- [21] T. de Lumley-Woodyear, P. Rocca, J. Lindsay, Y. Dror, A. Freeman, A. Heller, Polyacrylamide-Based Redox Polymer for Connecting Redox Centers of Enzymes to Electrodes, *Anal. Chem.* 67 (1995) 1332–1338. doi:10.1021/ac00104a006.
- [22] P. O Conghaile, D. MacAodha, B. Egan, P. Kavanagh, D. Leech, Tethering Osmium Complexes within Enzyme Films on Electrodes to Provide a Fully Enzymatic Membrane-Less Glucose/Oxygen Fuel Cell, *J. Electrochem. Soc.* 160 (2013) G3165–G3170. doi:10.1149/2.026307jes.
- [23] B.A. Gregg, A. Heller, Cross-linked redox gels containing glucose oxidase for amperometric biosensor applications, *Anal. Chem.* 62 (1990) 258–263. doi:10.1021/ac00202a007.
- [24] I. Osadebe, D. Leech, Effect of Multi-Walled Carbon Nanotubes on Glucose Oxidation by Glucose Oxidase or a Flavin-Dependent Glucose Dehydrogenase in Redox-Polymer-Mediated Enzymatic Fuel Cell Anodes, *ChemElectroChem.* 1 (2014) 1988–1993. doi:10.1002/celc.201402136.
- [25] D. MacAodha, M.L. Ferrer, P.Ó. Conghaile, P. Kavanagh, D. Leech, Crosslinked redox polymer enzyme electrodes containing carbon nanotubes for high and stable glucose oxidation current, *Phys. Chem. Chem. Phys.* 14 (2012) 14667–14672. doi:10.1039/c2cp42089a.
- [26] S. Boland, P. Kavanagh, D. Leech, Mediated Enzyme Electrodes for Biological Fuel Cell and Biosensor Applications, in: *ECS Trans.*, ECS, 2008: pp. 77–87. doi:10.1149/1.3036213.
- [27] R. Kumar, D. Leech, A glucose anode for enzymatic fuel cells optimized for current production under physiological conditions using a design of experiment approach., *Bioelectrochemistry.* 106 (2015) 41–46. doi:10.1016/j.bioelechem.2015.06.005.
- [28] I. Osadebe, P.Ó. Conghaile, P. Kavanagh, D. Leech, Glucose oxidation by osmium redox polymer mediated enzyme electrodes operating at low potential and in oxygen, for application to enzymatic fuel cells, *Electrochim. Acta.* 182 (2015) 320–326. doi:10.1016/j.electacta.2015.09.088.
- [29] P. Ó Conghaile, M. Falk, D. MacAodha, M.E. Yakovleva, C. Gonaus, C.K. Peterbauer, L. Gorton, S. Shleev, D. Leech, Fully Enzymatic Membraneless Glucose|Oxygen Fuel Cell That Provides 0.275 mA cm⁻² in 5 mM Glucose, Operates in Human Physiological Solutions, and Powers Transmission of Sensing Data, *Anal. Chem.* 88 (2016) 2156–2163. doi:10.1021/acs.analchem.5b03745.
- [30] M. Shao, M.N. Zafar, M. Falk, R. Ludwig, C. Sygmund, C.K. Peterbauer, D.A.

- Guschin, D. MacAodha, P. Ó Conghaile, D. Leech, M.D. Toscano, S. Shleev, W. Schuhmann, L. Gorton, Optimization of a Membraneless Glucose/Oxygen Enzymatic Fuel Cell Based on a Bioanode with High Coulombic Efficiency and Current Density, *ChemPhysChem*. 14 (2013) 2260–2269. doi:10.1002/cphc.201300046.
- [31] R. Bennett, I. Osadebe, R. Kumar, P.Ó. Conghaile, D. Leech, Design of Experiments Approach to Provide Enhanced Glucose-oxidising Enzyme Electrode for Membraneless Enzymatic Fuel Cells Operating in Human Physiological Fluids, *Electroanalysis*. 30 (2018) 1438–1445. doi:10.1002/elan.201600402.
- [32] S. Cosnier, A. Le Goff, M. Holzinger, Towards glucose biofuel cells implanted in human body for powering artificial organs: Review, *Electrochem. Commun.* 38 (2014) 19–23. doi:10.1016/J.ELECOM.2013.09.021.
- [33] S. Vaddiraju, D.J. Burgess, I. Tomazos, F.C. Jain, F. Papadimitrakopoulos, Technologies for Continuous Glucose Monitoring: Current Problems and Future Promises, *J. Diabetes Sci. Technol.* 4 (2010) 1540–1562. doi:10.1177/193229681000400632.
- [34] S. Rubenwolf, S. Sané, L. Hussein, J. Kestel, F. von Stetten, G. Urban, M. Krueger, R. Zengerle, S. Kerzenmacher, Prolongation of electrode lifetime in biofuel cells by periodic enzyme renewal, *Appl. Microbiol. Biotechnol.* 96 (2012) 841–849. doi:10.1007/s00253-012-4374-8.
- [35] S. Cosnier, A. J. Gross, A. Le Goff, M. Holzinger, Recent advances on enzymatic glucose/oxygen and hydrogen/oxygen biofuel cells: Achievements and limitations, *J. Power Sources*. 325 (2016) 252–263. doi:10.1016/J.JPOWSOUR.2016.05.133.
- [36] X. Li, L. Zhang, L. Su, T. Ohsaka, L. Mao, A Miniature Glucose/O₂ Biofuel Cell With a High Tolerance Against Ascorbic Acid, *Fuel Cells*. 9 (2009) 85–91. doi:10.1002/fuce.200800054.
- [37] E. Katz, A.F. Bückmann, I. Willner, Self-Powered Enzyme-Based Biosensors, *J. Am. Chem. Soc.* 123 (2001) 10752–10753. doi:10.1021/ja0167102.
- [38] V. Coman, R. Ludwig, W. Harreither, D. Haltrich, L. Gorton, T. Ruzgas, and S. Shleev, A Direct Electron Transfer-Based Glucose/Oxygen Biofuel Cell Operating in Human Serum, *Fuel Cells*. 10 (2009) 9–16. doi:10.1002/fuce.200900121.
- [39] J.P. Lowry, K. McAteer, S.S. El Atrash, A. Duff, R.D. O’Neill, Characterization of Glucose Oxidase-Modified Poly(phenylenediamine)-Coated Electrodes in vitro and in vivo: Homogeneous Interference by Ascorbic Acid in Hydrogen Peroxide Detection, *Anal. Chem.* 66 (1994) 1754–1761. doi:10.1021/ac00082a025.

- [40] J.P. Lowry, R.D. O'Neill, Homogeneous mechanism of ascorbic acid interference in hydrogen peroxide detection at enzyme-modified electrodes, *Anal. Chem.* 64 (1992) 453–456. doi:10.1021/ac00028a022.
- [41] J. Wang, J. Liu, L. Chen, F. Lu, Highly Selective Membrane-Free, Mediator-Free Glucose Biosensor, *Anal. Chem.* 66 (1994) 3600–3603. doi:10.1021/ac00093a011.
- [42] S. V. Sasso, R.J. Pierce, R. Walla, A.M. Yacynych, Electropolymerized 1,2-diaminobenzene as a means to prevent interferences and fouling and to stabilize immobilized enzyme in electrochemical biosensors, *Anal. Chem.* 62 (1990) 1111–1117. doi:10.1021/ac00210a004.
- [43] R.J. Forster, J.G. Vos, Synthesis, characterization, and properties of a series of osmium- and ruthenium-containing metallopolymers, *Macromolecules.* 23 (1990) 4372–4377. doi:10.1021/ma00222a008.
- [44] E.M. Kober, J. V. Caspar, B.P. Sullivan, T.J. Meyer, Synthetic routes to new polypyridyl complexes of osmium(II), *Inorg. Chem.* 27 (1988) 4587–4598. doi:10.1021/ic00298a017.
- [45] C. Sygmund, P. Staudigl, M. Klausberger, N. Pinotsis, K. Djinović-Carugo, L. Gorton, D. Haltrich, R. Ludwig, Heterologous overexpression of *Glomerella cingulata* FAD-dependent glucose dehydrogenase in *Escherichia coli* and *Pichia pastoris*., *Microb. Cell Fact.* 10 (2011) 106. doi:10.1186/1475-2859-10-106.
- [46] C.A. Burtis, E.R. Ashwood, D.E. Bruns, *Tietz Textbook of Clinical Chemistry and Molecular Diagnostics.*, Elsevier Health Sciences, 2012.
- [47] X. Xiao, P.Ó. Conghaile, D. Leech, R. Ludwig, E. Magner, An oxygen-independent and membrane-less glucose biobattery/supercapacitor hybrid device, *Biosens. Bioelectron.* 98 (2017) 421–427. doi:10.1016/j.bios.2017.07.023.
- [48] M.N. Zafar, N. Beden, D. Leech, C. Sygmund, R. Ludwig, L. Gorton, Characterization of different FAD-dependent glucose dehydrogenases for possible use in glucose-based biosensors and biofuel cells, *Anal. Bioanal. Chem.* 402 (2012) 2069–2077. doi:10.1007/s00216-011-5650-7.
- [49] D. MacAodha, P. Ó Conghaile, B. Egan, P. Kavanagh, C. Sygmund, R. Ludwig, D. Leech, Comparison of Glucose Oxidation by Crosslinked Redox Polymer Enzyme Electrodes Containing Carbon Nanotubes and a Range of Glucose Oxidising Enzymes, *Electroanalysis.* 25 (2013) 94–100. doi:10.1002/elan.201200536.
- [50] T. Siepenkoetter, U. Salaj-Kosla, X. Xiao, P.Ó. Conghaile, M. Pita, R. Ludwig, E. Magner, Immobilization of Redox Enzymes on Nanoporous Gold Electrodes:

- Applications in Biofuel Cells, *Chempluschem*. 82 (2017) 553–560.
doi:10.1002/cplu.201600455.
- [51] D. MacAodha, P.Ó. Conghaile, B. Egan, P. Kavanagh, D. Leech, Membraneless Glucose/Oxygen Enzymatic Fuel Cells Using Redox Hydrogel Films Containing Carbon Nanotubes, *ChemPhysChem*. 14 (2013) 2302–2307.
doi:10.1002/cphc.201300239.
- [52] R.D. Milton, K. Lim, D.P. Hickey, S.D. Minteer, Employing FAD-dependent glucose dehydrogenase within a glucose/oxygen enzymatic fuel cell operating in human serum, *Bioelectrochemistry*. 106 (2015) 56–63. doi:10.1016/J.BIOELECHEM.2015.04.005.
- [53] H. Ju, D. Leech, [Os(bpy)₂(PVI)₁₀Cl]Cl polymer-modified carbon fiber electrodes for the electrocatalytic oxidation of NADH, *Anal. Chim. Acta*. 345 (1997) 51–58.
doi:10.1016/S0003-2670(97)00093-7.
- [54] T.J. Ohara, R. Rajagopalan, A. Heller, Glucose electrodes based on cross-linked bis(2,2'-bipyridine)chloroosmium(+2+) complexed poly(1-vinylimidazole) films, *Anal. Chem*. 65 (1993) 3512–3517. doi:10.1021/ac00071a031.
- [55] B. Limoges, J. Moiroux, J.-M. Savéant, Kinetic control by the substrate and the cosubstrate in electrochemically monitored redox enzymatic immobilized systems. Catalytic responses in cyclic voltammetry and steady state techniques, *J. Electroanal. Chem*. 521 (2002) 8–15. doi:10.1016/S0022-0728(02)00658-7.
- [56] P.N. Bartlett, K.F.E. Pratt, Theoretical treatment of diffusion and kinetics in amperometric immobilized enzyme electrodes Part I: Redox mediator entrapped within the film, *J. Electroanal. Chem*. 397 (1995) 61–78. doi:10.1016/0022-0728(95)04236-7.
- [57] B. Limoges, J.-M. Savéant, Cyclic voltammetry of immobilized redox enzymes. Interference of steady-state and non-steady-state Michaelis–Menten kinetics of the enzyme–redox cosubstrate system, *J. Electroanal. Chem*. 549 (2003) 61–70.
doi:10.1016/S0022-0728(03)00285-7.
- [58] P. Bollella, Y. Hibino, K. Kano, L. Gorton, R. Antiochia, The influence of pH and divalent/monovalent cations on the internal electron transfer (IET), enzymatic activity, and structure of fructose dehydrogenase, *Anal. Bioanal. Chem*. 410 (2018) 3253–3264.
doi:10.1007/s00216-018-0991-0.
- [59] D. Kracher, K. Zahma, C. Schulz, C. Sygmond, L. Gorton, R. Ludwig, Inter-domain electron transfer in cellobiose dehydrogenase: modulation by pH and divalent cations, *FEBS J*. 282 (2015) 3136–3148. doi:10.1111/febs.13310.
- [60] C. Schulz, R. Ludwig, P.O. Micheelsen, M. Silow, M.D. Toscano, L. Gorton,

- Enhancement of enzymatic activity and catalytic current of cellobiose dehydrogenase by calcium ions, *Electrochem. Commun.* 17 (2012) 71–74.
doi:10.1016/j.elecom.2012.01.031.
- [61] F. Moussy, D.J. Harrison, D.W. O'Brien, R. V. Rajotte, Performance of subcutaneously implanted needle-type glucose sensors employing a novel trilayer coating, *Anal. Chem.* 65 (1993) 2072–2077. doi:10.1021/ac00063a023.
- [62] D.S. Bindra, Y. Zhang, G.S. Wilson, R. Sternberg, D.R. Thevenot, D. Moatti, G. Reach, Design and in vitro studies of a needle-type glucose sensor for subcutaneous monitoring, *Anal. Chem.* 63 (1991) 1692–1696. doi:10.1021/ac00017a008.
- [63] X. Xiao, T. Siepenkoetter, P.Ó. Conghaile, D. Leech, E. Magner, Nanoporous Gold-Based Biofuel Cells on Contact Lenses, *ACS Appl. Mater. Interfaces.* 10 (2018) 7107–7116. doi:10.1021/acsami.7b18708.
- [64] M. Cadet, S. Gounel, C. Stines-Chaumeil, X. Brilland, J. Rouhana, F. Louerat, N. Mano, Cadet, M., Gounel, S., Stines-Chaumeil, C., Brilland, X., Rouhana, J., Louerat, F., Mano, N., 2016. An enzymatic glucose/O₂ biofuel cell operating in human blood. *Biosens. Bioelectron.* 83, 60–67. doi:10.1016/j.bios.2016.04.016.
- [65] R.T. Kachoosangi, C.E. Banks, R.G. Compton, Simultaneous Determination of Uric Acid and Ascorbic Acid Using Edge Plane Pyrolytic Graphite Electrodes, *Electroanalysis.* 18 (2006) 741–747. doi:10.1002/elan.200603470.
- [66] P. Pinyou, A. Ruff, S. Pöller, S. Ma, R. Ludwig, W. Schuhmann, Design of an Os Complex-Modified Hydrogel with Optimized Redox Potential for Biosensors and Biofuel Cells, *Chemistry - A Eur. J.* 22 (2016) 5319–5326. doi:10.1002/chem.201504591.
- [67] H. Yoshida, G. Sakai, K. Mori, K. Kojima, S. Kamitori, K. Sode, Structural analysis of fungus-derived FAD glucose dehydrogenase, *Sci. Rep.* 5 (2015) 13498. doi:10.1038/srep13498.
- [68] K. Sode, N. Loew, Y. Ohnishi, H. Tsuruta, K. Mori, K. Kojima, W. Tsugawa, J.T. LaBelle, D.C. Klonoff, Novel fungal FAD glucose dehydrogenase derived from *Aspergillus niger* for glucose enzyme sensor strips, *Biosens. Bioelectron.* 87 (2017) 305–311. doi:10.1016/j.bios.2016.08.053.
- [69] M.G. Simic, S. V. Jovanovic, Antioxidation mechanisms of uric acid, *J. Am. Chem. Soc.* 111 (1989) 5778–5782. doi:10.1021/ja00197a042.
- [70] A. Cornish-Bowden, *Fundamentals of enzyme kinetics*, Butterworths, 1979.
- [71] M. Grattieri, P. Scodeller, C. Adam, E.J. Calvo, Non-Competitive Reversible

- Inhibition of Laccase by H₂O₂ in Osmium Mediated Layer-By-Layer Multilayer O₂ Biocathodes, *J. Electrochem. Soc.* 162 (2015) G82–G86. doi:10.1149/2.0831509jes.
- [72] R.D. Milton, S.D. Minter, Investigating the Reversible Inhibition Model of Laccase by Hydrogen Peroxide for Bioelectrocatalytic Applications, *J. Electrochem. Soc.* 161 (2014) H3011–H3014. doi:10.1149/2.0031413jes.
- [73] P. Bollella, L. Gorton, R. Ludwig, R. Antiochia, A Third Generation Glucose Biosensor Based on Cellobiose Dehydrogenase Immobilized on a Glassy Carbon Electrode Decorated with Electrodeposited Gold Nanoparticles: Characterization and Application in Human Saliva, *Sensors*. 17 (2017) 1912. doi:10.3390/s17081912.
- [74] M.N. Zafar, I. Aslam, R. Ludwig, G. Xu, L. Gorton, An efficient and versatile membraneless bioanode for biofuel cells based on *Corynebacterium thermophilus* cellobiose dehydrogenase, *Electrochim. Acta.* 295 (2019) 316–324. doi:10.1016/J.ELECTACTA.2018.10.047.

Chapter 5: Improved operational stability of mediated glucose enzyme electrodes for operation in human physiological solutions

Published as:

Improved operational stability of mediated glucose enzyme electrodes for operation in human physiological solutions

Richard Bennett and Dónal Leech. *Bioelectrochemistry*, (2020) 133, 107460.

Co-author contributions:

I synthesised the PVI-bound osmium redox polymer, performed the lab work, the analysis and wrote the first draft of the submitted manuscript.

Dónal Leech, as the project supervisor, contributed through advice and guidance and wrote the final draft of the submitted manuscript.

Improved operational stability of mediated glucose enzyme electrodes for operation in human physiological solutions

*Richard Bennett, Dónal Leech**

School of Chemistry & Ryan Institute, National University of Ireland Galway, University Road, Galway, Ireland

DOI: 10.1016/j.bioelechem.2020.107460

Abstract

Stability of glucose-oxidising enzyme electrodes is affected by substances in physiological solutions, hampering deployment as long-term implantable biosensors or fuel cells. The performance of Nafion over-coated enzyme electrodes, consisting of multiwalled carbon nanotubes and flavin adenine dinucleotide-dependent glucose dehydrogenase (FADGDH) or glucose oxidase (GOx) crosslinked with osmium-complex based redox polymer, was compared to uncoated electrodes in presence of uric acid and artificial plasma. Nafion over-coating resulted in lower glucose oxidation current densities compared to no over-coating. The highest initial current density for Nafion over-coated electrodes in artificial plasma in 100 mM glucose was $8.0 \pm 2.0 \text{ mA cm}^{-2}$ for GOx electrodes with 0.5 % w/v Nafion coating. These electrodes retained 83 % of initial current after 12 hours continuous operation in artificial plasma while similarly prepared FADGDH electrodes retained 58% signal. This is compared to retention of only 73 % or 31 % observed for GOx or FADGDH electrodes in artificial plasma with no Nafion membrane. Enzyme electrodes over-coated with Nafion maintain improved signal stability when tested continuously in the presence of uric acid, identified as being the main contributing substance to FADGDH enzyme electrode instability, showing promise for application to continuous use glucose-oxidising enzyme electrodes.

Introduction

Despite the significant progress made in continuous-use glucose sensing in recent decades major hurdles remain for long term function and stability of enzyme electrodes for such applications. Implantable or semi-implantable devices are subject to the foreign body response (FBR) as well as the effect of interfering compounds such as uric acid and ascorbic acid. [1,2] Similarly, the lack of stability of semi-implantable enzymatic fuel cell (EFC) performance can be attributed to the FBR and the effect of interfering compounds found *in-vivo* on the EFC. This remains a major obstacle to overcome before EFCs can be considered as continuous use power sources for implantable and semi-implantable devices. [3]

Fuel cells based on enzymatic power are an attractive alternative to metal based catalysts such as platinum as they can electrolyse fuels present in the body, have greater substrate selectivity, and operate under physiological conditions (pH 7.4, 37 °C). [4–6] EFCs as power sources allow for greater miniaturisation as there is no need for seals, casings and membranes which are necessary in battery assemblies. Development of EFCs capable of powering such devices is reliant on improvements to fuel cell power generation and long-term operational stability of enzyme electrodes. [3,7–10]

Electron transfer between enzyme active site and electrode surface is achieved either through direct electron transfer (DET) or mediated electron transfer (MET). [11,12] To achieve DET, orientation strategies are required to place the active site close to the electrode surface to allow for shuttling of electrons. This can be difficult to achieve and for this reason redox mediators are widely used to act as electron shuttles. Osmium-based polypyridyl redox complexes and polymers are attractive mediators as they operate at low potentials, are relatively stable in the Os (II/III) redox states and the redox potential can be tuned to the enzyme redox potential to achieve a compromise between cell voltage and current generation. [13–17] Inclusion of multi walled carbon nanotubes (MWCNTs) in the casting process for preparation of enzyme electrodes, with the nanomaterial retained using a poly(ethylene glycol) diglycidyl ether (PEGDGE) crosslinker between enzyme and polymer, results in higher current response and operational stability for enzyme electrodes. [18,19] EFCs based on co-immobilisation of nano-supports, osmium based redox mediators and enzyme have been widely reported. [20–24]

We recently reported a systematic analysis of the effect of each component of artificial plasma on glucose oxidation at electrodes assembled by co-immobilising a flavin adenine dinucleotide-dependent glucose dehydrogenase (FADGDH) with osmium-complex based redox polymer, MWCNTs and PEGDGE on graphite. [25] The lowest glucose oxidation current response generated was for phosphate buffered saline (PBS) in the presence of uric acid when compared

to results obtained in PBS alone. In addition, the lowest operational stability recorded was in the presence of uric acid, with 46 % of initial current retained after 12 hours of continuous polarisation of electrodes for glucose oxidation, compared to 72 % retained in PBS alone. Electrodes tested in artificial plasma maintained 27 % of operational stability over the same time frame. Comparison of enzyme electrodes showed that cellobiose dehydrogenase (CDH)-based electrodes retained 33 % current density in the presence of uric acid compared to 86 % in PBS, while GOx-based electrodes were least affected by the presence of uric acid maintaining 70 % of their initial current in the presence and absence of uric acid.

Here we report on the use of Nafion over-coating to protect enzyme electrodes from the effects of uric acid. The use of Nafion limits direct oxidation at electrode surfaces of negatively charged molecules such as ascorbic acid and uric acid, as it is a negatively charged ionomer. [15,26–32] In addition over-coating enzyme electrodes, formed by deposition of enzyme and polycationic redox polymers, with polyanionic films such as poly-acrylic acid [33] or a copolymer containing poly(styrene sulfonate) [34] has been reported to enhance enzyme electrode stability through improved retention of the redox polymer within the enzyme electrode film matrix. In this report enzyme electrodes were prepared using either FADGDH or GOx and tested in PBS, PBS containing physiological levels of uric acid, and in artificial plasma.

Experimental Section

2.1 Materials

All chemicals used in the study were purchased from Sigma-Aldrich, unless stated otherwise. The osmium redox polymer used poly(1-vinylimidazole)-[Os(2,2'-bipyridine)₂Cl]⁺ (Os(bpy)PVI), with a nominal ratio of one redox complex for every 10th vinyl-imidazole monomer unit, was synthesised according to previously published work. [35,36] The glucose oxidase is sourced from *Aspergillus niger* (GOx, EC 1.1.3.4., Sigma-Aldrich). The flavin adenine dinucleotide-dependent glucose dehydrogenase is from *Aspergillus sp.* (FADGDH 1.1.99.10, Sekisui, Cambridge, USA; product GLDE-70-1192). The MWCNTs were purchased from Sigma Aldrich and were refluxed in concentrated nitric acid for 6 hours before washing using copious amount of water until the run-off from the washing was neutral, and subsequently filtered. Milli-Q water (18 MΩcm) was used to prepare all aqueous solutions. The Nafion solution (5% w/v) was purchased from Sigma Aldrich and was diluted in ethanol to produce solutions containing 0.5% and 1% Nafion. The artificial plasma recipe used in the study

contained uric acid (68.5 mg L^{-1}), ascorbic acid (9.5 mg L^{-1}), fructose (36 mg L^{-1}), lactose (5.5 mg L^{-1}), urea (267 mg L^{-1}), cysteine (18 mg L^{-1}), sodium chloride (6.75 g L^{-1}), sodium bicarbonate (2.138 g L^{-1}), calcium sulfate (23.8 mg L^{-1}), magnesium sulfate (104.5 mg L^{-1}) and bovine serum albumin (7 g L^{-1}). [37]

2.2 Methods

All electrochemical testing was carried out using a CH Instruments 1030a multichannel potentiostat. Electrochemical testing was performed in PBS (50 mM phosphate buffer containing 150 mM NaCl, pH 7.4) at $37 \text{ }^{\circ}\text{C}$. No effort was made to exclude oxygen from the electrolyte. Graphite rods (Graphite store, USA, 3.0 mm diameter, NC001295) were cut, insulated with heat shrink tubing and polished at one end using fine grit paper to give graphite electrodes with a geometric working surface area of 0.0707 cm^2 . Graphite rods were used as the working electrodes with a custom-built Ag/AgCl (3M KCl) reference electrode and a platinum mesh as counter electrode. The electrochemical responses reported in this study are an average result obtained for four separate electrodes tested simultaneously.

Enzyme electrodes were prepared through deposition onto working electrode areas of $16 \text{ }\mu\text{L}$ of a 5 mg mL^{-1} redox polymer aqueous solution, $10 \text{ }\mu\text{L}$ of a 10 mg mL^{-1} aqueous enzyme solution (FADGDH or GOx), $8.88 \text{ }\mu\text{L}$ of a 46.25 mg mL^{-1} MWCNT aqueous dispersion and $2 \text{ }\mu\text{L}$ of a 15 mg mL^{-1} PEGDGE aqueous solution. Electrodes were allowed to stand for 24 hours prior to testing to ensure the film had cured. Nafion treated electrodes were prepared by allowing the film described above to cure for three hours followed by deposition of $10 \text{ }\mu\text{L}$ of either a 1% or 0.5 % w/v Nafion in ethanol dispersion. The electrodes were then allowed to stand for the remainder of the 24 hours to allow for the film to cure.

Results and Discussion

Relative quantities of each component for initial preparation of glucose-oxidising enzyme electrodes using the FADGDH enzyme are selected based on the previously described systematic analysis of the effect of each component on current response. [20,38,39] The stability of the current output recorded for these enzyme electrodes is greatly altered when comparing between PBS and artificial plasma, and a systematic analysis highlighted uric acid as the component responsible for the largest decrease in electrode stability in artificial plasma versus PBS. [25] Over-coating of the enzyme electrodes with Nafion is therefore targeted as a route towards protecting the enzyme electrode from uric acid, as the anionic charge of the Nafion film should limit access of the anionic uric acid to the enzyme electrode while allowing

for glucose to permeate through to the film. The redox Os(bpy)PVI redox polymer is selected for this study, despite the relatively positive redox potential, as it has been previously reported that lower potential redox polymers are subject to oxidation from dissolved molecular oxygen in solution [20, 40, 41]. As testing was carried out in solutions containing dissolved molecular oxygen, a redox polymer with a higher potential was used to seek to minimise this effect.

3.1 Nafion Coated Enzyme Electrodes

Slow-scan cyclic voltammetry in the presence and absence of glucose was used to initially characterise enzyme electrodes. Scans recorded in the absence of substrate (glucose) show a redox potential centred at approximately 0.22 V vs. Ag/AgCl (see Fig 1 for enzyme electrodes based on GOx and Fig S1 for enzyme electrodes based on FADGDH) which agrees with previously reported values for the Os(II/III) transition of the redox polymer. [42,43] At relatively slow scan rates ($< 20 \text{ mV s}^{-1}$) peak currents vary linearly with scan rate indicative of a surface-confined redox response. [44] Peak currents vary linearly with the square root of scan rate at higher scan rates ($>20 \text{ mV s}^{-1}$) indicative of semi-infinite diffusion as expected for multi-layer films. [44] The half-wave potential ($E_{1/2}$) recorded in the presence of a high concentration of substrate (100 mM glucose) is shifted negatively by $\sim 100 \text{ mV}$ when compared to the redox response in the absence of substrate (see Fig 1 for enzyme electrodes based on GOx and Fig S1 for enzyme electrodes based on FADGDH). This negative shift occurs for both the Nafion over-coated and uncoated electrodes. The basis for this shift is unclear at present, but it is not likely due to a charging process and instead may be indicative of substrate transport limitation that occurs for a mixed case between substrate and kinetic-limited conditions. [45,46]

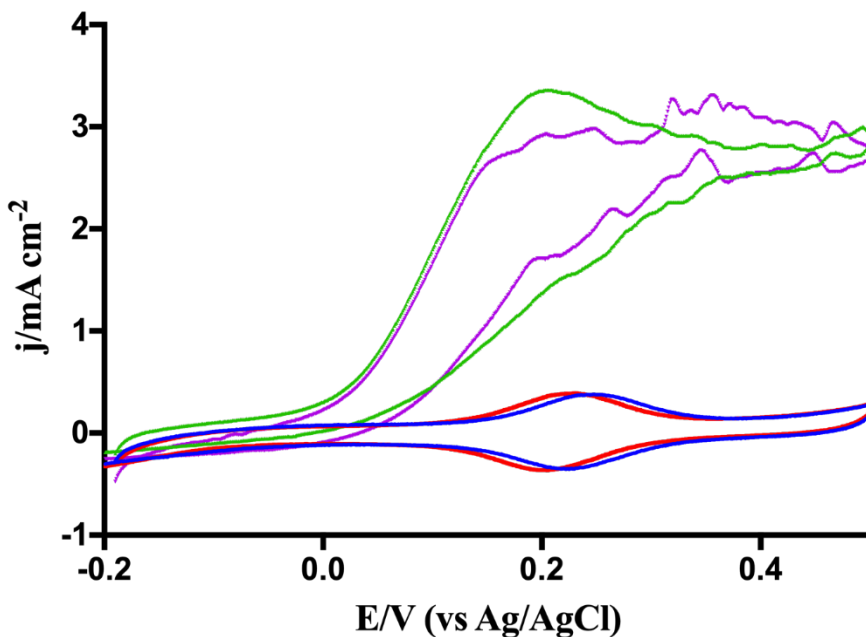


Figure 9: Slow scan (1 mV s^{-1}) cyclic voltammograms recorded for enzyme electrodes prepared with no Nafion coating tested in the presence (green) and absence (blue) of glucose (100 mM in quiescent PBS at $37 \text{ }^\circ\text{C}$) compared to enzyme electrodes prepared with a 0.5 % Nafion coating tested in the presence (purple) or absence of glucose (red) (100 mM in quiescent PBS at $37 \text{ }^\circ\text{C}$). Enzyme electrodes consisted of GOx (100 μg), Os(bpy)PVI (80 μg), MWCNTs (410 μg) and PEGDGE (30 μg).

Slow scan CVs recorded in the presence of 100 mM glucose are similar for Nafion-coated and uncoated electrodes showing a sigmoidal response, characteristic of an electrocatalytic process (EC') (see Fig 1 for enzyme electrodes based on GOx and Fig S1 for enzyme electrodes based on FADGDH), with the noise in the steady-state current most likely due to mass transport limitations. Enzyme electrodes prepared using FADGDH (Fig S1) produce similar shaped CV responses for glucose oxidation in PBS as electrodes prepared using GOx. Over-coating electrodes with a layer produced by addition of a volumes of either 0.5 % or 1 % Nafion does not alter significantly the shape for the slow scan CV, when compared to electrodes that are not over-coated, for both FADGDH and GOx enzyme electrodes, although a slight negative shift in redox potential is observed with over-coating which may be due to counter-ion effect within the films. Surface coverage of Os redox centres obtained through integrating the area under the redox peak for 1 mV s^{-1} scan rate CVs in the absence of glucose as substrate provide values of 202 ± 25 , 246 ± 37 and $172 \pm 13 \text{ nmol cm}^{-2}$ for FADGDH electrodes with no Nafion coating, 0.5 % Nafion coating and 1 % Nafion coating respectively. Surface coverage values of 323 ± 12 , 337 ± 21 and $341 \pm 14 \text{ nmol cm}^{-2}$ were obtained for otherwise identical electrodes containing GOx instead of FADGDH. The increased osmium surface coverage for GOx electrodes suggests a greater retention of the redox polymer at the surface due to electrostatic

interaction between the GOx and polycationic redox polymer compared to that for FADGDH and redox polymer. This may be due to differences in isoelectric point (pI) for each enzyme as the pI of GOx is 4.05 while the pI for FADGDH is 4.4 leading to a greater negative charge of GOx under test conditions (pH 7.4): however further testing over a range of pH values is required to confirm the results. [47–49]

Further characterisation of the Nafion coated electrodes consisting of FADGDH and GOx was performed in PBS using amperometry. Higher current densities were recorded for amperometric measurements when compared to slow scan CVs at the same potential as stirring of the test solution was performed during amperometric measurements to prevent substrate depletion at the enzyme electrode. [50] Amperometric measurements were performed at 0.45 V, selected as steady state currents are achieved at this potential as observed in Fig. 1: this also permits comparison with results previously reported. [25] Apparent K_m values and maximum saturation currents (j_{max}) were estimated from non-linear fitting of the amperometric current response as a function of glucose with a Michaelis-Menten model (Fig. 2), with the data presented in Table 1. [51] Maximum linear ranges were estimated from linear fitting of the current density versus concentration and selection of the glucose concentration that retained a correlation co-efficient >0.99 , with the enzyme electrode sensitivity values equal to the slope of the linear plot to that concentration (Table 1).

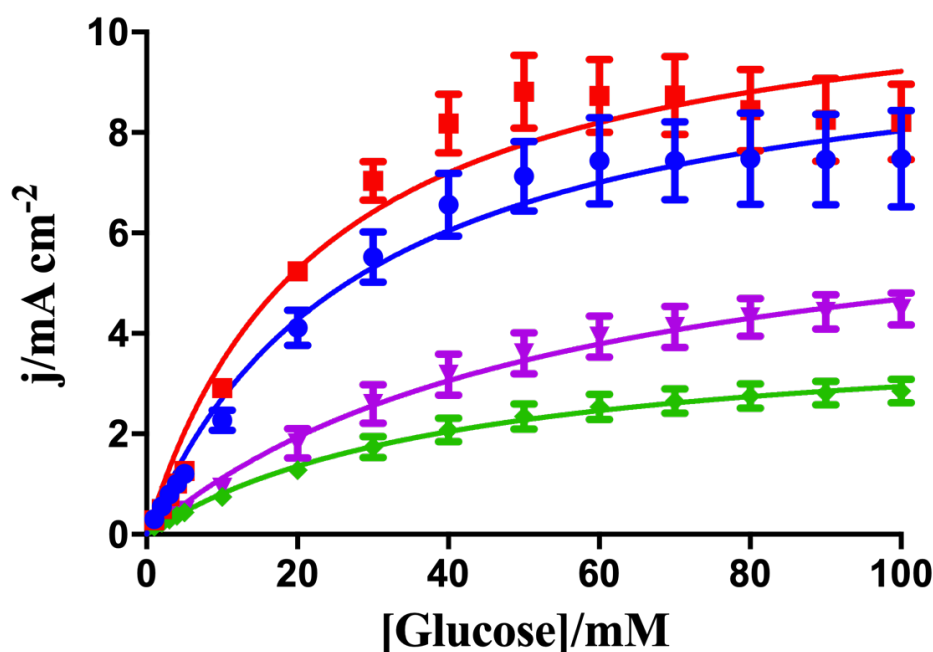


Figure 2: Glucose oxidation current densities as a function of glucose concentration, extracted from amperometry at 0.45 V vs. Ag/AgCl in PBS (37 °C) with stirring at 150 rpm for electrodes (n=4) consisting of enzyme (100 μ g), Os(bpy)PVI (80 μ g), MWCNTs (410 μ g) and PEGDGE (30 μ g). Current responses for electrodes consisting of GOx (red squares), or FADGDH (blue circles) with no Nafion coating, and GOx (purple triangles) or FADGDH (green diamonds) with 0.5% w/v Nafion coating.

To assess which Nafion coating was most suitable for testing in human physiological solutions, current density values recorded in PBS in the presence of 5 mM glucose, to represent typical human physiological values, and in 100 mM glucose, are presented in Table 1. The decrease in current response, decrease in sensitivity, and increase in linear range, as a result of over-coating of enzyme electrodes with Nafion is in agreement with previously published work, and is because the Nafion layer acts as a barrier that decreases the glucose flux. [15,52,53]

The glucose oxidation current density under physiological glucose concentrations (5 mM), and the linear range, is similar for enzyme electrodes prepared with GOx and FADGDH, although the GOx enzyme electrode response produces a slightly higher current density than that for FADGDH at higher glucose concentrations (100 mM), and a higher sensitivity over the linear range, as has been reported on previously for enzyme electrodes prepared with the same protocol, but using a redox polymer with a lower redox potential. [25,50]

Table 1: Enzyme electrode responses (n=4) for electrodes consisting of enzyme (100 μg), Os(bpy)PVI (80 μg), MWCNTs (410 μg) and PEGDGE (30 μg). Amperometry performed at 0.45 V vs. Ag/AgCl in PBS (37 $^{\circ}\text{C}$, pH 7.4) with stirring at 150 rpm.

Enzyme electrode	Current density in 5 mM glucose (mA cm^{-2})	Current density in 100 mM glucose (mA cm^{-2})	K_m^{app} (mM)	j_{max} (mA cm^{-2})	Maximum linear range (mM)	Sensitivity ($\text{mA cm}^{-2}\text{mM}^{-1}$)
GOx	1.3 ± 0.1	8.2 ± 0.8	23 ± 2.9	11.3 ± 0.5	30	0.240
GOx (0.5% w/v Nafion)	0.5 ± 0.1	4.5 ± 0.3	54.9 ± 6.3	7.3 ± 0.4	40	0.080
GOx (1 % w/v Nafion)	0.4 ± 0.2	4.4 ± 1.4	80.8 ± 34.3	8.1 ± 1.9	50	0.064
FADGDH	1.2 ± 0.4	7.5 ± 1.0	28.1 ± 3.4	10.3 ± 0.4	30	0.182
FADGDH (0.5% w/v Nafion)	0.4 ± 0.1	2.9 ± 0.2	41.3 ± 4.1	4.2 ± 0.2	40	0.050
FADGDH (1% w/v Nafion)	0.4 ± 0.1	2.6 ± 0.4	45.1 ± 7.6	3.8 ± 0.3	40	0.044

3.2 Enzyme electrode response under pseudo-physiological conditions

The effect of physiological solutions on enzyme electrode performance has been previously published, showing a significant drop off in electrode performance in complex physiological solutions when compared to electrodes tested in PBS. [20,54–58] We reported on a systematic study of the effect of components in artificial plasma on the operational stability of the current for glucose oxidising electrodes, based on co-immobilisation of enzymes with an osmium redox polymer. [25] Uric acid was identified as the component of artificial plasma resulting in the most significant change to current response and operational stability for electrodes based on FADGDH. It should be noted there is evidence of direct oxidation of uric acid at these physiological concentrations at the enzyme electrode, but not of ascorbic acid. Current response to increasing glucose concentrations and continuous operation over a 12-hour window was measured to assess the performance of the Nafion over-coating on the operational stability of the glucose-oxidising enzyme electrodes, with Fig. 3 showing the current responses as a function of glucose concentration for each electrode set tested in artificial plasma and Fig S2 showing current response over the 12 hour window for the enzyme electrodes. The decay curves differ for electrodes in different electrolytes or with different over-coating, demonstrating that glucose mass transport is not solely responsible for the current decay.

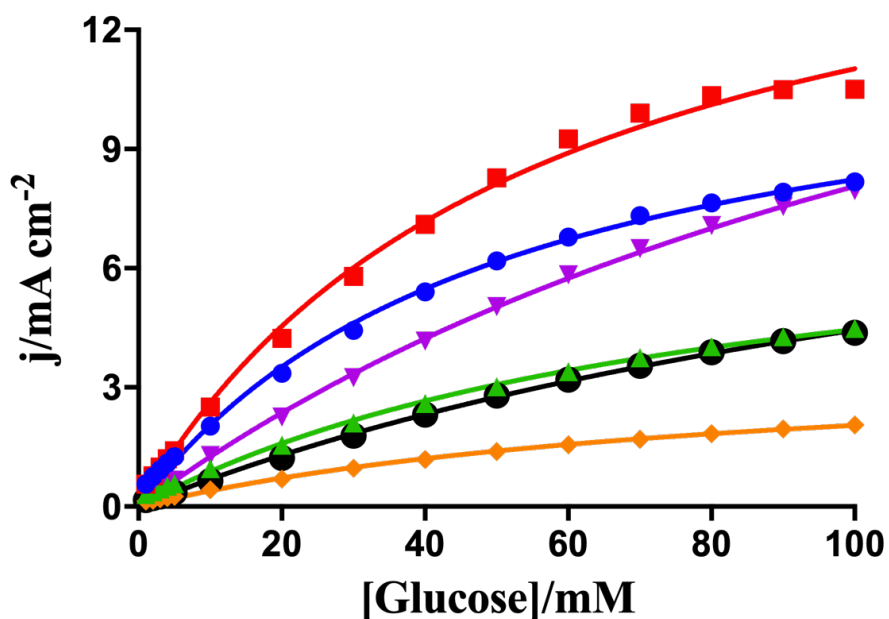


Figure 3: Average current responses (n=4) from amperometry at 0.45 V vs. Ag/AgCl in artificial plasma (37 °C) with stirring at 150 rpm at enzyme electrodes consisting of enzyme (100 μg), Os(bpy)PVI (80 μg), MWCNTs (410 μg) and PEGDGE (30 μg). Enzyme electrodes are GOx (red squares) or FADGDH (blue circles) with no Nafion coating, GOx (purple triangles) or FADGDH (green triangles) with 0.5% w/v Nafion coating, and GOx (black circles) or FADGDH (orange diamonds) with 1% w/v Nafion coating.

Table 2: % Retained current after 12 hours operation for enzyme electrodes (n=4) consisting of enzyme (100 μg), Os(bpy)PVI (80 μg), MWCNTs (410 μg) and PEGDGE (30 μg). The values recorded are amperometric current responses at 0.45 V vs. Ag/AgCl in test solutions (37 °C) containing 100 mM glucose with stirring at 150 rpm.

Electrode/Test solution	Retained current in PBS (%)	Retained current in PBS plus uric acid (%)	Retained current in artificial plasma (%)
GOx	80 \pm 5	78 \pm 4	73 \pm 8
GOx (0.5% w/v Nafion)	79 \pm 3	90 \pm 9	83 \pm 8
GOx (1 % w/v Nafion)	84 \pm 3	100 \pm 19	84 \pm 6
FADGDH	80 \pm 5	35 \pm 6	31 \pm 3
FADGDH (0.5% w/v Nafion)	76 \pm 6	71 \pm 2	58 \pm 2
FADGDH (1% w/v Nafion)	90 \pm 9	90 \pm 11	66 \pm 6

The FADGDH electrodes without Nafion over-coating retained 31 % of their initial current response after 12 hours in artificial plasma compared to the GOx electrodes which retained 73 % of their initial output. The better performance of GOx electrodes over FADGDH electrodes is in agreement with previous work published on continuous operation in complex solutions. [25,50,59] The significant decrease in operational current stability in the presence of uric acid for the enzyme electrodes prepared using FADGDH, falling from 80% to 35% retained current after 12 hours, compared to those prepared using GOx, with retained current not changing

significantly, highlights the effect of the presence of this component on the enzyme, as reported previously. [25] The operational stability of the electrodes, for FADGDH and GOx, was improved by over-coating with Nafion when compared to enzyme electrodes without Nafion, presumably because the anionic Nafion acts as a barrier repelling anions such as uric acid in the artificial plasma from interacting with the enzyme electrode films and the electrode. [30,31,52] Over-coating GOx enzyme electrodes with Nafion results in an improved operational stability when comparing performance in uric acid to that in PBS alone, with retained current increasing from 84% to 100% when 1 % Nafion solution is used to over-coat, most likely due to improved retention of redox polymer within the film once over-coated with the Nafion, as reported on previously [58]. Over-coating of the FADGDH enzyme electrodes with Nafion results in a similar retained current of 90% in the presence of uric acid compared to PBS alone, compared to retained current of 80% in PBS or 35% in uric acid for electrodes without Nafion over-coating. Improved operational stability in artificial plasma is observed for each enzyme electrode when over-coating of Nafion is implemented. The retained current is however lower in the presence of artificial plasma compared to uric acid indicating that other component(s) in the artificial plasma contribute to the decreased stability of these enzyme electrodes. [25] Lower current density is however observed for electrodes over-coated with Nafion compared to those which are not, reflected also in the higher K_m^{app} values, increased linear range and lower sensitivity, due to mass transport limitations on glucose. It should be noted therefore that electrodes over-coated from a solution of 0.5 % w/v Nafion result in higher currents compared to electrodes over-coated from a solution of 1 % w/v Nafion, while maintaining similar operational stability values.

Conclusions

Glucose oxidising electrodes were prepared with and without over-coating of Nafion to investigate if coating with the anionic polymer could shield the enzyme electrode from the effect of uric acid and other components present in artificial plasma. Electrodes prepared using co-immobilised GOx resulted in higher current densities than FADGDH based electrodes. Enzyme electrodes coated with a 0.5% w/v Nafion membrane produced significantly higher currents than electrodes coated with 1% w/v Nafion in artificial plasma while having similar operational stability. The highest initial current density recorded for Nafion over-coated electrodes in artificial plasma was $8.0 \pm 2.0 \text{ mA cm}^{-2}$ for the GOx electrodes with 0.5 % w/v Nafion coating. These electrodes retained 84 % of their initial current after 12 hours while

operating continuously in artificial plasma. The FADGDH electrodes with 0.5% w/v Nafion over-coating produced $4.5 \pm 0.7 \text{ mA cm}^{-2}$ in artificial plasma initially with a retained current after 12 hours of 58% of that signal. The GOx-based enzyme electrodes over-coated with Nafion therefore produce higher current densities and maintained higher current signal when tested continuously in the presence of uric acid and in artificial plasma, showing promise for application to continuous use glucose-oxidising enzyme electrodes.

Acknowledgements

R. Bennett acknowledges support by NUI Galway College of Science fellowship and an Irish Research Council Postgraduate Scholarship (GOIPG/2016/505).

References

- [1] G. Reach, G.S. Wilson, Can Continuous Glucose Monitoring Be Used for the Treatment of Diabetes, *Anal. Chem.* 64 (1992) 381A-386A. doi:10.1021/ac00030a718.
- [2] J. Wang, Electrochemical Glucose Biosensors, *Chem. Rev.* 108 (2008) 814–825. <https://pubs.acs.org/doi/abs/10.1021/ac00030a718> (accessed September 16, 2019).
- [3] X. Xiao, H. Xia, R. Wu, L. Bai, L. Yan, E. Magner, S. Cosnier, E. Lojou, Z. Zhu, A. Liu, Tackling the Challenges of Enzymatic (Bio)Fuel Cells, *Chem. Rev.* (2019) acs.chemrev.9b00115. doi:10.1021/acs.chemrev.9b00115.
- [4] S. Cosnier, A.J. Gross, F. Giroud, M. Holzinger, Beyond the hype surrounding biofuel cells: What's the future of enzymatic fuel cells?, *Curr. Opin. Electrochem.* (2018). doi:10.1016/J.COEELEC.2018.06.006.
- [5] P. Kavanagh, D. Leech, Mediated electron transfer in glucose oxidising enzyme electrodes for application to biofuel cells: recent progress and perspectives, *Phys. Chem. Chem. Phys.* 15 (2013) 4859. doi:10.1039/c3cp44617d.
- [6] A. Heller, Miniature biofuel cells, *Phys. Chem. Chem. Phys.* 6 (2004) 209. doi:10.1039/b313149a.
- [7] J.A. Cracknell, K.A. Vincent, F.A. Armstrong, Enzymes as Working or Inspirational Electrocatalysts for Fuel Cells and Electrolysis, *Chem. Rev.* 108 (2008) 2439–2461. doi:10.1021/cr0680639.
- [8] D. Leech, P. Kavanagh, W. Schuhmann, Enzymatic fuel cells: Recent progress, *Electrochim. Acta.* 84 (2012) 223–234. doi:10.1016/j.electacta.2012.02.087.
- [9] S. Calabrese Barton, J. Gallaway, P. Atanassov, Enzymatic Biofuel Cells for

- Implantable and Microscale Devices, *Chem. Rev.* 104 (2004) 4867–4886.
doi:10.1021/cr020719k.
- [10] M. Rasmussen, S. Abdellaoui, S.D. Minter, Enzymatic biofuel cells: 30 years of critical advancements, *Biosens. Bioelectron.* 76 (2016) 91–102.
doi:10.1016/J.BIOS.2015.06.029.
- [11] M. Yuan, S.D. Minter, Redox polymers in electrochemical systems: From methods of mediation to energy storage, *Curr. Opin. Electrochem.* 15 (2019) 1–6.
doi:10.1016/J.COEELEC.2019.03.003.
- [12] A.L. Ghindilis, P. Atanasov, E. Wilkins, Enzyme-catalyzed direct electron transfer: Fundamentals and analytical applications, *Electroanalysis.* 9 (1997) 661–674.
doi:10.1002/elan.1140090902.
- [13] F. Mao, N. Mano, A. Heller, Long Tethers Binding Redox Centers to Polymer Backbones Enhance Electron Transport in Enzyme “Wiring” Hydrogels, *J. Am. Chem. Soc.* 125 (2003) 4951–4957. doi:10.1021/ja029510e.
- [14] J. Michl, A. Heller, Electrical Wiring of Redox Enzymes, *Acc. Chem. Res.* 23 (1990) 128–134. <https://pubs.acs.org/doi/pdf/10.1021/ar00173a002> (accessed April 25, 2018).
- [15] T.J. Ohara, R. Rajagopalan, A. Heller, “Wired” Enzyme Electrodes for Amperometric Determination of Glucose or Lactate in the Presence of Interfering Substances, *Anal. Chem.* 66 (1994) 2451–2457. doi:10.1021/ac00087a008.
- [16] P. Ó Conghaile, S. Pöller, D. MacAodha, W. Schuhmann, D. Leech, Coupling osmium complexes to epoxy-functionalised polymers to provide mediated enzyme electrodes for glucose oxidation, *Biosens. Bioelectron.* 43 (2013) 30–37.
doi:10.1016/j.bios.2012.11.036.
- [17] P. O Conghaile, D. MacAodha, B. Egan, P. Kavanagh, D. Leech, Tethering Osmium Complexes within Enzyme Films on Electrodes to Provide a Fully Enzymatic Membrane-Less Glucose/Oxygen Fuel Cell, *J. Electrochem. Soc.* 160 (2013) G3165–G3170. doi:10.1149/2.026307jes.
- [18] T. de Lumley-Woodyear, P. Rocca, J. Lindsay, Y. Dror, A. Freeman, A. Heller, Polyacrylamide-Based Redox Polymer for Connecting Redox Centers of Enzymes to Electrodes, *Anal. Chem.* 67 (1995) 1332–1338. doi:10.1021/ac00104a006.
- [19] B.A. Gregg, A. Heller, Cross-linked redox gels containing glucose oxidase for amperometric biosensor applications, *Anal. Chem.* 62 (1990) 258–263.
doi:10.1021/ac00202a007.
- [20] R. Bennett, I. Osadebe, R. Kumar, P.Ó. Conghaile, D. Leech, Design of Experiments

- Approach to Provide Enhanced Glucose-oxidising Enzyme Electrode for Membraneless Enzymatic Fuel Cells Operating in Human Physiological Fluids, *Electroanalysis*. 30 (2018). doi:10.1002/elan.201600402.
- [21] S. Boland, P. Kavanagh, D. Leech, Mediated Enzyme Electrodes for Biological Fuel Cell and Biosensor Applications, in: *ECS Trans.*, ECS, 2008: pp. 77–87. doi:10.1149/1.3036213.
- [22] P. Ó Conghaile, M. Falk, D. MacAodha, M.E. Yakovleva, C. Gonaus, C.K. Peterbauer, L. Gorton, S. Shleev, D. Leech, Fully Enzymatic Membraneless Glucose|Oxygen Fuel Cell That Provides 0.275 mA cm⁻² in 5 mM Glucose, Operates in Human Physiological Solutions, and Powers Transmission of Sensing Data, *Anal. Chem.* 88 (2016) 2156–2163. doi:10.1021/acs.analchem.5b03745.
- [23] M. Shao, M.N. Zafar, M. Falk, R. Ludwig, C. Sygmund, C.K. Peterbauer, D.A. Guschin, D. MacAodha, P. Ó Conghaile, D. Leech, M.D. Toscano, S. Shleev, W. Schuhmann, L. Gorton, Optimization of a Membraneless Glucose/Oxygen Enzymatic Fuel Cell Based on a Bioanode with High Coulombic Efficiency and Current Density, *ChemPhysChem*. 14 (2013) 2260–2269. doi:10.1002/cphc.201300046.
- [24] R. Kumar, D. Leech, A glucose anode for enzymatic fuel cells optimized for current production under physiological conditions using a design of experiment approach., *Bioelectrochemistry*. 106 (2015) 41–6. doi:10.1016/j.bioelechem.2015.06.005.
- [25] R. Bennett, E. Blochouse, D. Leech, Effect of individual plasma components on the performance of a glucose enzyme electrode based on redox polymer mediation of a flavin adenine dinucleotide-dependent glucose dehydrogenase, *Electrochim. Acta*. 302 (2019) 270–276. doi:10.1016/J.ELECTACTA.2019.02.039.
- [26] R.F.B. Turner, D.J. Harrison, R.V. Rajotte, H.P. Baltes, A biocompatible enzyme electrode for continuous in vivo glucose monitoring in whole blood, *Sensors Actuators B Chem.* 1 (1990) 561–564. doi:10.1016/0925-4005(90)80273-3.
- [27] J.-A. Ni, H.-X. Ju, H.-Y. Chen, D. Leech, Amperometric determination of epinephrine with an osmium complex and Nafion double-layer membrane modified electrode, *Anal. Chim. Acta*. 378 (1999) 151–157. doi:10.1016/S0003-2670(98)00569-8.
- [28] D.S. Bindra, G.S. Wilson, Pulsed amperometric detection of glucose in biological fluids at a surface-modified gold electrode, *Anal. Chem.* 61 (1989) 2566–2570. doi:10.1021/ac00197a022.
- [29] K.A. Mauritz, R.B. Moore, State of Understanding of Nafion, *Chem. Rev.* 104 (2004) 4535–4586. doi:10.1021/cr0207123.

- [30] R. Vaidya, P. Atanasov, E. Wilkins, Effect of interference on the performance of glucose enzyme electrodes using Nafion® coatings, *Med. Eng. Phys.* 17 (1995) 416–424. doi:10.1016/1350-4533(94)00006-U.
- [31] D.J. Harrison, R.F.B. Turner, H.P. Baltes, Characterization of perfluorosulfonic acid polymer coated enzyme electrodes and a miniaturized integrated potentiostat for glucose analysis in whole blood, *Anal. Chem.* 60 (1988) 2002–2007. doi:10.1021/ac00170a003.
- [32] S.H. Lim, J. Wei, J. Lin, Q. Li, J. KuaYou, A glucose biosensor based on electrodeposition of palladium nanoparticles and glucose oxidase onto Nafion-solubilized carbon nanotube electrode, *Biosens. Bioelectron.* 20 (2005) 2341–2346. doi:10.1016/J.BIOS.2004.08.005.
- [33] X. Xiao, P.Ó. Conghaile, D. Leech, E. Magner, Use of Polymer Coatings to Enhance the Response of Redox-Polymer-Mediated Electrodes, *ChemElectroChem.* 6 (2019) 1344–1349. doi:10.1002/celec.201800983.
- [34] J. Szczesny, N. Marković, F. Conzuelo, S. Zacarias, I.A.C. Pereira, W. Lubitz, N. Plumeré, W. Schuhmann, A. Ruff, A gas breathing hydrogen/air biofuel cell comprising a redox polymer/hydrogenase-based bioanode, *Nat. Commun.* 9 (2018) 4715. doi:10.1038/s41467-018-07137-6.
- [35] E.M. Kober, J. V. Caspar, B.P. Sullivan, T.J. Meyer, Synthetic routes to new polypyridyl complexes of osmium(II), *Inorg. Chem.* 27 (1988) 4587–4598. doi:10.1021/ic00298a017.
- [36] R.J. Forster, J.G. Vos, Synthesis, characterization, and properties of a series of osmium- and ruthenium-containing metallopolymers, *Macromolecules.* 23 (1990) 4372–4377. doi:10.1021/ma00222a008.
- [37] C.A. Burtis, E.R. Ashwood, D.E. Bruns, *Tietz Textbook of Clinical Chemistry and Molecular Diagnostics.*, Elsevier Health Sciences, 2012.
- [38] C. Mercer, R. Bennett, P.Ó. Conghaile, J.F. Rusling, D. Leech, Glucose biosensor based on open-source wireless microfluidic potentiostat, *Sensors Actuators B Chem.* (2019). doi:10.1016/j.snb.2019.02.031.
- [39] D. MacAodha, M.L. Ferrer, P.Ó. Conghaile, P. Kavanagh, D. Leech, Crosslinked redox polymer enzyme electrodes containing carbon nanotubes for high and stable glucose oxidation current, *Phys. Chem. Chem. Phys.* 14 (2012) 14667. doi:10.1039/c2cp42089a.
- [40] A. Prévotau, N. Mano, Oxygen reduction on redox mediators may affect glucose

- biosensors based on “wired” enzymes, *Electrochim. Acta* 68, 128.
doi.org/10.1016/j.electacta.2012.02.053
- [41] A. PrévotEAU, N. Mano, How the reduction of O₂ on enzymes and/or redox mediators affects the calibration curve of “wired” glucose oxidase and glucose dehydrogenase biosensors, *Electrochim. Acta* 112 (2013) 318. doi.org/10.1016/j.electacta.2013.08.173
- [42] T.J. Ohara, R. Rajagopalan, A. Heller, Glucose electrodes based on cross-linked bis(2,2'-bipyridine)chloroosmium(+2+) complexed poly(1-vinylimidazole) films, *Anal. Chem.* 65 (1993) 3512–3517. doi:10.1021/ac00071a031.
- [43] H. Ju, D. Leech, [Os(bpy)₂(PVI)₁₀Cl]Cl polymer-modified carbon fiber electrodes for the electrocatalytic oxidation of NADH, *Anal. Chim. Acta.* 345 (1997) 51–58. doi:10.1016/S0003-2670(97)00093-7.
- [44] A.J. Bard, L.R. Faulkner, *Electrochemical methods : fundamentals and applications*, Wiley, 2001. <https://www.wiley.com/en-ie/Electrochemical+Methods:+Fundamentals+and+Applications,+2nd+Edition-p-9780471043720> (accessed March 27, 2018).
- [45] B. Limoges, J. Moiroux, J.-M. Savéant, Kinetic control by the substrate and the cosubstrate in electrochemically monitored redox enzymatic immobilized systems. Catalytic responses in cyclic voltammetry and steady state techniques, *J. Electroanal. Chem.* 521 (2002) 8–15. doi:10.1016/S0022-0728(02)00658-7.
- [46] P.N. Bartlett, K.F.E. Pratt, Theoretical treatment of diffusion and kinetics in amperometric immobilized enzyme electrodes Part I: Redox mediator entrapped within the film, *J. Electroanal. Chem.* 397 (1995) 61–78. doi:10.1016/0022-0728(95)04236-7.
- [47] S. Diagnostics, Glucose Dehydrogenase FAD Dependent Product Document, (n.d.). www.sekisuidiagnostics.com (accessed June 22, 2019).
- [48] J.G. Voet, J. Coe, J. Epstein, V. Matossian, T. Shipley, Electrostatic control of enzyme reactions: effect of ionic strength on the pK_a of an essential acidic group on glucose oxidase, *Biochemistry.* 20 (1981) 7182–7185. doi:10.1021/bi00528a020.
- [49] N. Mano, Engineering glucose oxidase for bioelectrochemical applications, *Bioelectrochemistry.* 128 (2019) 218–240. doi:10.1016/J.BIOELECHEM.2019.04.015.
- [50] D. MacAodha, P. Ó Conghaile, B. Egan, P. Kavanagh, C. Sygmund, R. Ludwig, D. Leech, Comparison of Glucose Oxidation by Crosslinked Redox Polymer Enzyme Electrodes Containing Carbon Nanotubes and a Range of Glucose Oxidising Enzymes, *Electroanalysis.* 25 (2013) 94–100. doi:10.1002/elan.201200536.

- [51] I. Osadebe, D. Leech, Effect of Multi-Walled Carbon Nanotubes on Glucose Oxidation by Glucose Oxidase or a Flavin-Dependent Glucose Dehydrogenase in Redox-Polymer-Mediated Enzymatic Fuel Cell Anodes, *ChemElectroChem*. 1 (2014) 1988–1993. doi:10.1002/celec.201402136.
- [52] C.P. Andrieux, P. Audebert, P. Bacchi, B. Divisia-Blohorn, Kinetic behaviour of an amperometric biosensor made of an enzymatic carbon paste and a Nafion® gel investigated by rotating electrode studies, *J. Electroanal. Chem.* 394 (1995) 141–148. doi:10.1016/0022-0728(95)04037-O.
- [53] C.P. Andrieux, P. Audebert, B. Divisia-Blohorn, S. Linquette-Maillet, A new glucose sensor made of a Nafion-gel-layer covered carbon paste, *J. Electroanal. Chem.* 353 (1993) 289–296. doi:10.1016/0022-0728(93)80305-2.
- [54] T. Siepenkoetter, U. Salaj-Kosla, X. Xiao, P.Ó. Conghaile, M. Pita, R. Ludwig, E. Magner, Immobilization of Redox Enzymes on Nanoporous Gold Electrodes: Applications in Biofuel Cells, *ChemPlusChem*. 82 (2017) 553–560. doi:10.1002/cplu.201600455.
- [55] D. MacAodha, P.Ó. Conghaile, B. Egan, P. Kavanagh, D. Leech, Membraneless Glucose/Oxygen Enzymatic Fuel Cells Using Redox Hydrogel Films Containing Carbon Nanotubes, *ChemPhysChem*. 14 (2013) 2302–2307. doi:10.1002/cphc.201300239.
- [56] R.D. Milton, K. Lim, D.P. Hickey, S.D. Minteer, Employing FAD-dependent glucose dehydrogenase within a glucose/oxygen enzymatic fuel cell operating in human serum, *Bioelectrochemistry*. 106 (2015) 56–63. doi:10.1016/J.BIOELECHEM.2015.04.005.
- [57] V. Coman, R. Ludwig, W. Harreither, D. Haltrich, L. Gorton, T. Ruzgas, and S. Shleev, A Direct Electron Transfer-Based Glucose/Oxygen Biofuel Cell Operating in Human Serum, *Fuel Cells*. (2009). doi:10.1002/fuce.200900121.
- [58] M. Cadet, S. Gounel, C. Stines-Chaumeil, X. Brilland, J. Rouhana, F. Louerat, N. Mano, Cadet, M., Gounel, S., Stines-Chaumeil, C., Brilland, X., Rouhana, J., Louerat, F., Mano, N., 2016. An enzymatic glucose/O₂ biofuel cell operating in human blood. *Biosens. Bioelectron.* 83, 60–67. <https://doi.org/10.1016/j.bios.2016.04.016> An enzymatic gluc, *Biosens. Bioelectron.* 83 (2016) 60–67. doi:10.1016/j.bios.2016.04.016.
- [59] X. Xiao, T. Siepenkoetter, P.Ó. Conghaile, D. Leech, E. Magner, Nanoporous Gold-Based Biofuel Cells on Contact Lenses, *ACS Appl. Mater. Interfaces*. 10 (2018) 7107–7116. doi:10.1021/acsami.7b18708.

Supporting Information

Improved operational stability of mediated glucose enzyme electrodes for operation in human physiological solutions

Richard Bennett, Dónal Leech*

School of Chemistry & Ryan Institute, National University of Ireland Galway, University Road, Galway, Ireland

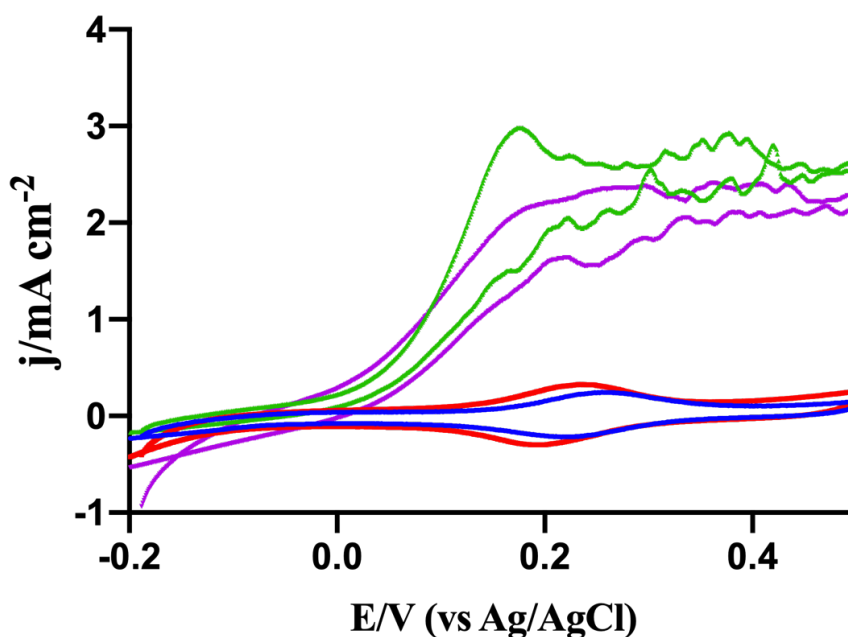


Figure S10: Slow scan (1 mV s^{-1}) cyclic voltammograms recorded for enzyme electrodes prepared with no Nafion coating tested in the presence (green) and absence (blue) of glucose (100 mM in quiescent PBS at 37°C) compared to enzyme electrodes prepared with a 0.5 % Nafion coating tested in the presence (purple) or absence of glucose (red) (100 mM in quiescent PBS at 37°C). Enzyme electrodes consisted of FADGDH ($100 \mu\text{g}$), Os(bpy)PVI ($80 \mu\text{g}$), MWCNTs ($410 \mu\text{g}$) and PEGDGE ($30 \mu\text{g}$).

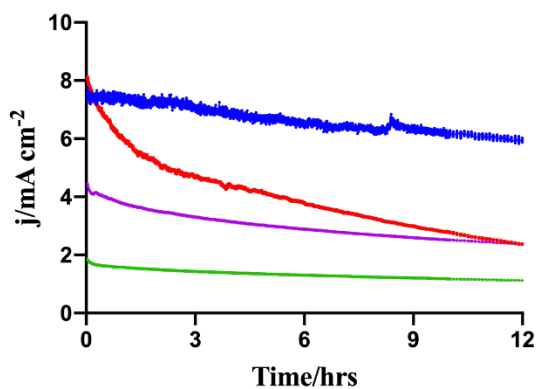
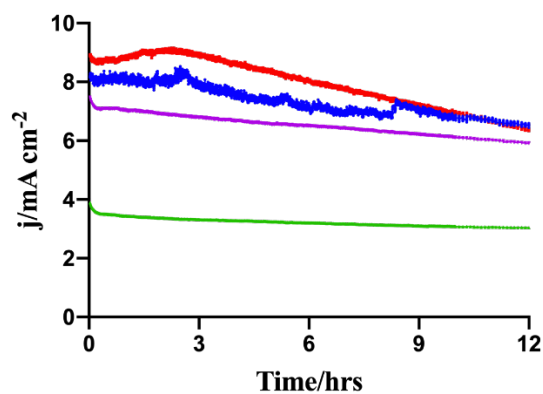
A**B**

Figure S2: Average current response ($n=4$) from continuous use amperometry at 0.45 V vs. Ag/AgCl in test solutions (37 °C) containing 100 mM glucose with stirring at 150 rpm. Enzyme electrodes consisted of either FADGDH (100 μg) **A** or GOx (100 μg) **B** co-immobilised with Os(bpy)PVI (80 μg), MWCNTs (410 μg) and PEGDGE (30 μg) prepared with no Nafion over-coating and tested in PBS (blue) and artificial plasma (red), with 0.5% w/v Nafion over-coating and tested in artificial plasma (magenta) and with 1% w/v Nafion over-coating and tested in artificial plasma (green).

Chapter 6: Conclusions and future directions

Conclusions

This thesis focused on improving the performance of glucose oxidising enzyme electrodes for application as biosensors and in biofuel cells as well as improving the understanding of why such enzyme electrodes suffer from reduced performance in complex human physiological solutions. The aim of the thesis was to focus on improving current density and operational stability of mediated enzyme electrodes which could be utilised under *in-vivo* conditions.

Chapter 2 focused on using an alternative immobilisation strategy with the electropolymerisation of L-Dopa to poly(L-Dopa). The aim was to show proof of concept of the poly(L-Dopa) films as a route for immobilising the enzyme, mediator and MWCNTs at an electrode surface. These poly(L-Dopa) enzyme electrodes were then tested for performance in the presence of increasing concentrations of glucose and benchmarked against PEGDGE crosslinked electrodes.

Chapter 3 demonstrated the application of a design of experiments approach for the optimisation of surface components for a mediated glucose oxidising electrode. The optimised electrodes were compared with previously optimised electrodes using an OFAT approach. The DoE approach was used to optimise amounts of osmium redox polymer, FADGDH and MWCNTs at an electrode surface for current density in the presence of 5 mM glucose. Current densities of $1.22 \pm 0.1 \text{ mA cm}^{-2}$ in PBS at 37 °C in the presence of 5 mM glucose were achieved. This was a 52 % increase on previously reported OFAT optimised enzyme electrodes. Manipulation of component amounts allowed for high current densities $0.78 \pm 0.11 \text{ mA cm}^{-2}$ with 34 % less enzyme.

Chapter 4 reported on the effect of individual components of artificial plasma on the performance of glucose oxidising electrodes containing FADGDH, osmium redox polymer, MWCNTs and the crosslinker PEGDGE. The testing was performed to gain a better understanding of enzyme electrode performance in human physiological solutions. Electrodes tested in the presence of uric acid produced showed a significant decrease in performance in 5 mM glucose and operational stability over a 12-hour window in 100 mM glucose. GOx based electrodes maintained 70 % of operational stability over 12 hours when compared to 46 % for FADGDH electrodes in the presence of uric acid. CDH electrodes maintained 86 % of their initial current in PBS testing over 12 hours but only 33 % in the presence of uric acid.

Chapter 5 followed on from chapter 4 with application of Nafion membranes to mediated glucose oxidising electrodes as a strategy to mitigate the effect of artificial plasma on electrode

performance. Glucose oxidising electrodes containing either FADGDH or GOx with Nafion coatings were prepared and tested in PBS, PBS containing uric acid and in artificial plasma. GOx electrodes with a 0.5 % Nafion coating produced $8.0 \pm 2.0 \text{ mA cm}^{-2}$ in 100 mM glucose and maintained 84 % of the initial current after 12 hours in artificial plasma. In comparison the FADGDH electrodes with a 0.5 % Nafion coating generated $4.5 \pm 0.7 \text{ mA cm}^{-2}$ in 100 mM with an operational stability of 58 %. Further work is required to investigate surface coatings on enzyme electrodes for improved performance in human physiological solutions.

Future directions

There are significant hurdles which need to be overcome before enzyme-based electrodes can be relied on for power generation or long term biosensing. A recent review by Xiao *et al.* suggested four major challenges facing EFC development. These were limited voltage output, low power density, partial oxidation of fuels and poor operational stability. [1] Throughout my research project detailed in the previous chapters, novel strategies and methodologies were used to understand and improve the low power output as well as tackling the poor operational stability of enzyme electrodes. Low power output from EFCs (typically on a $\mu\text{W cm}^{-2}$ scale) when compared to Li-ion batteries or metal-based fuel cells limit their potential applications. This is due to the active site being buried deep within a protein shell, complicating electron transfer to the electrode surface. [1,2]

A potential route towards overcoming this low power output is to look at engineering of wild type enzymes to provide mutants with increased catalytic activity, and thus improved current density. Mano recently published a review article detailing strategies employed to improve the performance of GOx based electrodes through protein engineering. The two main requirements for new GOx mutations are to reduce its inherent oxygen sensitivity and to increase electron transfer rate from active site to the electrode surface. [3] Another route towards improved enzyme electrode performance is directed evolution of the enzyme. This evolution can occur with the aim of improving the catalytic properties of the enzyme or in the case of GOx, reducing oxygen sensitivity. Holland *et al.* redesigned a GOx for improved catalytic performance. They obtained 4 mutants demonstrating 3 to 4.5 fold improvement of the catalytic rate constant, with the T110S identified as the mutant with the highest activity. [5] Zhu *et al.* reported on directed evolution of GOx from *Aspergillus niger* for mediated electron transfer using ferrocenemethanol. Over 4000 mutants were screened with a double mutant (T30S/I94V) showing increased pH and thermal stability and a 1.9 fold increase in enzymatic activity when

compared with the wild type GOx. [6] Further work is needed in the area of protein engineering to develop enzymes that are capable of producing higher current densities when immobilised at electrode surface while also demonstrating robust operational stabilities.

An alternate route towards improved performance of glucose oxidase is the deglycosylation of the protein. Glycosylations increase the size of the enzyme and result in greater distance between active site and electrode thus acting as an insulating membrane. PrévotEAU *et al.* compared deglycosylated GOx with native GOx when co-immobilised at glassy carbon electrodes with an osmium redox polymer. Glucose oxidation currents produced by the deglycosylated enzyme electrodes were 38 % than the native enzyme. [4]

A further route towards improving power density of EFCs is the use of enzyme cascades. These work by immobilising more than one enzyme within the film at an electrode surface. The first enzyme would oxidise a fuel, such as glucose, with the second enzyme oxidising the product from the first enzyme. This continued oxidation of a fuel can occur with the inclusion of the relevant enzymes in the electrode film to allow for complete oxidation of a fuel, thus increasing the coulombic efficiency of an EFC. [7,8] One such example is the complete oxidation of glycerol using a three enzyme cascade at an anode, with glycerol/air fuel cells yielding power densities of 1.32 mW cm⁻². [9] Future work on enzyme cascades coupled with protein engineering strategies could focus on complete oxidation of fuels (such as the conversion of glucose to carbon dioxide) to produce higher power densities while also addressing the operational stability of immobilised enzymatic films.

The inclusion of nano-supports such as nanoporous gold and MWCNTs in enzyme electrode assembly has resulted in higher current densities as well as improved operational stabilities. [1,10,11] Further examples of nano-supports included in electrode assemblies are carbon nanofibres, graphene and buckypaper. [12–14] Nanomaterials are not fully understood and require further investigation for electrochemical performance and toxicity before they can be implemented in potentially implantable or semi-implantable devices. However, in certain cases they have improved electrode performance and as a result novel nano-supports should be tested in electrode assemblies as they are discovered. [15]

One of the biggest challenges facing EFC prototypes is their performance under *in-vivo* conditions. There are multiple facets to this challenge with two of the most significant being achieving acceptable performance of enzyme electrodes in human physiological solutions and mitigating the foreign body response for implantable or semi-implantable devices. Further work is required to understand the basis for poor enzyme electrode performance in human solutions. [16–18] Chapter 4 of this thesis reported on the effect of individual plasma

components on glucose oxidising electrodes in an attempt to understand reduced electrode performance. Further experiments are required to understand the impact human physiological solutions have on each component of the enzymatic film. While electrochemical testing in PBS is an important step in reporting on novel electrode assemblies, testing in more complex solutions should be carried out in parallel to give a greater understanding of electrode performance. Any device once implanted in the body will be subjected to the foreign body response, resulting in biofouling of the electrodes with the adsorption of layers of cells and proteins. The end result of this is mass transport and diffusion limitations with reduced power output from the electrodes. One potential route is the use of biocompatible coatings to reduce biofouling. Trouillon *et al.* reported on the ability of various coatings to reduce biofouling at an electrode. [19] Biofouling was induced using albumin in solution with fibronectin coatings reported as the most satisfactory of the tested membranes. Chapter 5 of this thesis reported on the use of Nafion coatings to mitigate the effects of artificial plasma on enzyme electrode performance. Further work is required to find an acceptable level of protection from plasma components while allowing for glucose diffusion through the coating. The use of dialysis bags for carbon electrodes placed in a Dacron sleeve to prevent leakage and improve biocompatibility has been reported previously. [20,21] Cadet *et al.* described the use of cellulose dialysis bags for enzyme electrodes tested in whole human blood. [22] The dialysis coated system retained twice the current signal of the unprotected system when tested continuously in blood for 6 hours. The reduced performance in blood was attributed to mass transport issues at both electrodes. Further work is required on strategies to improve electrode performance when operated in blood.

References

- [1] X. Xiao, H. Xia, R. Wu, L. Bai, L. Yan, E. Magner, S. Cosnier, E. Lojou, Z. Zhu, A. Liu, Tackling the Challenges of Enzymatic (Bio)Fuel Cells, *Chem. Rev.* (2019) [acs.chemrev.9b00115](https://doi.org/10.1021/acs.chemrev.9b00115). doi:10.1021/acs.chemrev.9b00115.
- [2] D. Leech, P. Kavanagh, W. Schuhmann, Enzymatic fuel cells: Recent progress, *Electrochim. Acta.* 84 (2012) 223–234. doi:10.1016/j.electacta.2012.02.087.
- [3] N. Mano, Engineering glucose oxidase for bioelectrochemical applications, *Bioelectrochemistry.* 128 (2019) 218–240. doi:10.1016/J.BIOELECTHEM.2019.04.015.
- [4] A. PrévotEAU, O. Courjean, N. Mano, Deglycosylation of glucose oxidase to improve

- biosensors and biofuel cells, *Electrochem. Commun.* 12 (2010) 213–215.
doi:10.1016/j.elecom.2009.11.027.
- [5] J.T. Holland, J.C. Harper, P.L. Dolan, M.M. Manginell, D.C. Arango, J.A. Rawlings, C.A. Ablett, S.M. Brozik, Rational Redesign of Glucose Oxidase for Improved Catalytic Function and Stability, *PLoS One.* 7 (2012) e37924.
doi:10.1371/journal.pone.0037924.
- [6] Z. Zhu, M. Wang, A. Gautam, J. Nazor, C. Momeu, R. Prodanovic, U. Schwaneberg, Directed evolution of glucose oxidase from *Aspergillus niger* for ferrocenemethanol-mediated electron transfer, *Biotechnol. J.* 2 (2007) 241–248.
doi:10.1002/biot.200600185.
- [7] S.D. Minter, B.Y. Liaw, M.J. Cooney, Enzyme-based biofuel cells, *Curr. Opin. Biotechnol.* 18 (2007) 228–234. doi:10.1016/J.COPBIO.2007.03.007.
- [8] D. Sokic-Lazic, S.D. Minter, Citric acid cycle biomimic on a carbon electrode, *Biosens. Bioelectron.* 24 (2008) 939–944. doi:10.1016/j.bios.2008.07.043.
- [9] R.L. Arechederra, S.D. Minter, Complete Oxidation of Glycerol in an Enzymatic Biofuel Cell, *Fuel Cells.* 9 (2009) 63–69. doi:10.1002/fuce.200800029.
- [10] X. Xiao, T. Siepenkoetter, P.Ó. Conghaile, D. Leech, E. Magner, Nanoporous Gold-Based Biofuel Cells on Contact Lenses, *ACS Appl. Mater. Interfaces.* 10 (2018) 7107–7116. doi:10.1021/acsami.7b18708.
- [11] D. MacAodha, M.L. Ferrer, P.Ó. Conghaile, P. Kavanagh, D. Leech, Crosslinked redox polymer enzyme electrodes containing carbon nanotubes for high and stable glucose oxidation current, *Phys. Chem. Chem. Phys.* 14 (2012) 14667.
doi:10.1039/c2cp42089a.
- [12] J. Filip, J. Tkac, Is graphene worth using in biofuel cells?, *Electrochim. Acta.* 136 (2014) 340–354. doi:10.1016/j.electacta.2014.05.119.
- [13] M. Bourourou, M. Holzinger, K. Elouarzaki, A. Le Goff, F. Bossard, C. Rossignol, E. Djurado, V. Martin, D. Curtil, D. Chaussy, A. Maaref, S. Cosnier, Laccase wiring on free-standing electrospun carbon nanofibres using a mediator plug, *Chem. Commun.* 51 (2015) 14574–14577. doi:10.1039/C5CC03906A.
- [14] A.J. Gross, M. Holzinger, S. Cosnier, Buckypaper bioelectrodes: emerging materials for implantable and wearable biofuel cells, *Energy Environ. Sci.* 11 (2018) 1670–1687.
doi:10.1039/C8EE00330K.
- [15] M. Holzinger, A. Le Goff, S. Cosnier, Nanomaterials for biosensing applications: a review, *Front. Chem.* 2 (2014). doi:10.3389/fchem.2014.00063.

- [16] V. Coman, R. Ludwig, W. Harreither, D. Haltrich, L. Gorton, T. Ruzgas, and S. Shleev, A Direct Electron Transfer-Based Glucose/Oxygen Biofuel Cell Operating in Human Serum, *Fuel Cells*. (2009) NA-NA. doi:10.1002/fuce.200900121.
- [17] R.D. Milton, K. Lim, D.P. Hickey, S.D. Minteer, Employing FAD-dependent glucose dehydrogenase within a glucose/oxygen enzymatic fuel cell operating in human serum, *Bioelectrochemistry*. 106 (2015) 56–63. doi:10.1016/J.BIOELECHEMA.2015.04.005.
- [18] P. Ó Conghaile, M. Falk, D. MacAodha, M.E. Yakovleva, C. Gonaus, C.K. Peterbauer, L. Gorton, S. Shleev, D. Leech, Fully Enzymatic Membraneless Glucose|Oxygen Fuel Cell That Provides 0.275 mA cm⁻² in 5 mM Glucose, Operates in Human Physiological Solutions, and Powers Transmission of Sensing Data, *Anal. Chem.* 88 (2016) 2156–2163. doi:10.1021/acs.analchem.5b03745.
- [19] R. Trouillon, Z. Combs, B.A. Patel, D. O'Hare, Comparative study of the effect of various electrode membranes on biofouling and electrochemical measurements, *Electrochem. Commun.* 11 (2009) 1409–1413. doi:10.1016/j.elecom.2009.05.018.
- [20] P. Cinquin, C. Gondran, F. Giroud, S. Mazabrard, A. Pellissier, F. Boucher, J.-P. Alcaraz, K. Gorgy, F. Lenouvel, S. Mathé, P. Porcu, S. Cosnier, A Glucose BioFuel Cell Implanted in Rats, *PLoS One*. 5 (2010) e10476. doi:10.1371/journal.pone.0010476.
- [21] A. Zebda, S. Cosnier, J.-P. Alcaraz, M. Holzinger, A. Le Goff, C. Gondran, F. Boucher, F. Giroud, K. Gorgy, H. Lamraoui, P. Cinquin, Single Glucose Biofuel Cells Implanted in Rats Power Electronic Devices, *Sci. Rep.* 3 (2013) 1516. doi:10.1038/srep01516.
- [22] M. Cadet, S. Gounel, C. Stines-Chaumeil, X. Brilland, J. Rouhana, F. Louerat, N. Mano, 2016. An enzymatic glucose/O₂ biofuel cell operating in human blood. *Biosens. Bioelectron.* 83, 60–67. <https://doi.org/10.1016/j.bios.2016.04.016>An enzymatic gluc, *Biosens. Bioelectron.* 83 (2016) 60–67. doi:10.1016/j.bios.2016.04.016.

Appendix

Publications

- **Bennett, R.**, Osadebe, I., Kumar, R., Ó Conghaile, P., & Leech, D. (2018) Design of Experiments Approach to Provide Enhanced Glucose-Oxidising Enzyme Electrode for Membrane-Less Enzymatic Fuel Cells Operating in Human Physiological Fluids. *Electroanalysis*, 30(7), 1438-1445 doi:10.1002/elan.201600402
- **Bennett, R.**, Blochouse, E., & Leech, D. (2019) Effect of individual plasma components on the performance of a glucose enzyme electrode based on redox polymer mediation of a flavin adenine dinucleotide-dependent glucose dehydrogenase. *Electrochimica Acta*, 302, 270-276 doi:10.1016/j.electacta.2019.02.039
- Mercer, C., **Bennett, R.**, Ó Conghaile, P., Rusling, J.F., & Leech, D. (2019) Glucose biosensor based on open-source wireless microfluidic potentiostat. *Sensors and Actuators B: Chemical*, 290, 616-624 doi:10.1016/j.snb.2019.02.031
- **Bennett, R.** & Leech, D. (2020) Improved operational stability of mediated glucose enzyme electrodes for operation in human physiological solutions. *Bioelectrochemistry*, 133, 107460 doi:10.1016/j.bioelechem.2020.107460

Oral presentations

- Royal Society of Chemistry Electrochemistry Conference, University of Birmingham, September '17
- Conference for Analytical Sciences in Ireland, Maynooth University, May '18
- Summer Meeting of Bio Electrochemistry, Antwerp University, August '18
- Chemistry Research Day, NUI Galway, January '19
- XXV BES Symposium, University of Limerick, May '19
- 70th ISE Conference, Durban, South Africa, August '19

Poster presentations

- Conference for Analytical Sciences in Ireland, Dublin City University, April '16

Awards

- NUI Galway Ryan Institute Travel award recipient 2019
- Best speaker at the Conference for Analytical Sciences in Ireland 2018